Computational investigations of small molecule activation

Thesis Submitted to AcSIR for the Award of the Degree of

DOCTOR OF PHILOSOPHY

in Chemical Sciences

By

Amrita Pal

Registration Number: 10CC12A26055

Under the guidance of

Dr. Kumar Vanka

Physical Chemistry Division CSIR-

National Chemical Laboratory,

Pune - 411008, India

August 2015

सीएसआयआर–राष्ट्रीय रासायनिक प्रयोगशाला
(वैज्ञानिक तथा औद्योगिक अनुसंधान परिषद)
डॉ. होमी भाभा मार्ग, पुणे – 411 008. भारत
CSIR-NATIONAL CHEMICAL LABORATORY
(Council of Scientific & Industrial Research)
Dr. Homi Bhabha Road, Pune - 411008. India

Certificate

This is to certify that the work incorporated in this Ph.D. thesis entitled ***Computational investigations of small molecule activation*** submitted by ***Ms. Amrita Pal*** to Academy of Scientific and Innovative Research (AcSIR) in fulfillment of the requirements for the award of the Degree of ***Doctor of Philosophy in Chemical Sciences***, embodies original research work under my supervision. I further certify that this work has not been submitted to any other University or Institution in part or full for the award of any degree or diploma. Research material obtained from other sources has been duly acknowledged in the thesis. Any text, illustration, table etc., used in the thesis from other sources, have been duly cited and acknowledged.

Amrita Pal
(Student)

Dr. Kumar Vanka
(Supervisor)

Date: 13/08/2015

Place: Pune

Communications Channels
NCL Level DID : 2590
NCL Board No. : +91-20-25902000
Four PRI Lines : +91-20-25902000
FAX
Director's Office : +91-20-25902601
COA's Office : +91-20-25902660
SPO's Office : +91 20 25902664
WEBSITE
www.ncl-india.org

Dedicated to

My Parents...

ACKNOWLEDGEMENT

First of all, I am thankful to my research supervisor **Dr. Kumar Vanka** for his sincere guidance, constant support and inspiration throughout my PhD. He familiarized me with the exciting research that has been performed on small molecule activation and also guided me to envisage future prospects. His constructive suggestions and criticisms on my research topics shaped the work described in this thesis.

I specially thank **Dr. Sourav Pal**, former Director CSIR-National Chemical Laboratory, for his immense help throughout the PhD process, whether it was teaching core concepts of quantum mechanics, assistance in proceeding through coursework or thesis submission. Dr. Pal's support and encouragement will always motivate me throughout my life. I would also like to acknowledge the contributions from my DAC committee members (**Dr. Sayam Sengupta, Dr. Neelanjana Sengupta, Dr. Sudip Roy** and **Dr. Nayana Vaval**) for their consistent research suggestions and fruitful evaluations at every stage of my PhD. I also thank Dr. Sakya Sen for his helpful discussions and suggestions.

I am thankful to CSIR, New Delhi for senior research fellowship support. I acknowledge the teaching, non-teaching and administrative staff of CSIR-NCL for their help at various stages. I thank all my labmates Kamalika, Sneha, Jaya, Debaratidi, Deepthidi, Achintya, Susanta, Manzoor, Turbasu, Himadri, Sayali, Anagha, Saba, Vidhika, Deepak, Sudip, Prathit, Samik, Rahul, Shantanu, Yuvraj, Nisha, Manoj, Jugal, Tamal, Subrashish, Mrityunjoy for their assistance on many occasions.

I thank all the CSIR-NCL research scholars for maintaining a jovial relationship. I am particularly thankful to Kamalika for her help and suggestions. I also thank Swagata, Debarotidi, Niveditadi, Sumantrada, Abhik, Munmun for making my NCL days joyful. Also, I am grateful to my friends Priya and Jagadish for their support.

I am grateful to Dr. Pillai, Director, and Dr. Pal, former director, CSIR-National Chemical Laboratory for allowing me to work in NCL and providing the necessary facilities and work environment to complete the results described in this thesis. I acknowledge Academy of Scientific & Innovative Research (AcSIR) for registering for a PhD course and providing me the opportunity to obtain a PhD degree.

I thank my family members and particularly my elder sister Moumita for her invariable care and good wishes. I am also thankful to my husband for his support. Last but not the least; I

would like to pay deep respect to my parents. They have shown utmost patience and provided constant blessing and encouragement that helped me through my tough times. I therefore dedicate my thesis in the name of my parents, which is the least I can do to acknowledge their effort in the long run.

Amrita Pal

Abstract

Small molecule activation has been an important area of research since the emergence of catalytic processes. It has been relevant both industrially and biologically due to the scope and opportunities related to the substrates and the concerned pathways. The wide variety of bond strength, polarity, reactivity and the availability of suitable orbitals has made it possible to explore a wide range of catalysts for the activation processes. A rational design and computational screening of such catalysts to observe the activation mechanisms can prove fruitful for practical syntheses of such catalysts and for testing their activity in small molecular activation.

Discussed in chapter 1 are different systems for small molecule activation and their distinction based on their nature (i.e., metallic or non-metallic), reactivity, operating conditions and respective pathways or mechanisms. Beginning with transition metal catalysts, the chapter then describes the evolution to more effective forms of metal ligand cooperativity. The subsequent discussion has focused on main group catalysts, such as carbenes, silylenes and frustrated Lewis pairs (FLPs), which are the greener alternatives to the transition metal catalysts.

Chapter 2 focuses on the computational details of the methods that have been used throughout the calculations. The fundamental concepts and equations, such as the Schrödinger equation and the Born-Oppenheimer approximation have been discussed. In the following sections, the Thomas-Fermi model, the Hohenberg-Kohn theorems, the Kohn-Sham approach, concepts of functionals and the Møller–Plesset (MP2) theory have been discussed. Furthermore, the RI-J and MARI-J approximations and the COSMO model for solvent correction, which have been implemented in Turbomole software, have been elucidated.

In Chapter 3, it has been shown that late transition metals that can cooperate with ligands (bearing phosphines as pendant groups) can work as metal analogues to frustrated Lewis pairs (FLPs) and participate in a variety of important reactions. A suitably adapted palladium complex has been studied as a specimen of a potential late transition metal based FLP and explored with detailed quantum mechanical calculations. Calculations indicate that this complex would be an effective catalyst for the ammonia borane dehydrogenation reaction. The chances of competing side reactions, for example, the reductive elimination process, have also been taken under consideration. It has been observed that such processes would also yield stable products that could also act as a FLP in the catalytic dehydrogenation process of ammonia borane, thereby expanding the

horizon of metal based FLPs having late transition metals (*Dalton Trans.*, 2013, 42, 13866-13873).

In Chapter 4, new zero dimensional cage structures have been identified for the ammonia borane dehydrogenation reactions. The basic cage (containing four phenyl rings separated by imine connectors) has been synthesized recently. By using detailed computational investigations with the help of density functional theory (DFT), it has been shown that the modification of such cages by replacing the 2, 4, 6 carbon atoms in the phenyl rings with phosphorous or germanium yields new rings having interesting prospects for small molecule activation. Also demonstrated is that the replacement of the imine moiety in the connector by other electronegative atoms (such as phosphorous in place of nitrogen) can also be efficient in catalyzing reactions such as the dehydrogenation of ammonia borane. Interestingly, the predicted phosphorus-nitrogen pairs (phosphorus in the 2, 4, 6 positions in the ring, nitrogen in the linker position), germanium-nitrogen and germanium-phosphorus pair combinations can generate Lewis pairs that would work in tandem to dehydrogenate ammonia borane. (*Chem. Commun.*, 2011, 47, 11417-11419 and *Phys. Chem. Chem. Phys.*, 2013, 15, 20857-20867.)

In Chapter 5, it has been demonstrated that contrary to the conventional bond weakening process, the bond-strengthening back-donation to a π-diborene (recently discovered for transition metal systems by Braunschweig and co-workers, *Nat. Chem.*, 2013, **5**, 115-121) would be similarly favored for main group silylene complexes. These results have been performed by full quantum chemical calculations with density functional theory (DFT), and have expanded the range and applicability of the bond-strengthening back-bonding interaction. Calculations also demonstrate the potential of main group complexes to perform new and exciting chemistry, for example, the cooperative activation of carbon monoxide and carbon dioxide. (*Chem. Commun.*, 2014, 50, 8522-8525.)

Presented in chapter 6 is an exciting constrained, “flat”, phosphorus based complex and its use to catalyze reactions such as the dehydrogenation of ammonia borane and the activation of the N-H bond in primary amines. This development in main group chemistry has been exploited to show that when properly designed, such compounds can be as efficient as transition metal complexes for performing different chemical transformations. The detailed computational studies employing density functional theory (DFT) reveals that a common, general mechanism exists to account for the behavior of the flat phosphorus compound in different reaction conditions that have been observed experimentally to date. The proposed mechanism shows a base as a proton transfer agent that is simpler and energetically more favorable than the previous mechanisms that have

been proposed for the same reactions in the literature. The mechanism provides important new insights into phosphorus chemistry. (*Inorg. Chem.*, 2016, 55, 558–565)

Finally, in chapter 7, a summary and conclusion of the overall work presented in this thesis has been provided.

Amrita Pal

CONTENTS

Chapter 5

Chapter 6

Chapter 7

List of Abbreviations

DFT	density functional theory
AB	ammonia borane
MP2	second-order Møller–Plesset perturbation theory
SCS-MP2	spin-component scaled - MP2
RI	resolution of identity
MARIJ	multipole accelerated resolution of identity
NHC	N-heterocyclic carbene
0D	zero dimensional
Dipp	2,6-$iPr_2C_6H_3$
CI	configuration interaction
CC	coupled cluster
KS	Kohn-Sham
LDA	local density approximation
GGA	generalized gradient approximation
PW	Perdew and Wang
LYP	Lee, Yang and Parr
PBE	Perdew, Burke and Ernzerhof
TS	transition state
COSMO	conductor-like screening model
QM	quantum mechanical
PCM	polarizable continuum model
NBO	natural bond orbital
HOMO	highest occupied molecular orbitals
LUMO	lowest unoccupied molecular orbitals
MO	molecular orbital
FLP	frustrated Lewis pair

List of Publications

(1) **Amrita Pal** and Kumar Vanka, A DFT investigation of the potential of porous cages for the catalysis of ammonia borane dehydrogenation, *Chem. Commun*., 2011, 47, 11417-11419.

(Featured in inside back cover of the journal)

(2) **Amrita Pal** and Kumar Vanka, Proposing late transition metal complexes as frustrated Lewis pairs – a computational investigation, *Dalton Trans*., 2013, 42, 13866-13873.

(3) **Amrita Pal** and Kumar Vanka, Exploring the effectiveness of different Lewis pair combinations in caged structures for the catalysis of ammonia borane dehydrogenation: a DFT study, *Phys. Chem. Chem. Phys*., 2013, 15, 20857-20867.

(4). **Amrita Pal** and Kumar Vanka, Can Silylenes Rival Transition Metal Systems in Bond-Strengthening Pi-Back Donation? A Computational Investigation, *Chem. Commun*., 2014, 50, 8522-8525.

(5) **Amrita Pal** and Kumar Vanka, Small molecule activation by Constrained Phosphorus Compounds: Insights from Theory, *Inorg. Chem*., 2016, 55, 558–565.

Chapter 1

Introduction to Small Molecule Activation

1.1 Introduction

Environmental problems have become a very significant issue today because of the continuous and ever increasing burning of non-renewable fossil fuel resources over several decades. This has led to the generation of large amounts of greenhouse gases such as CO_2 and other pollutants. This has spurred the search for new, greener fuels for energy generation and their use in on-board applications such as transportation. Furthermore, this has also led to strategies to convert the harmful gases into an environmentally benign form. The chemistry community holds enormous responsibility for developing clean and green energy alternatives for the global community. In this regard, hydrogen has attracted much attention in recent years for being potentially the cleanest of fuels, as it emits only water as the by-product. However, the key roadblock towards using hydrogen as a fuel is its storage, and the lack of effective and realistic methods for its extensive use, as it is almost non-compressable and highly flammable. Thus, the current worldwide goal is to implement safe and practical methods for the on-board storage of hydrogen. Several groups have investigated diverse approaches in the past decade to make hydrogen an effective fuel source, including the problem of its storage[1-6]. One potential solution to this problem is to use a compound that can chemically store hydrogen so that one can easily produce hydrogen from the compound *via* a reversible chemical reaction[7-9]. In this regard, ammonia borane (AB) is one of the promising candidates for the chemical storage of hydrogen, as it contains 19.6 weight % of hydrogen[10-12]. Furthermore, it is a solid species as well as moisture stable at ambient temperatures, which is an important aspect for the ease of storage and transportation.

Another important issue is the chemical conversion of several important small molecules such as H_2O, CH_4, CO_2, CO, N_2 and O_2 - molecules that have profound biological and industrial relevance. For example, methanol production by the activation of CO, CO_2 and CH_4 helps to reduce the greenhouse gases[13-19]4. The splitting of water is also an important reaction that generates O_2 and H_25[20-26]. All these processes need efficient catalysts for the overall conversion, which has promoted the search for catalysts that can effectively activate important small molecules.

1.2 Transition Metal Based Systems

Several transition metal complexes are known to successfully catalyze the dehydrogenation reaction of ammonia borane[7, 9, 27-34] and activate small molecules[35-45]. In general, three types of strategic approaches have been employed in transition metal systems: 1) single site catalysts[31, 46-50], where only the central transition metal is involved in the chemical transformation of the substrate (see Figure 1, Ia); 2) metal-ligand cooperativity, where the central metal atom can cooperate with the attached ligands to facilitate the reaction[24, 32, 51-56](see Figure 1, IIa); 3) metal-metal cooperativity[57-62], where two or more metal atoms can interact in the same or different complexes in order to catalyze the chemical reactions. In this chapter, only the first two types of reactivity in transition metal complexes will be discussed for several chemical conversions and small molecule activations.

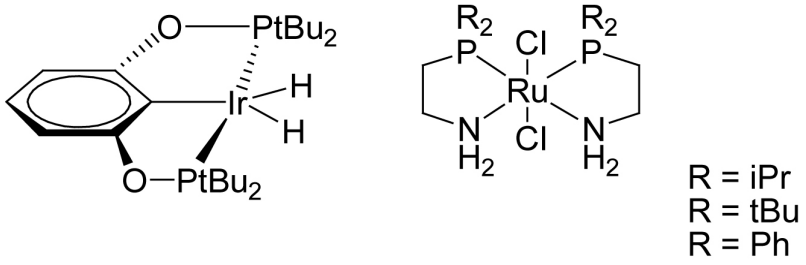

Ia IIa

Figure 1. The different strategies in transition metal systems for small molecule activation.

1.2.1 Single Site Activation by the Transition Metal Complexes

Ammonia borane (AB) and related amine boranes are species that are isoelectronic with alkanes. As a result, the previously known efficient homogeneous catalysts for alkane dehydrogenation can be thought to also be applicable for the AB dehydrogenation reaction. In this regard, Goldberg and coworkers have synthesized the iridium based pincer complex (POCOP)Ir(H)$_2$ (POCOP = [η^3-1,3-(OP^{t}Bu$_2$)$_2$C$_6$H$_3$]), which is an active single site catalyst for the AB dehydrogenation reaction[31]. When the catalyst is employed in an inert environment to a THF solution of ammonia borane, vigorous evolution of

hydrogen is observed. Within 14 minutes, the quantitative conversion of AB with the release of one equivalent of dihydrogen is observed with respect to an initial AB concentration of 0.5 M and a catalyst loading of 0.5 mol%. After complete AB consumption, a dehydrogenated product (white precipitate) is formed that resembled the data reported for the cyclic pentamer having the formula $[H_2NBH_2]_5$[31]. The fast rates of the dehydrogenation reaction and the rapid catalyst regeneration have overcome the formation of the dormant species by the reaction of BH_3 with the iridium pincer complex. In addition, Manners *et al.* have reported a rhodium catalyst $[Rh(COD)(Cl)]_2$ (COD = 1,5 cyclooctadiene) for the dehydrogenation of a number of amine boranes at ambient temperature[63]. Later, they have extended the idea and showed that the same catalyst could dehydrogenate the amine boranes and ammonia borane to form borazine and other spent fuel[64, 65]. However, they have also showed that the heterogeneous rhodium cluster of 2 nm size was responsible for the catalysis process[66]. Thus, the iridium pincer system is a very important report of homogeneous transition metal catalysts for the AB dehydrogenation reactions.

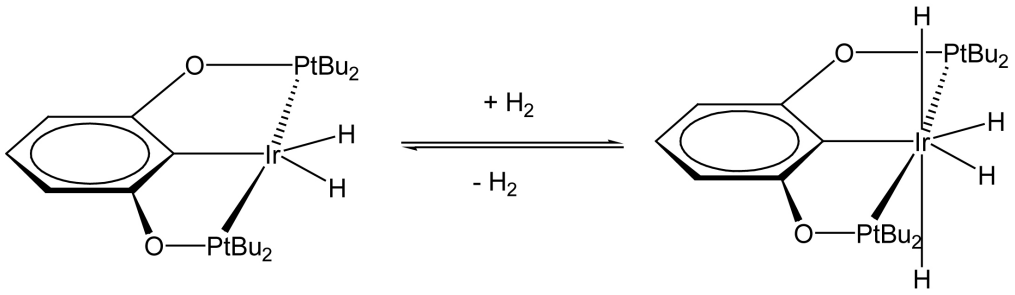

Figure 2. The dehydrogenation of AB by the iridium pincer complex.

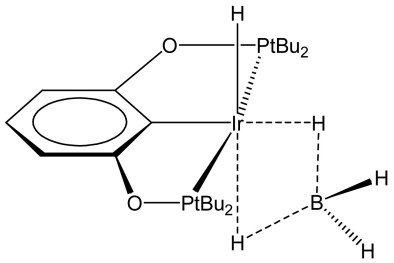

Figure 3. The structure of the dormant species that formed by the reaction of free BH_3 with the iridium pincer complex.

Another study has focused on the development of cationic Pd(II) complexes for the dehydrogenation reaction of AB[30]. They have investigated a series of palladium complexes such as [Pd(allyl)][BF_4], [Pd(allyl)(2,4-hexadiene)][BF_4] and [$Pd(MeCN)_4$][BF_4]$_2$. The catalysts show excellent dehydrogenation kinetics for the dehydrogenation reaction of ammonia borane. The [Pd(allyl)][BF_4] shows the best performance among them to release 2 equivalent of H_2 in 20 s. On the other hand, complex [$Pd(MeCN)_4$][BF_4]$_2$ is used to release H_2 from AB and alkylated amine boranes. However, the dehydrogenation product precipitated with the Pd, and did not catalyze the dehydrogenation of a second batch of AB due to the heterogeneity for this case. Interestingly, the amount of H_2 released depends on the number of hydrogen atoms at the boron center, as the spent fuels contain no B-H bond. They have computationally proposed the possible mechanism for this process, where they have demonstrated that the α-agostic interaction is responsible for the binding between the palladium atom and the hydrogen attached to the boron of AB. The direct evidence supports the fact that the boron-hydrogen bond that forms the agostic interaction is nearly 0.2 Å longer than the B-H bond in free AB. Also, one of the isocyanide (MeCN) ligands is replaced by the AB molecule that forms a hydrogen bond with a protic hydrogen atom of NH_3BH_3. Thus, the palladium complexed with AB is 30.2 kcal/mol exothermic in comparison to the separated species. The hydridic hydrogen then transfers to the palladium atom and forms the hydrogen molecule by the interaction with the second hydrogen attached to the boron of AB. The explanation of the hydrogen transfer to the palladium center has been given by the natural charge and molecular orbital analysis. The feasibility of both the electron transfer from the filled B-H bonding orbital to the empty metal orbital and the filled metal orbital to the empty antibonding B-H orbital is primarily responsible for the weakening of the B-H bond. Thus, the proton transfers to the palladium center and hydrogen forms in the next step. The overall cycle was found to be a barrierless process.

$$n\,H_3B{-}NH_3 \xrightarrow{\text{Pd (II) catalysts}} 2n\,H_2 + (BNH_x)_n$$

Figure 4. The dehydrogenation reaction by the palladium catalysts.

1.2.2 Activation by the Transition Metal-Ligand Cooperativity

In the aforementioned section, we have discussed some typical examples related to the small molecule activation by single site transition metal catalysts. In this section, we will discuss the metal–ligand cooperativity in various transition metal systems. Noyori *et al.* have first introduced the concept of cooperativity between the amino ligands and the transition metals in bifunctional catalysts for the reactions of hydrogenation and transfer hydrogenation (TH) of polar double bonds[67-69]. Similarly, Schneider and coworkers have reported that the ruthenium (II) compound bearing the PNP ligand undergoes reversible hydrogenation-dehydrogenation reactions[32]. They have also demonstrated a Noyori–Morris-type[70] concerted mechanism where the hydride and a proton of AB transfer from the AB to the catalyst. The amido chelate ligand cooperates by using its backbone nitrogen that is connected with the alkene of the ligand system (see Figure 5a). The alkene of the ligand system can also take part in the hydrogenation reaction *via* a reversible reaction with hydrogen. The active catalyst has been employed in the THF solution, and Schneider *et al.* have demonstrated that it can spontaneously evolve hydrogen from AB at room temperature. They have also checked that the high catalytic activity also remains unaltered with a small catalytic loading. Thus, under mild conditions, the amido complex shows excellent activity and high turnover numbers for the AB dehydrogenation reaction. DFT calculations show that the enamido complex is a distorted square-pyramidal structure while the amido complex is trigonal-bipyramidal with a Y-shaped distortion (see Figure 5a). Such a distortion indicates that the π interaction between the nitrogen of the enamido ligand and the ruthenium metal is very weak, whereas the electron lone pair of the nitrogen is delocalized into the vinylene group, which also supports the experimental structure of the compounds.

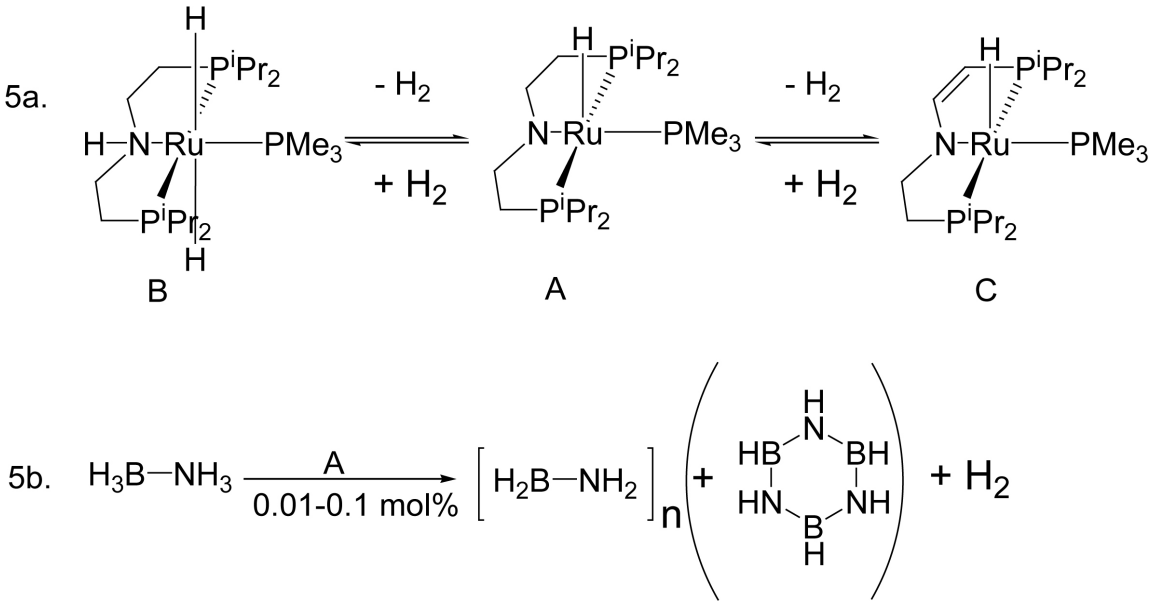

Figure 5. a) The equilibria for the hydrogenation-dehydrogenation reaction by the ruthenium complexes; b) the dehydrogenation reaction of AB.

Baker *et al.* have demonstrated the first example of a long-lived, Ni-NHC complex that dehydrogenates ammonia borane (AB) and releases hydrogen to an exceptional extent[7] (2.5 equiv). They have explored the use of NHC as an alternative to phosphines in order to avoid the decomposition problem and synthesized an active catalyst *in situ* by the reaction between $Ni(cod)_2$ and 2 equiv of NHC, which immediately evolved H_2 by AB addition at 60˚C.

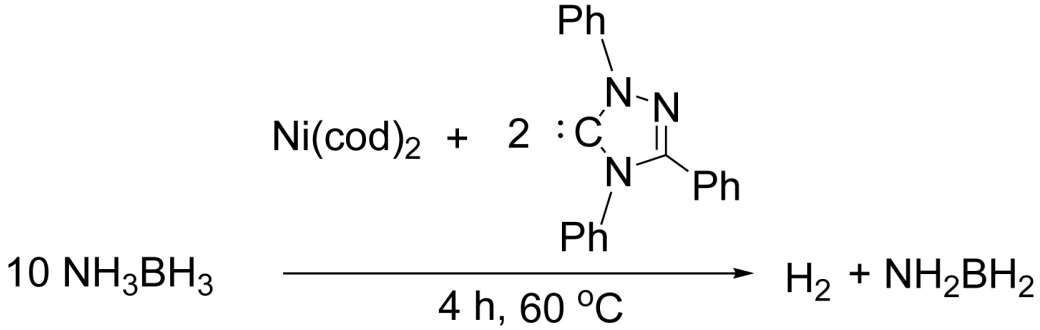

Figure 6. The dehydrogenation reaction of AB by the nickel-NHC complex.

In another account, Manners *et al.*[71] have synthesized titanium metallocene catalysts for dehydrogenating Me_2HNBH_3 to form the cyclic dimer $(Me_2NBH_2)_2$. They have also explored the Wilkinson's catalyst, $RhCl(PPh_3)_3$[72, 73] for the same reaction, where the dehydrogenation process took 19 hrs to complete[74]. Later, they have reported rhodium and iridium analogues of Wilkinson's catalyst connected by the secondary phosphine $PHCy_2$ (Cy = cyclohexyl) ligand. Those complexes are not effective for the AB dehydrogenation; however with various amine and phosphine boranes, they exhibit different rates of hydrogen loss. They have also demonstrated that the rate of dehydrogenation is commonly enhanced by the addition of $B(C_6F_5)_3$ as a co-catalyst.

Fagnou and coworkers have demonstrated that the ruthenium catalyst, which was initially developed for alcohol redox processes[68, 70, 75-77], released 1 equiv of H_2 from AB within 5 min at room temperature when only a small concentration of the ruthenium complex was employed[28]. Interestingly, a higher concentration of MeAB rapidly liberated 2 equivalents of H_2 at 22 °C. Moreover, they have also shown that the evolution of hydrogen increases by introducing an AB/MeAB mixture at 50 °C with small catalytic loading. The precatalysts are activated through the treatment with KO^tBu in THF under inert atmosphere to produce the active ruthenium amide species, which reacts with AB in the reaction vessel. It is to be noted here that the insoluble precipitate of a polymeric aminoborane species has been found in these cases as well. Interestingly, no insoluble precipitate was observed for the dehydrogenation reaction of methyl ammonia borane (MeAB) even with highly concentrated conditions (11 M [MeAB]). In addition to that, the hydrogenated intermediate can easily hydrogenate the carbon-oxygen and carbon-nitrogen double bonds. The DFT calculations indicate that the ruthenium cooperates with the nitrogen atom of the ligand and thus dehydrogenates AB.

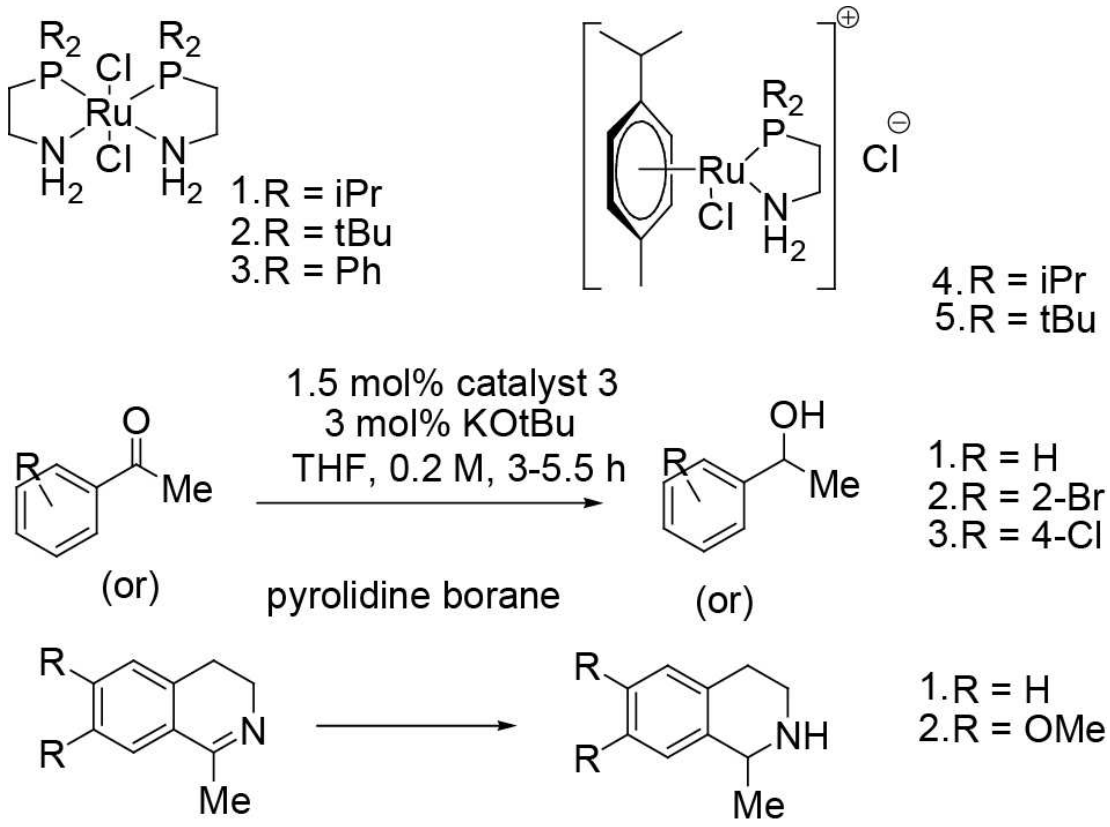

Figure 7. The ruthenium catalysts for the dehydrogenation reaction of ammonia borane and the hydrogenation of carbon-oxygen and carbon-carbon double bonds.

1.3 Activation of Metal Free Main Group Systems

Although the reactivity of the transition metal complexes towards the homogeneous catalytic dehydrogenation of AB and other small molecule activations are found to show promising activities, the metal free greener systems are also necessary for large scale productions as the transition metals are non-renewable, expensive and toxic. Therefore, metal free catalysis may be the only cost effective and environmentally benign route to the dehydrogenations of AB and related amine boranes, as well as other small molecule activations. In this regard, the carbene[78-81], silylene[82-86] and higher analogues[87-91] are important as they effectively imitate the single site reactivity of the transition metal complexes. The novel concept of frustrated Lewis pairs[92-96] developed by Douglas Stephan and coworkers has expanded the field of cooperativity in main group chemistry. In the following sections, we will be discussing the reactivity of such main group systems

for different types of small molecule activation. Very recently, phosphorus based planner[97, 98], distorted planner[99] and pyramidal[100] systems have also gained significant attention for their important role in small molecule activation reactions.

1.3.1 Carbenes

Since their discovery in 1950, carbenes have played an extraordinary role in the vast area of both organic and organometallic chemistry. The carbon atom in carbenes is divalent with six valence electrons, among which two are nonbonding, with either paired (singlet) or unpaired (triplet) configurations. The singlet carbenes are nucleophilic as well as electrophilic in nature because of the presence of a vacant orbital and a lone pair of electrons, whereas the triplet carbenes resemble radicals in terms of reactivity.

For quite some time, carbenes were thought to be the reactive intermediate in various chemical processes. However, the discovery and the enormous applications of stable carbenes as an exceptional ligand in organic synthesis and catalysis, as well as in organometallic reactions, have led to the classification of carbenes as a separate class of compounds[79, 101-103]. The N-heterocyclic carbenes (NHCs) are the new set of carbenes where the carbon atom of the NHC is flanked by two nitrogen atoms that are attached by a ring system[104-115]. Several research groups, such as those of Wanzlick [116-118], Arduengo [79, 101, 119], Enders [81, 103, 108] and others[80, 102, 120] have contributed to the understanding of the stability and reactivity of carbenes and N-heterocyclic carbene (NHC) complexes[78, 105-107, 109, 111-115]. Bertrand and coworkers have reported the splitting of hydrogen and ammonia by carbenes[121], a reaction that had been previously in the domain of transition metal systems.

1.3.2 Silylenes

After carbon, silicon is the next most abundant element in the earth's crust, and exists mostly in the form of silica and silicates. Its elemental form is non-toxic and exhibits semi-metal character. This has led to its utilization as the basic material for energy storage and information technologies. In addition, organosilicon compounds have been known for their biocompatibility and are widely used in cosmetic and food industries. Thus, the chemical usefulness of the silicon compounds can be further tuned to expand

the horizons of sustainable technologies. For example, the rational design of subvalent silicon compounds could be useful for developing similar or higher activity in comparison to expensive transition metal catalysts for the small molecule activation processes[83, 84, 122-126]. However, such silylene (R_2Si:) species exist mostly under cryogenic conditions and are short-lived and very reactive. In 1994, West and coworker reported the first example of a stable N-heterocyclic silylene (NHSi) under ambient temperatures having sterically hindered substituents at the nitrogen ends[127]. Later, Kira and co-workers synthesized the first cyclic silylene system by the reaction of dibromo silane with potassium graphite[85]. The electronic stability of such NHSi systems is presumed to be because of the π-lone pair donation from the nitrogen atoms to the empty 3p orbital of the silicon. Interestingly, although such silylenes are monomeric in dilute solution, some of them exhibit oligomerization in the concentrated state. Enormous synthetic progresses have been performed on the stability of silylene compounds and their potential for the activation of important small molecules such as O_2[124, 126], CO_2[128, 129] and H_2O[125, 130].

Several research groups have shown interest towards the structure and reactivity of silylene compounds[86, 122, 123, 131-138]. For example, in 2006, Matthias Driess and coworkers introduced the modified β-diketiminate ligand for the synthesis of stable N-heterocyclic silylenes[88, 139]. They have described that the exocyclic methylene group can cooperate with both the lone pair and the empty 3p orbital of the silicon center, which enables the silylenes to behave in a particularly reactive manner towards electrophiles as well as nucleophiles. For example, the reaction between H_2O and the silylene leads to the formation of a mixed-valent siloxy silylene that activates the small molecules such as N_2O and CO_2 to generate the corresponding silanoic silyl esters[136, 139]. The NHSi also exhibits excellent propensity for C-H[131, 133, 135] and N-H[135, 136] bond activation, for example, when dry NH_3 and NH_2NH_2 are passed over NHSi a 1,1 insertion reaction at the N-H center takes place[136]. A similar reaction happens when PH_3 and AsH_3 are employed. However, for the AsH_3 case, a tautomerism is observed. In the same year, the group of Roesky has reported the amidinate backbone stabilized NHSi, which has an interesting terminal Si(II)-Cl bond[123]. The bis-NHSi is also emerged as prospective candidates with a Si(I)-Si(I) bond that exhibits interesting chemistry in small-molecule activation[132]. In

2013, Kato *et al.* have explored the unique reactivity of cyclic silylene by using a silacyclopropylidene that is stabilized by the coordinating base[140]. The silylene generates sila-β-lactone upon reaction with dioxygen, which further reacts with the protic solvent ethanol to afford silanoic acid, an unprecedented analogue of carboxylic acid. Further DFT calculations pinpoint the role of the backbone for stabilizing the silanoic acid without modifying its acidity.

In this regard, Simon Aldridge's group has reported the first two-coordinate acyclic silylenes, Si{B(NDippCH)$_2$}{N-(SiMe$_3$)Dipp} by using strong σ-donors and a highly sterically crowded B(NDippCH)$_2$ group where Dipp = 2,6-^{i}Pr$_2$C$_6$H$_3$. Such species exhibit high thermal stability in the solid state (up to 130 °C)[141]39. The acylic silylene species display high reactivity with a low singlet−triplet gap (103.9 kJ mol−1) and undergo oxidative addition reactions in the presence of dihydrogen at lower temperatures. Interestingly, intramolecular activation of one of the methine C−H bonds of the Dipp substituents by the silylene compound efficiently mimics the ortho metalation reaction of the transition metal systems. Rekken and coworkers have synthesized another stable silylene complex Si{S(C$_6$H$_3$-2,6(C$_6$H$_2$-2,4,6-Me$_3$)$_2$)}$_2$ that is attached to two sulphur groups[138]. However, it does not activate the hydrogen molecule. A few examples of other acyclic silylenes are also known in the literature[25, 135, 142-144].

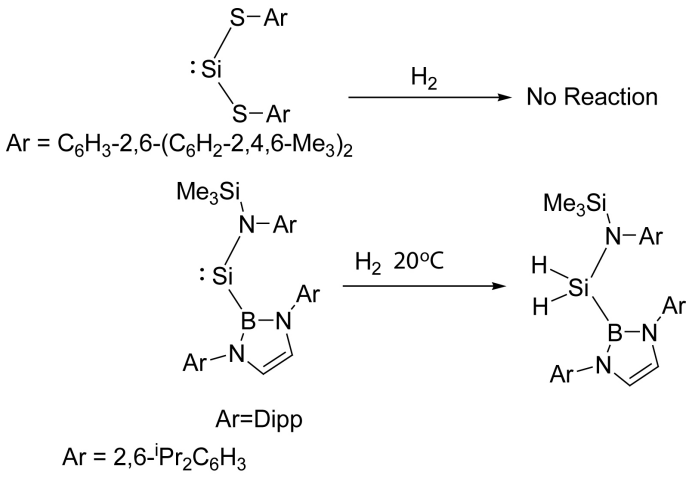

Figure 8. The examples of acyclic silylene systems with different reactivity towards the hydrogen activation reaction.

1.3.3 Frustrated Lewis Pairs

In 1923 G. N. Lewis described Lewis acids and bases as a class of compounds that can accept and donate an electron lone pair to and from another molecule respectively to make a stable adduct[145]. The molecular orbital analysis shows that Lewis acids have lowest unoccupied molecular orbitals (LUMOs) that can accept the lone electron-pair from the highest occupied molecular orbital (HOMO) of the Lewis bases. As a result, the interactions between the HOMO of one molecule and the LUMO of the other are used to rationalize various reactions of Lewis acids and bases.

In the late 2000s, Douglas Stephan and co-workers demonstrated that the classical Lewis adduct formation can be precluded by introducing the steric hindrance between the Lewis acid and the Lewis base[95]. Thus, these pairs are known as frustrated Lewis pairs (FLPs). They have reported the phosphino-borane species $(C_6H_2Me_3)_2P(C_6F_4)B(C_6F_5)_2$ where the electron donating phosphorus atom and the electron deficient boron atom are separated by the phenyl ring. This is the very first example of FLP systems that can rapidly split the hydrogen molecule and form a zwitterionic species where the protic hydrogen is attached to the phosphorus atom and the hydridic hydrogen is bonded with the electron deficient Lewis acidic boron atom (as shown in Figure 9). The zwitterionic species is air and moisture stable to a fair degree even under ambient conditions. However, above 150 °C, it stoichiometrically looses hydrogen. Thus, the remarkable concept of metal free systems for the activation of hydrogen molecule has opened up a whole new research area based on the main group elements.

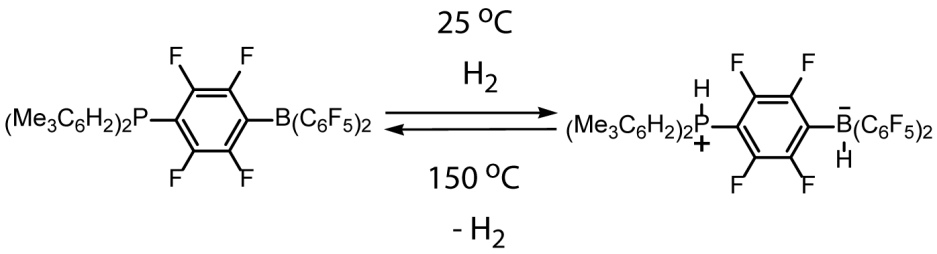

Figure 9. The first example of hydrogen activation by the frustrated Lewis pairs.

As discussed above, the idea of FLP has generated novel and potential strategies towards reactivity and catalysis[93, 94, 96, 146-154]. The wide applicability of such a concept has been observed for a range of various sterically precluded combinations between the electron donating groups (containing N, P as the electron donor atom)[94, 96, 106, 148-153] and the electron deficient groups (containing B, Al as the electron acceptor atom)[94, 96, 147, 151, 152, 155-158].

1.3.4 Varieties of Frustrated Lewis Pair (FLP) Systems

According to the structure and the nature of the interaction between the Lewis acidic and basic components, the FLPs can be classified into two parts:

1) The intramolecular FLP[92, 155, 159], where the acidic and basic sites are incorporated in the same molecule, i.e., one molecule has both the charged fragments.

2) The intermolecular FLP[93, 147, 160, 161], where both the acidic and the basic sites are part of different molecules, which are sterically separated from each other. Shown in Figure 10A below is an example of an intramolecular FLP and shown in Figure 10B is the example of an intermolecular type of FLP.

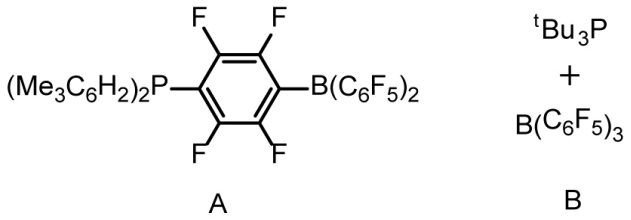

Figure 10. A. The example of an intramolecular FLP; B. the example of an intermolecular FLP.

1.3.4.1 Phosphorus-Boron FLPs

The Phosphorus-boron FLPs are one of the most widely studied systems in the area of FLPs, where the phosphine and the borane systems are separated by conjugated aromatic or aliphatic[159] moieties. Stephan and coworkers have demonstrated that the intermolecular type of phosphine borane where the Lewis basic phosphine [P(^{t}Bu)$_3$,

$P(C_6H_2Me_3)_3]$ and Lewis acidic borane $B(C_6F_5)_3]$ are separated due to the steric congestion can also be very effective for the heterolytic cleavage of the hydrogen molecule[96]. The successful combination of $tBu_2P(C{\equiv}CCH_3)$ as the phosphine and $HB(C_6F_5)_2$ as the borane unit - the "Piers borane", is another example of phosphorus-boron FLPs. The FLP is formed by the hydroboration reaction of the phosphine and the borane[96]. However, the system is inactive towards dihydrogen activation under ambient conditions. This arguably indicates that the reactivity of such systems is low. However, the dihydrogen splitting is achievable at a much higher pressure (60 bar), which generates the zwitterions where the phosphonium cation is next to the hydridoborate anion separated by conjugated species. However, increasing the bulk around the reactive centers ($(C_6H_2Me_3)_2PC{\equiv}CPh$) and subsequent formation of FLPs with the "Piers borane" would lead to complete inactivation of the species towards dihydrogen activation[96]. The activity can be restored by adding any reactive conjugated phosphonium hydridoborate in a catalytic amount (10%) which would accelerate rapid proton and hydride transfer through dihydrogen splitting to generate the hydrogenated species in a near quantitative yield[96].

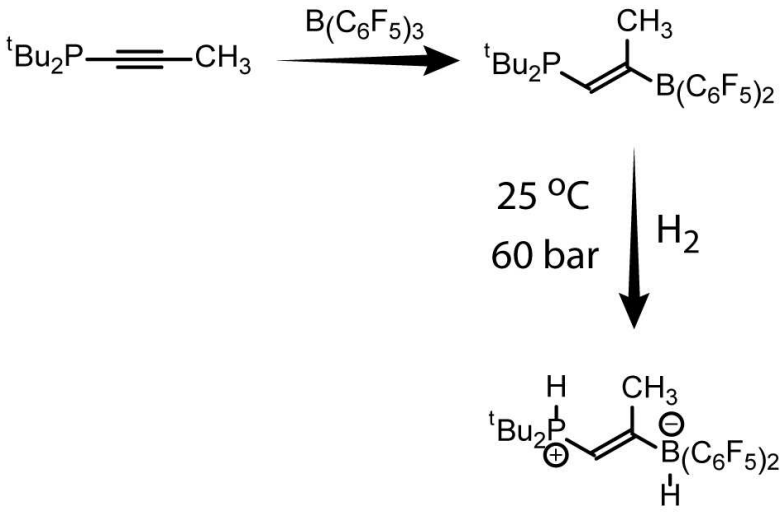

Figure 11. The reaction of the alkyne phosphine with borane and the hydrogenation product.

In addition to the aforementioned systems, an intermolecular type of FLP has been synthesized by combining 1-8-bis(diphenylphosphino)-naphthalene and $B(C_6F_5)_3$ in an equimolar ratio[162]. This system exhibits characteristic Lewis acid base pair separation and can also perform dihydrogen activation through the formation of an asymmetric zwitterionic species.

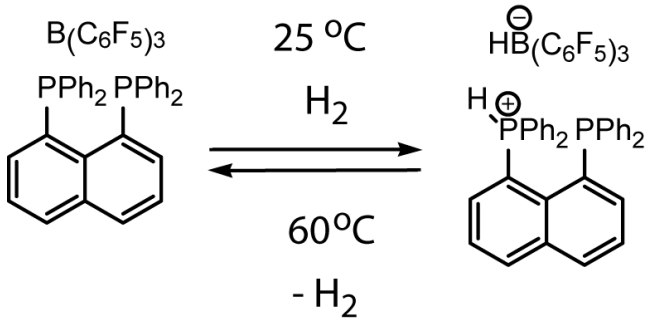

Figure 12. The hydrogen activation by the phosphino-naphthalene and borane FLP.

Another example of a phosphorus based frustrated Lewis pair is the family of the phosphino-metallocene based compounds that have also emerged as an interesting class of sterically hindered Lewis pairs[163]. For example, the reaction of the mono(phosphino)ferrocene $[(C_5H_4P^tBu_2)Fe(C_5H_5)]$ with $(C_6F_5)_3B$ forms an FLP that can conveniently activate H_2[163]. Dimeric phosphido-borane FLPs have been synthesized by reacting secondary lithium phosphides with $(C_6F_5)_2BCl$[164]. This interesting intermolecular FLP has bulky substituents such as Cy and ^{t}Bu and is capable of activating H_2[164]. There are several examples of other phosphorus base FLPs in the literature, which have showed the unique reactivity towards the small molecule activation reactions[165-168].

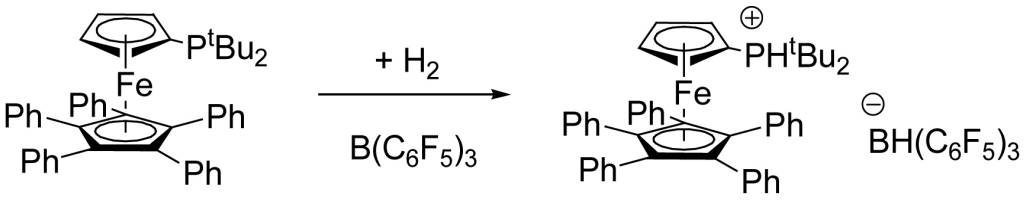

Figure 13. The hydrogen activation by the phosphino-metallocene and borane FLP.

The phosphorus boron FLPs are readily accessible for the dehydrogenation and the transfer hydrogenation reaction. Stephan and coworkers have demonstrated the reduction of imines, nitriles, and aziridines by the phosphorus boron based FLPs[148]. The first step of the reaction is the formation of the zwitterionic species by the heterolytic cleavage of hydrogen. Then, the salt is stoichiometrically treated with the respective aldimines to form the desired amine adducts by the protonation of the imine centre (Figure 14). The next step is the borohydride transfer to the carbon of the iminium intermediate comleting the reduction. A similar catalytically reductive ring opening reaction of the N-aryl aziridine to produce the corresponding amine can also be achieved under mild reaction conditions. A similar reduction mechanism for nitriles gives the corresponding amine-$B(C_6F_5)_3$ products in excellent yields using a phosphonium-borate catalyst. However, a slightly higher temperature or pressure of H_2 or higher concentration of the catalysts is required for the reduction of the bulky electron withdrawing imines and nitriles. In a similar manner, the activation of a variety of aldehydes can also be achieved[148]. Furthermore, the findings showcase the novel chemical root to the main group alternatives of metal systems that are important for both the academic as well as industrial processes. The reduction process is catalytic in nature for the metal free systems that replace the stoichiometric behaviour for the metal systems. Moreover, it largely reduces the waste production cost.

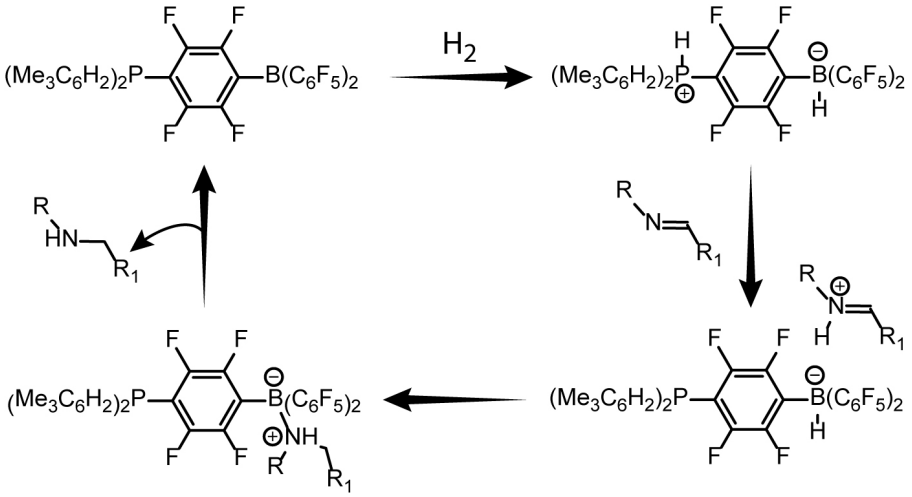

Figure 14. The cycle for the hydrogen activation and simultaneous hydrogenation of imine by FLP.

1.3.4.2 Nitrogen-Boron FLPs

The rational replacement of the phosphorus atom in FLP by the nitrogen atom as the donor group has extended the field of main group catalysis[169-171]. The reaction between imines and $B(C_6F_5)_3$ produces the amine-borane in the presence of dihydrogen (Figure 15), which implies the temporary formation of a hydrogenated zwitterionic species - the iminium hydridoborate intermediate, followed by the hydride transfer to the iminium carbon atom to form the amine[146]. This adduct affords the heretolytic cleavage of H_2 upon heating at 80 °C for 1 h under H_2 atmosphere and a high pressure of 4–5 atmospheres (Figure 15).

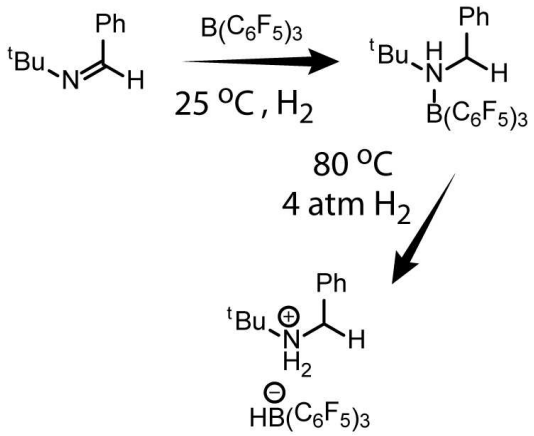

Figure 15. The reduction of imine by borene and hydrogen to form a FLP.

Similar to the phosphino-metallocene, Erker and co-workers have shown that an aminomethyl-substituted zirconocene can be treated as a Lewis base in a frustrated amine-$B(C_6F_5)_3$ complex and can activate more than one equivalent of H_2 under ambient conditions[172]. Another example of nitrogen-boron FLPs is the lutidine and $B(C_6F_5)_3$ combination. It is well known that the lutidine does not make any Lewis acid-base adduct with $B(C_6F_5)_3$[160]. Stephan's group has managed to make a lutidine-boron combination that can act as an intermolecular FLP. Also, the treatment of the lutidine-$B(C_6F_5)_3$ adduct with THF was found to yield a zwitterionic species (Figure 16)[160].

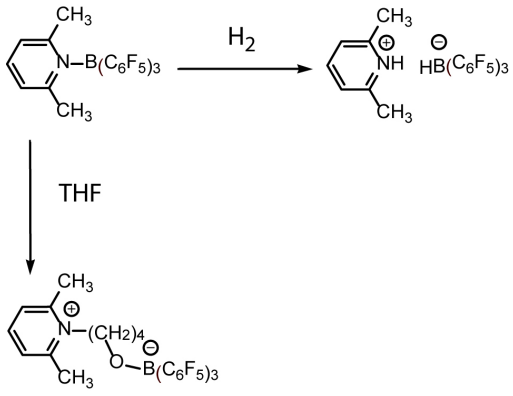

Figure 16. The reaction of lutidine and boranes with hydrogen and THF.

1.3.4.3 Nitrogen-Phosphorus FLPs

Stephan's group has synthesized an amidophosphorane ($Ph_2PF(o\text{-}C_6H_4NMe)$ where the phosphorus was seen to have a distorted trigonal bipyramidal geometry, which is constrained within the four-membered ring (Figure 17)[150]. As shown below, here the phosphorus, being less electronegative than the nitrogen, acts as an acid, while the Lewis base is the nitrogen counterpart for the FLP.

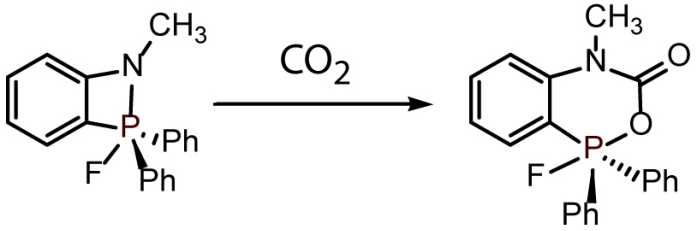

Figure 17. The reaction of amino phosphine FLP with CO_2.

1.3.4.4 Carbon-Boron FLPs

The N-heterocyclic carbenes (NHCs) do not react with H_2 under ambient conditions[121]. However, the monoaminocarbene is capable of heterolytically breaking the H-H and N-H bond of H_2 and NH_3 respectively[121]. The moderately bulky N-heterocyclic carbenes form a conventional Lewis acid-base adduct with $B(C_6F_5)_3$ [147, 161, 173]. Tamm and co-workers have shown that the more sterically congested NHC backbone facilitates the formation of a frustrated Lewis pair that conveniently generates the imidazolium

hydridoborate zwitterion upon H_2 exposure (Figure 18)[161]. Such a system can also afford the ring opening reaction of THF (Figure 18).

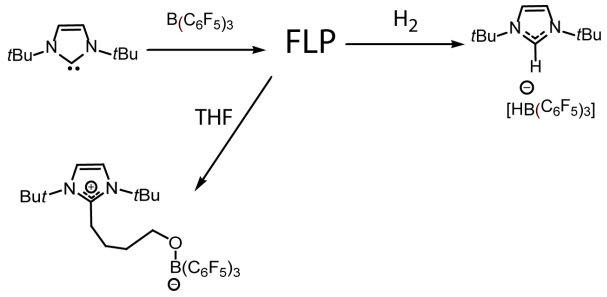

Figure 18. The H_2 and the THF activation reactions by carbene and borane FLP.

1.3.5 Catalytic Dehydrogenation of Ammonia Borane by FLPs

The frustrated Lewis pairs can also dehydrogenate the ammonia borane (AB)[155, 158, 174]. Bercaw and coworkers have reported the dehydrogenation reaction of AB with the bulky tertiary phosphine-borane Lewis pairs $P^tBu_3/B(C_6F_5)_3$ at 25^oC[175]. They have also shown that the FLPs are effective as catalysts for the dehydrogenation of AB as well as of relative amine boranes. It is to be noted here that at high temperatures, the $B(C_6F_5)_3$ itself can dehydrogenate AB but in the presence of the bulky phosphine, the reactions become highly feasible at nearly room temperature. Moreover, $B(C_6F_5)_3$ does not react with Me_2NHBH_3 even at elevated temperatures. Thus, the formation of the bulky phosphine-borane FLP is essential for the dehydrogenation reactions of AB and Me_2NHBH_3. Similarly, the Al-phosphine pair has been employed by Uhl and coworkers for the same dehydrogenation reaction, where they have shown that the reaction of free ammonia and the free borane BH_3 with FLP readily forms adducts with FLP[155]. However, the treatment of FLP with AB does not form any adduct - it effectively dehydrogenates AB at room temperature. They have also demonstrated by DFT calculations that the N-H bond in AB is first activated, followed by the hydride transfer to form the hydrogen molecule.

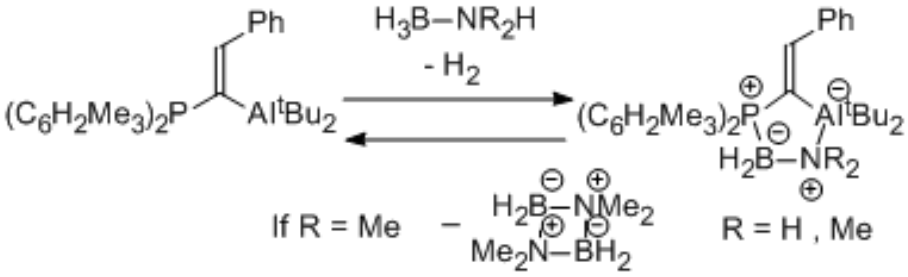

Figure 19. The dehydrogenation of ammonia borane by FLP.

1.3.6 Activation of CO_2 by FLPs:

The development of new processes for the activation of CO_2 is increasingly drawing attention. There are a large number of reactions reported for the activation of CO_2 with both the metal based or main group reagents[16, 19, 37, 39, 128, 129, 150, 157, 176, 177]. Similarly, CO_2 also reacts with frustrated Lewis pairs. For example, the reaction of CO_2 with the $^tBu_3P$-$B(C_6F_5)_3$ pair forms two new P–C and O–B bonds at room temperature[153] 65. Upon heating to 70 °C, the CO_2 evolves, which suggests that the CO_2 addition reaction to FLP is reversible. Similar to the intermolecular frustrated Lewis pair, the intramolecular FLP also reacts with CO_2 (2 bar), which results in the formation of the stoichiometric FLP-CO_2 adduct[153]. Besides the stoichiometric activation of CO_2, there are other examples reported for the catalytic activations of CO_2. The research groups of O'Hare and Ashley have demonstrated the first example of such catalytic processes[176]. They have described that the reaction of CO_2 and H_2 with the tetramethylpiperidine (TMP)/$B(C_6F_5)_3$ FLP reduces CO_2 catalytically.

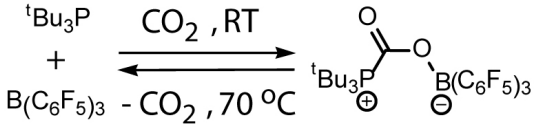

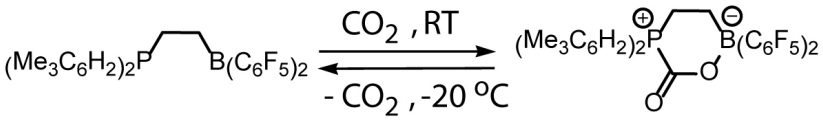

Figure 20. The activation of CO_2 by the FLPs.

1.3.7 Metal Based FLPs

The concepts of frustrated Lewis pairs have also expanded into the metal based systems, where the metal and the main group ligand cooperate to mimic the role of FLPs. There are several examples of such metal based systems for various small molecule activation reactions[178-181]. For example, Wass and coworkers have synthesized the zirconium based FLP to dehydrogenate AB and activation of other small molecules[182, 183]. Stephan and coworkers have synthesized another late transition metal based FLP system, which also activates CO_2 in presence of excess boranes[177]. Thus, the metal based FLPs also serve as effective catalysts for small molecule activations.

1.4 Conclusion

In this chapter, at first we have discussed the key problems of hydrogen storage and their possible solutions, focusing mainly in terms of ammonia borane dehydrogenation reactions. In this regard, we have elaborated the role of traditional single site metal catalysts and the metal-ligand cooperativity in different ammonia borane dehydrogenation pathways. Later, diverse metal free systems have emerged as greener alternatives towards toxic and costly metal catalysts. We have pinpointed their advantages and role in important activation reactions. The main group systems such as carbenes and N-heterocyclic carbenes (NHCs) emerged as very effective catalysts for various organic transformations. On the other hand, silylenes displayed a wide range of reactivity. Although silylenes are thought to be unstable, scientists are able to stabilize them incorporating various functionalities that also add to the tenability of the reactivity of such systems. Last but not the least, the frustrated Lewis pairs (FLPs) are a useful class of main group molecules that can exhibit similar reactivity compared to the metal catalysts due to internal (intramolecular or intermolecular) frustration. Different types of FLPs have been discussed in terms of their structure and reactivity in terms of activating dihydrogen, ammonia borane and other important molecules.

1.5 References

1. P. Jena, *J. Phys. Chem. Lett.*, 2011, 2, 206-211.
2. S. Yuan, D. White, A. Mason, D.-J. Liu, *Int. J. Energ. Res.*, 2013, 37, 732-740.
3. L. Schlapbach, A. Zuttel, *Nature*, 2001, 414, 353-358.
4. G. Li, H. Kobayashi, J. M. Taylor, R. Ikeda, Y. Kubota, K. Kato, M. Takata, T. Yamamoto, S. Toh, S. Matsumura, H. Kitagawa, *Nat. Mater*, 2014, 13, 802-806.
5. M. Schlichtenmayer, M. Hirscher, *J. Mat. Chem.*, 2012, 22, 10134-10143.
6. Y. Xia, Z. Yang, Y. Zhu, *J. Mat. Chem. A*, 2013, 1, 9365-9381.
7. R. J. Keaton, J. M. Blacquiere, R. T. Baker, *J. Am. Chem. Soc.*, 2007, 129, 1844-1845.
8. J. Weitkamp, M. Fritz, S. Ernst, *Int. J. Hydrogen Energ.*, 1995, 20, 967-970.
9. J.-M. Yan, X.-B. Zhang, S. Han, H. Shioyama, Q. Xu, *Angew. Chem. Int. Ed.*, 2008, 47, 2287-2289.
10. A. Staubitz, A. P. M. Robertson, I. Manners, *Chem. Rev.*, 2010, 110, 4079-4124.
11. A. Staubitz, A. P. M. Robertson, M. E. Sloan, I. Manners, *Chem. Rev.*, 2010, 110, 4023-4078.
12. T. B. Marder, *Angew. Chem. Int. Ed.*, 2007, 46, 8116-8118.
13. C.-T. Wu, K. M. K. Yu, F. Liao, N. Young, P. Nellist, A. Dent, A. Kroner, S. C. E. Tsang, *Nat. Commun.*, 2012, 3, 1050.
14. C. Benjamín, C. E. Gigola, N. B. Brignole, *Ind. Eng. Chem. Res.*, 2014, 53, 7103-7112.
15. L. C. Grabow, M. Mavrikakis, *ACS Catal.*, 2011, 1, 365-384.
16. J.-y. Xin, Y.-x. Zhang, S. Zhang, C.-g. Xia, S.-b. Li, *J. Basic Microb.*, 2007, 47, 426-435.
17. H. D. Gesser, N. R. Hunter, C. B. Prakash, *Chem. Rev.*, 1985, 85, 235-244.
18. E. E. Barton, D. M. Rampulla, A. B. Bocarsly, *J. Am. Chem. Soc.*, 2008, 130, 6342-6344.
19. T. Sakakura, J.-C. Choi, H. Yasuda, *Chem. Rev.*, 2007, 107, 2365-2387.
20. S. Y. Reece, J. A. Hamel, K. Sung, T. D. Jarvi, A. J. Esswein, J. J. H. Pijpers, D. G. Nocera, *Science*, 2011, 334, 645-648.
21. H. Kato, K. Asakura, A. Kudo, *J. Am. Chem. Soc.*, 2003, 125, 3082-3089.
22. X. Wang, K. Maeda, A. Thomas, K. Takanabe, G. Xin, J. M. Carlsson, K. Domen, M. Antonietti, *Nat. Mater.*, 2009, 8, 76-80.
23. S. W. Kohl, L. Weiner, L. Schwartsburd, L. Konstantinovski, L. J. W. Shimon, Y. Ben-David, M. A. Iron, D. Milstein, *Science*, 2009, 324, 74-77.
24. D. G. H. Hetterscheid, J. I. van der Vlugt, B. de Bruin, J. N. H. Reek, *Angew. Chem. Int. Ed.*, 2009, 48, 8178-8181.
25. K. Maeda, K. Teramura, D. Lu, T. Takata, N. Saito, Y. Inoue, K. Domen, *Nature*, 2006, 440, 295-295.
26. L. Liao, Q. Zhang, Z. Su, Z. Zhao, Y. Wang, Y. Li, X. Lu, D. Wei, G. Feng, Q. Yu, X. Cai, J. Zhao, Z. Ren, H. Fang, F. Robles-Hernandez, S. Baldelli, J. Bao, *Nat. Nano.*, 2014, 9, 69-73.
27. Z. Li, G. Zhu, G. Lu, S. Qiu, X. Yao, *J. Am. Chem. Soc.*, 2010, 132, 1490-1491.

28. N. Blaquiere, S. Diallo-Garcia, S. I. Gorelsky, D. A. Black, K. Fagnou, *J. Am. Chem. Soc.*, 2008, 130, 14034-14035.
29. B. L. Conley, D. Guess, T. J. Williams, *J. Am. Chem. Soc.*, 2011, 133, 14212-14215.
30. S.-K. Kim, W.-S. Han, T.-J. Kim, T.-Y. Kim, S. W. Nam, M. Mitoraj, Ł. Piekoś, A. Michalak, S.-J. Hwang, S. O. Kang, *J. Am. Chem. Soc.*, 2010, 132, 9954-9955.
31. M. C. Denney, V. Pons, T. J. Hebden, D. M. Heinekey, K. I. Goldberg, *J. Am. Chem. Soc.*, 2006, 128, 12048-12049.
32. B. Askevold, J. T. Nieto, S. Tussupbayev, M. Diefenbach, E. Herdtweck, M. C. Holthausen, S. Schneider, *Nat. Chem.*, 2011, 3, 532-537.
33. W. R. H. Wright, E. R. Berkeley, L. R. Alden, R. T. Baker, L. G. Sneddon, *Chem. Commun.*, 2011, 47, 3177-3179.
34. F. H. Stephens, R. T. Baker, M. H. Matus, D. J. Grant, D. A. Dixon, *Angew. Chem. Int. Ed.*, 2007, 46, 746-749.
35. J. A. Labinger, J. E. Bercaw, *Nature*, 2002, 417, 507-514.
36. A. A. Toutov, W.-B. Liu, K. N. Betz, A. Fedorov, B. M. Stoltz, R. H. Grubbs, *Nature*, 2014, 518, 80-84.
37. M. Cokoja, C. Bruckmeier, B. Rieger, W. A. Herrmann, F. E. Kühn, *Angew. Chem. Int. Ed.*, 2011, 50, 8510-8537.
38. R. Tanaka, M. Yamashita, K. Nozaki, *J. Am. Chem. Soc.*, 2009, 131, 14168-14169.
39. S. Chakraborty, J. Zhang, J. A. Krause, H. Guan, *J. Am. Chem. Soc.*, 2010, 132, 8872-8873.
40. S. Wesselbaum, T. vom Stein, J. Klankermayer, W. Leitner, *Angew. Chem.*, 2012, 124, 7617-7620.
41. B. Su, Z.-C. Cao, Z.-J. Shi, *Acc. Chem. Res.*, 2015, 48, 886-896.
42. G. E. Dobereiner, R. H. Crabtree, *Chem. Rev.*, 2010, 110, 681-703.
43. T. Punniyamurthy, S. Velusamy, J. Iqbal, *Chem. Rev.*, 2005, 105, 2329-2364.
44. GreeleyJ, I. E. L. Stephens, A. S. Bondarenko, T. P. Johansson, H. A. Hansen, T. F. Jaramillo, RossmeislJ, ChorkendorffI, J. K. NÃ¸rskov, *Nat. Chem.*, 2009, 1, 552-556.
45. D. V. Yandulov, R. R. Schrock, *Science*, 2003, 301, 76-78.
46. B. K. Langlotz, H. Wadepohl, L. H. Gade, *Angew. Chem. Int. Ed.*, 2008, 47, 4670-4674.
47. G. W. Coates, *Chem. Rev.*, 2000, 100, 1223-1252.
48. S. Mecking, *Angew. Chem. Int. Ed.*, 2001, 40, 534-540.
49. E. Y. X. Chen, *Chem. Rev.*, 2009, 109, 5157-5214.
50. J. Takaya, N. Iwasawa, *J. Am. Chem. Soc.*, 2008, 130, 15254-15255.
51. C. Gunanathan, D. Milstein, *Acc. Chem. Res.*, 2011, 44, 588-602.
52. D. Benito-Garagorri, K. Kirchner, *Acc. Chem. Res.*, 2008, 41, 201-213.
53. H. Grützmacher, *Angew. Chem. Int. Ed.*, 2008, 47, 1814-1818.
54. C. Gunanathan, B. Gnanaprakasam, M. A. Iron, L. J. W. Shimon, D. Milstein, *J. Am. Chem. Soc.*, 2010, 132, 14763-14765.
55. T. Zell, D. Milstein, *Acc. Chem. Res.*, 2015, 48, 1979-1994.

56. M. Feller, E. Ben-Ari, Y. Diskin-Posner, R. Carmieli, L. Weiner, D. Milstein, *J. Am. Chem. Soc.*, 2015, 137, 4634-4637.
57. T. J. Mazzacano, N. P. Mankad, *J. Am. Chem. Soc.*, 2013, 135, 17258-17261.
58. J. R. Torkelson, F. H. Antwi-Nsiah, R. McDonald, M. Cowie, J. G. Pruis, K. J. Jalkanen, R. L. DeKock, *J. Am. Chem. Soc.*, 1999, 121, 3666-3683.
59. T. J. Steiman, C. Uyeda, *J. Am. Chem. Soc.*, 2015, 137, 6104-6110.
60. M. E. Broussard, B. Juma, S. G. Train, W.-J. Peng, S. A. Laneman, G. G. Stanley, *Science*, 1993, 260, 1784-1788.
61. O. Iranzo, T. Elmer, J. P. Richard, J. R. Morrow, *Inorg. Chem.*, 2003, 42, 7737-7746.
62. J. Park, S. Hong, *Chem. Soc. Rev.*, 2012, 41, 6931-6943.
63. C. A. Jaska, K. Temple, A. J. Lough, I. Manners, *Chem. Commun.*, 2001, 962-963.
64. C. A. Jaska, I. Manners, *J. Am. Chem. Soc.*, 2004, 126, 9776-9785.
65. C. A. Jaska, K. Temple, A. J. Lough, I. Manners, *J. Am. Chem. Soc.*, 2003, 125, 9424-9434.
66. C. A. Jaska, K. Temple, A. J. Lough, I. Manners, *Phosphorus Sulfur Silicon Relat. Elem.*, 2004, 179, 733-736.
67. R. Noyori, T. Ohkuma, *Angew. Chem. Int. Ed.*, 2001, 40, 40-73.
68. S. E. Clapham, A. Hadzovic, R. H. Morris, *Coord. Chem. Rev.*, 2004, 248, 2201-2237.
69. K. Muñiz, *Angew. Chem. Int. Ed.*, 2005, 44, 6622-6627.
70. K. Abdur-Rashid, S. E. Clapham, A. Hadzovic, J. N. Harvey, A. J. Lough, R. H. Morris, *J. Am. Chem. Soc.*, 2002, 124, 15104-15118.
71. T. J. Clark, C. A. Russell, I. Manners, *J. Am. Chem. Soc.*, 2006, 128, 9582-9583.
72. J. A. Osborn, F. H. Jardine, J. F. Young, G. Wilkinson, *J. Chem. Soc. A: Inorg., Phys., Theor.*, 1966, 1711-1732.
73. J. A. Osborn, G. Wilkinson, J. J. Mrowca, *Inorg. Synth., John Wiley & Sons, Inc.*, 2007, pp. 67-71.
74. M. E. Sloan, T. J. Clark, I. Manners, *Inorg. Chem.*, 2009, 48, 2429-2435.
75. T. Li, R. l. Churlaud, A. J. Lough, K. Abdur-Rashid, R. H. Morris, *Organometallics*, 2004, 23, 6239-6247.
76. R. Noyori, S. Hashiguchi, *Acc. Chem. Res.*, 1997, 30, 97-102.
77. T. Ikariya, A. J. Blacker, *Acc. Chem. Res.*, 2007, 40, 1300-1308.
78. I. Abdellah, C. Lepetit, Y. Canac, C. Duhayon, R. Chauvin, *Chem. Eur. J.*, 2010, 16, 13095-13108.
79. A. J. Arduengo, H. V. R. Dias, R. L. Harlow, M. Kline, *J. Am. Chem. Soc.*, 1992, 114, 5530-5534.
80. J. W. Bode, *Nat. Chem.*, 2013, 5, 813-815.
81. D. Enders, T. Balensiefer, *Acc. Chem. Res.*, 2004, 37, 534-541.
82. M. Haaf, T. A. Schmedake, R. West, *Acc. Chem. Res.*, 2000, 33, 704-714.
83. M. Haaf, A. Schmiedl, T. A. Schmedake, D. R. Powell, A. J. Millevolte, M. Denk, R. West, *J. Am. Chem. Soc.*, 1998, 120, 12714-12719.
84. N. J. Hill, R. West, *J. Organomet. Chem.*, 2004, 689, 4165-4183.

85. M. Kira, S. Ishida, T. Iwamoto, C. Kabuto, *J. Am. Chem. Soc.*, 1999, 121, 9722-9723.
86. F. Lips, J. C. Fettinger, A. Mansikkamäki, H. M. Tuononen, P. P. Power, *J. Am. Chem. Soc.*, 2014, 136, 634-637.
87. M. E. Alberto, N. Russo, E. Sicilia, *Chem. Eur. J.*, 2013, 19, 7835-7846.
88. M. Driess, S. Yao, M. Brym, C. van Wüllen, *Angew. Chem. Int. Ed.*, 2006, 45, 4349-4352.
89. J. D. Erickson, J. C. Fettinger, P. P. Power, *Inorg. Chem.*, 2015, ASAP.
90. M. Z. Kassaee, M. R. Momeni, F. A. Shakib, M. Ghambarian, *J. Organomet. Chem.*, 2010, 695, 760-765.
91. S. Krupski, C. Schulte to Brinke, H. Koppetz, A. Hepp, F. E. Hahn, *Organometallics*, 2015, 34, 2624-2631.
92. P. Spies, G. Erker, G. Kehr, K. Bergander, R. Frohlich, S. Grimme, D. W. Stephan, *Chem. Commun.*, 2007, 5072-5074.
93. D. W. Stephan, *Dalton Trans.*, 2009, 3129-3136.
94. D. W. Stephan, G. Erker, *Angew. Chem. Int. Ed.*, 2010, 49, 46-76.
95. G. C. Welch, R. R. S. Juan, J. D. Masuda, D. W. Stephan, *Science*, 2006, 314, 1124-1126.
96. G. C. Welch, D. W. Stephan, *J. Am. Chem. Soc.*, 2007, 129, 1880-1881.
97. N. L. Dunn, M. Ha, A. T. Radosevich, *J. Am. Chem. Soc.*, 2012, 134, 11330-11333.
98. S. M. McCarthy, Y.-C. Lin, D. Devarajan, J. W. Chang, H. P. Yennawar, R. M. Rioux, D. H. Ess, A. T. Radosevich, *J. Am. Chem. Soc.*, 2014, 136, 4640-4650.
99. W. Zhao, S. M. McCarthy, T. Y. Lai, H. P. Yennawar, A. T. Radosevich, *J. Am. Chem. Soc.*, 2014, 136, 17634-17644.
100. J. Cui, Y. Li, R. Ganguly, A. Inthirarajah, H. Hirao, R. Kinjo, *J. Am. Chem. Soc.*, 2014, 136, 16764-16767.
101. A. J. Arduengo, R. L. Harlow, M. Kline, *J. Am. Chem. Soc.*, 1991, 113, 361-363.
102. K. H. Dötz, *Angew. Chem. Int. Ed. Eng.*, 1984, 23, 587-608.
103. D. Enders, U. Kallfass, *Angew. Chem. Int. Ed.*, 2002, 41, 1743-1745.
104. D. A. Culkin, W. Jeong, S. Csihony, E. D. Gomez, N. P. Balsara, J. L. Hedrick, R. M. Waymouth, *Angew. Chem.*, 2007, 119, 2681-2684.
105. M. Albrecht, *Angew. Chem. Int. Ed.*, 2015, 54, 5822-5822.
106. J. W. Bode, S. S. Sohn, *J. Am. Chem. Soc.*, 2007, 129, 13798-13799.
107. X. Bugaut, F. Glorius, *Chem. Soc. Rev.*, 2012, 41, 3511-3522.
108. D. Enders, O. Niemeier, A. Henseler, *Chem. Rev.*, 2007, 107, 5606-5655.
109. W. A. Herrmann, *Angew. Chem. Int. Ed.*, 2002, 41, 1290-1309.
110. M. N. Hopkinson, C. Richter, M. Schedler, F. Glorius, *Nature*, 2014, 510, 485-496.
111. O. Kuhl, *Chem. Soc. Rev.*, 2007, 36, 592-607.
112. F. Li, Z. Wu, J. Wang, *Angew. Chem. Int. Ed.*, 2014, 54, 656-659.
113. J. Mahatthananchai, J. W. Bode, *Acc. Chem. Res.*, 2014, 47, 696-707.
114. R. S. Menon, A. T. Biju, V. Nair, *Chem. Soc. Rev.*, 2015, 44, 5040-5052.
115. U. Siemeling, C. Farber, C. Bruhn, M. Leibold, D. Selent, W. Baumann, M. von Hopffgarten, C. Goedecke, G. Frenking, *Chem. Sci.*, 2010, 1, 697-704.

116. H. W. Wanzlick, *Angew. Chem. Int. Ed. Eng.*, 1962, 1, 75-80.
117. H. W. Wanzlick, H. J. Kleiner, *Angew. Chem.*, 1963, 75, 1204-1204.
118. H. W. Wanzlick, H. J. Schönherr, *Angew. Chem. Int. Ed. Eng.*, 1968, 7, 141-142.
119. A. J. Arduengo, *Acc. Chem. Res.*, 1999, 32, 913-921.
120. D. Bourissou, O. Guerret, F. o. P. GabbaÃ¯, G. Bertrand, *Chem. Rev.*, 2000, 100, 39-92.
121. G. D. Frey, V. Lavallo, B. Donnadieu, W. W. Schoeller, G. Bertrand, *Science*, 2007, 316, 439-441.
122. S. S. Sen, S. Khan, P. P. Samuel, H. W. Roesky, *Chem. Sci.*, 2011, 3, 659-682.
123. C.-W. So, H. W. Roesky, J. Magull, R. B. Oswald, *Angew. Chem. Int. Ed.*, 2006, 45, 3948-3950.
124. R. Becerra, S.-J. Bowes, J. Steven Ogden, J. Pat Cannady, I. Adamovic, M. S. Gordon, M. J. Almond, R. Walsh, *Phys. Chem. Chem. Phys.*, 2005, 7, 2900-2908.
125. R. Becerra, J. P. Cannady, R. Walsh, *J. Phys. Chem. A*, 2003, 107, 11049-11056.
126. J. O. Chu, D. B. Beach, R. D. Estes, J. M. Jasinski, *Chem. Phys. Lett.*, 1988, 143, 135-139.
127. M. Denk, R. Lennon, R. Hayashi, R. West, A. V. Belyakov, H. P. Verne, A. Haaland, M. Wagner, N. Metzler, *J. Am. Chem. Soc.*, 1994, 116, 2691-2692.
128. R. Becerra, J. P. Cannady, R. Walsh, *J. Phys. Chem. A*, 2002, 106, 4922-4927.
129. X. Liu, X.-Q. Xiao, Z. Xu, X. Yang, Z. Li, Z. Dong, C. Yan, G. Lai, M. Kira, *Organometallics*, 2014, 33, 5434-5439.
130. R. Becerra, N. Goldberg, J. P. Cannady, M. J. Almond, J. S. Ogden, R. Walsh, *J. Am. Chem. Soc.*, 2004, 126, 6816-6824.
131. R. Azhakar, S. P. Sarish, H. W. Roesky, J. Hey, D. Stalke, *Organometallics*, 2011, 30, 2897-2900.
132. S. S. Sen, A. Jana, H. W. Roesky, C. Schulzke, *Angew. Chem. Int. Ed.*, 2009, 48, 8536-8538.
133. S. S. Sen, H. W. Roesky, D. Stern, J. Henn, D. Stalke, *J. Am. Chem. Soc.*, 2010, 132, 1123-1126.
134. M. Driess, *Nat. Chem.*, 2012, 4, 525-526.
135. A. Meltzer, S. Inoue, C. Präsang, M. Driess, *J. Am. Chem. Soc.*, 2010, 132, 3038-3046.
136. S. Yao, Y. Xiong, M. Driess, *Organometallics*, 2011, 30, 1748-1767.
137. F. Lips, A. Mansikkamäki, J. C. Fettinger, H. M. Tuononen, P. P. Power, *Organometallics*, 2014, 33, 6253-6258.
138. B. D. Rekken, T. M. Brown, J. C. Fettinger, H. M. Tuononen, P. P. Power, *J. Am. Chem. Soc.*, 2012, 134, 6504-6507.
139. S. Yao, M. Brym, C. van Wüllen, M. Driess, *Angew. Chem. Int. Ed.*, 2007, 46, 4159-4162.
140. R. Rodriguez, D. Gau, T. Troadec, N. Saffon-Merceron, V. Branchadell, A. Baceiredo, T. Kato, *Angew. Chem. Int. Ed.*, 2013, 52, 8980-8983.
141. A. V. Protchenko, K. H. Birjkumar, D. Dange, A. D. Schwarz, D. Vidovic, C. Jones, N. Kaltsoyannis, P. Mountford, S. Aldridge, *J. Am. Chem. Soc.*, 2012, 134, 6500-6503.

142. P. Jutzi, K. Leszczynska, A. Mix, B. Neumann, B. Rummel, W. Schoeller, H.-G. Stammler, *Organometallics*, 2010, 29, 4759-4761.
143. P. Jutzi, K. Leszczyńska, B. Neumann, W. W. Schoeller, H.-G. Stammler, *Angew. Chem. Int. Ed.*, 2009, 48, 2596-2599.
144. S. Inoue, K. Leszczyńska, *Angew. Chem. Int. Ed.*, 2012, 51, 8589-8593.
145. G. N. Lewis, W. L. Jolly, *Valence, the structure of atoms, molecules, The Chemical Catalog Company, inc.*, New York, 1923.
146. P. A. Chase, T. Jurca, D. W. Stephan, *Chem. Commun.*, 2008, 1701-1703.
147. P. A. Chase, D. W. Stephan, *Angew. Chem. Int. Ed.*, 2008, 47, 7433-7437.
148. P. A. Chase, G. C. Welch, T. Jurca, D. W. Stephan, *Angew. Chem. Int. Ed.*, 2007, 46, 8050-8053.
149. L. Greb, P. Oña-Burgos, B. Schirmer, S. Grimme, D. W. Stephan, J. Paradies, *Angew. Chem. Int. Ed.*, 2012, 51, 10164-10168.
150. L. J. Hounjet, C. B. Caputo, D. W. Stephan, *Angew. Chem. Int. Ed.*, 2012, 51, 4714-4717.
151. J. S. J. McCahill, G. C. Welch, D. W. Stephan, *Angew. Chem. Int. Ed.*, 2007, 46, 4968-4971.
152. G. Ménard, D. W. Stephan, *J. Am. Chem. Soc.*, 2010, 132, 1796-1797.
153. C. M. Mömming, E. Otten, G. Kehr, R. Fröhlich, S. Grimme, D. W. Stephan, G. Erker, *Angew. Chem. Int. Ed.*, 2009, 48, 6643-6646.
154. E. Otten, R. C. Neu, D. W. Stephan, *J. Am. Chem. Soc.*, 2009, 131, 9918-9919.
155. C. Appelt, J. C. Slootweg, K. Lammertsma, W. Uhl, *Angew. Chem. Int. Ed.*, 2013, 52, 4256-4259.
156. C. Appelt, J. C. Slootweg, K. Lammertsma, W. Uhl, *Angew. Chem. Int. Ed.*, 2012, 51, 5911-5914.
157. C. Appelt, H. Westenberg, F. Bertini, A. W. Ehlers, J. C. Slootweg, K. Lammertsma, W. Uhl, *Angew. Chem. Int. Ed.*, 2011, 50, 3925-3928.
158. W. Uhl, C. Appelt, J. Backs, H. Westenberg, A. Wollschlager, J. Tannert, *Organometallics*, 2014, 33, 1212-1217.
159. P. Spies, S. Schwendemann, S. Lange, G. Kehr, R. Fröhlich, G. Erker, *Angew. Chem. Int. Ed.*, 2008, 47, 7543-7546.
160. S. J. Geier, D. W. Stephan, *J. Am. Chem. Soc.*, 2009, 131, 3476-3477.
161. D. Holschumacher, T. Bannenberg, C. G. Hrib, P. G. Jones, M. Tamm, *Angew. Chem. Int. Ed.*, 2008, 47, 7428-7432.
162. H. Wang, R. Frohlich, G. Kehr, G. Erker, *Chem. Commun.*, 2008, 5966-5968.
163. A. Ramos, A. J. Lough, D. W. Stephan, *Chem. Commun.*, 2009, 1118-1120.
164. S. J. Geier, T. M. Gilbert, D. W. Stephan, *J. Am. Chem. Soc.*, 2008, 130, 12632-12633.
165. M. H. Holthausen, J. M. Bayne, I. Mallov, R. Dobrovetsky, D. W. Stephan, *J. Am. Chem. Soc.*, 2015, 137, 7298-7301.
166. M.-A. L. Marc-André Courtemanche, Laurent Maron,, Frédéric-Georges Fontaine, *J. Am. Chem. Soc.*, 2014, 136, 10708-10717.
167. T. Xu, E. Y. X. Chen, *J. Am. Chem. Soc.*, 2014, 136, 1774-1777.
168. Y. Cao, J. K. Nagle, M. O. Wolf, B. O. Patrick, *J. Am. Chem. Soc.*, 2015, 137, 4888-4891.

169. P. Pyykko, C. Wang, *Phys. Chem. Chem. Phys.*, 2010, 12, 149-155.
170. Z. Lu, Z. Cheng, Z. Chen, L. Weng, Z. H. Li, H. Wang, *Angew. Chem. Int. Ed.*, 2011, 50, 12227-12231.
171. S. Schwendemann, R. Frohlich, G. Kehr, G. Erker, *Chem. Sci.*, 2011, 2, 1842-1849.
172. K. V. Axenov, G. Kehr, R. Frohlich, G. Erker, *J. Am. Chem. Soc.*, 2009, 131, 3454-3455.
173. E. L. Kolychev, T. Bannenberg, M. Freytag, C. G. Daniliuc, P. G. Jones, M. Tamm, *Chem. Eur. J.*, 2012, 18, 16938-16946.
174. Y. Guo, X. He, Z. Li, Z. Zou, *Inorg. Chem.*, 2010, 49, 3419-3423.
175. A. J. M. Miller, J. E. Bercaw, *Chem. Commun.*, 2010, 46, 1709-1711.
176. A. E. Ashley, A. L. Thompson, D. O'Hare, *Angew. Chem. Int. Ed.*, 2009, 48, 9839-9843.
177. M. J. Sgro, D. W. Stephan, *Angew. Chem. Int. Ed.*, 2012, 51, 11343-11345.
178. S. R. Flynn, D. F. Wass, *ACS Catal.*, 2013, 3, 2574-2581.
179. S. K. Podiyanachari, R. Fröhlich, C. G. Daniliuc, J. L. Petersen, C. Mück-Lichtenfeld, G. Kehr, G. Erker, *Angew. Chem.*, 2012, 124, 8960-8963.
180. A. Berkefeld, W. E. Piers, M. Parvez, L. Castro, L. Maron, O. Eisenstein, *J. Am. Chem. Soc.*, 2012, 134, 10843-10851.
181. M. J. Sgro, D. W. Stephan, *Chem. Commun.*, 2013, 49, 2610-2612.
182. A. M. Chapman, M. F. Haddow, D. F. Wass, *J. Am. Chem. Soc.*, 2011, 133, 18463-18478.
183. A. M. Chapman, M. F. Haddow, D. F. Wass, *J. Am. Chem. Soc.*, 2011, 133, 8826-8829.

Chapter 2

Theoretical Methods

Abstract

In the previous chapter, we have discussed about the different organometallic and non-metallic main group catalysts and their use in the small molecule activation reaction. In this chapter, we will try to demonstrate the theoretical background that forms the basis of the state of the art computational methods that have been employed in our calculations. We have first started the chapter by discussing the Schrödinger equation and the Born-Oppenheimer approximation. In the subsequent sections, we have discussed the Thomas-Fermi model, the Hohenberg-Kohn theorems, the Kohn-Sham approach and the concepts of functional and the Møller–Plesset (MP2) theory. Furthermore, we have discussed the RI-J and MARI-J approximations and the COSMO model for solvent correction that have been implemented in the Turbomole software.

2.1 The Time Independent Schrödinger Equation

The Schrödinger equation deals with the determination of the N-electronic atomic or molecular system, which can be presented in the form of standing waves. They are also called stationary states as the Hamiltonian does not depend on time. Thus, the time independent, non-relativistic Schrödinger equation[1] for any atomic or molecular systems can be represented as,

$$\hat{H}\Psi = E\Psi \qquad (2.1)$$

Where $\hat{H}$ = Hamiltonian operator for a system of nuclei and electrons, $\Psi = \Psi(x_1, x_2, ..., x_N)$ is the wave function which does not depend on time and E= electronic energy. The Hamiltonian operator for any system can be expressed as Equation 2.2 (in atomic units).

$$\hat{H} = -\sum_{i=1}^{N}\frac{1}{2m}\Delta_i^2 - \sum_{A=1}^{M}\frac{1}{2M_A}\Delta_A^2 - \sum_{i=1}^{N}\sum_{A=1}^{M}\frac{Z_A}{r_{iA}} + \sum_{i=1}^{N}\sum_{j>i}^{N}\frac{1}{r_{ij}} + \sum_{A=1}^{M}\sum_{B>A}^{M}\frac{Z_A Z_B}{R_{AB}} \qquad (2.2)$$

The first term of the Equation 2.2 is the kinetic energy operator of the electrons of mass m. The second term indicates the operator for the kinetic energy of the nuclei having mass M_A. The third term illustrates the coulombic attraction force between the electrons and the nuclei and the distance between them is r_{iA}. The fourth and fifth term represents both the repulsive force between each of the the electrons and the nuclei themselves. The electrons are separated by the distance of r_{ij} i.e the distance amongst the ith and jth electron. Similarly, the nucles are separated by the distance of R_{AB} (where A and B are the nuclei). Thus, the contributions from all the terms make the Hamiltonian operator for our systems of interest, which can eventually provide the energy of the systems once the wave function is known.

2.1.1 The Born-Oppenheimer Approximation

In the above section, we have discussed the Schrödinger equation, which cannot be solved exactly for multi-electron systems. Thus simplification of the Equation 2.2 is

needed to reach nearly the exact energy values for the systems. In this context, the Born-Oppenheimer approximation was postulated in order to decouple the motion of the electrons from the motion of the nucleus, as it is well known that the mass of the nucleus is 1836 times the mass of the electron[2]. By this approximation, for a given position of the nuclei, all the electrons move in the fixed nuclei field as the electronic wavefunction only depends on the position of the nuclei. Thus, according to the Born-Oppenheimer approximation, the overall Schrödinger equation can be written in a simpler form where the nuclei are assumed to be fixed. Therefore, only the electronic Hamiltonian, which depends parametrically on the nuclear coordinates, is the Hamiltonian that we have to be concerned with. The modified form of the electronic Hamiltonian is written in Equation 2.3. Thus, for the fix nuclei, the total energy is equal to the sum of the electronic energy and the nuclear repulsion energy. Essentially, in this way, one calculates the kinetic and potential energy in the electrostatic field of nuclei along with the electron-electron repulsion energy.

$$\hat{H}_{ele} = -\sum_{i=1}^{N} \frac{1}{2}\Delta_i^2 - \sum_{i=1}^{N}\sum_{A=1}^{M} \frac{Z_A}{r_{iA}} + \sum_{i=1}^{N}\sum_{j>i}^{N} \frac{1}{r_{ij}} \tag{2.3}$$

$$E_{tot} = E(\text{electron}) + E(\text{nucler repulsion}) \tag{2.4}$$

Now, the electronic Schrödinger equation for the many-electron systems needs to be solved. In this regard, it is well known that any solution for the many-electron system is the approximation to the true solution for the system. Various approaches with diverse approximation and computational cost have been reported for solving the electronic Hamiltonian. The simplest approach in this regards is the Hartree-Fock approximation. To improve the accuracy of the electronic energy, several other approximations have been studied. The configuration interaction (CI)[3], the coupled cluster (CC)[4] and the many body Møller-Plesset (MP)[5] perturbation theory are the well established methods for solving the electronic Schrödinger equation. However, the huge computational cost makes these methods practically impossible to apply for the large, practical system of interest. In this context, density functional theory (DFT) is very useful, where the ground state properties can be determined from the electron density of many-electron systems. In

addition to this, the DFT methods are computationally less expensive and versatile for many-body systems.

2.2 Density Functional Theory

The density functional theory (DFT)[6] has addressed the major drawback of the *ab initio* mathods, i.e., the energy depends on the determination of the N-electron wave function, which is not a physical observable. In DFT, the ground state properties of the molecules can be determined by the determination of the electron density $\rho(r)$ of that particular molecule.

2.2.1 Thomas Fermi Model

In 1920s, Thomas[7] and Fermi[8,9] approximated the electron distribution in an atom by the statistical approach. They postulated that the electrons are uniformly distributed along the six-dimensional phase space and the kinetic energy of the non-interacting electrons in a homogeneous gas can be written as the functional form of the local density. The energy term for the Thomas-Fermi model in terms of electron density is expressed in Equation 2.5[6],

$$E_{TF}[\rho(r)] = C_F \int \rho^{5/3}(r)dr - Z\int \frac{\rho(r)}{r}dr + \frac{1}{2}\iint \frac{\rho(r_1)\rho(r_2)}{r_1 - r_2}dr_1 dr_2 \qquad (2.5)$$

where C_F is the Thomas-Fermi coefficient.

Equation 2.5 contains three terms. The first one is the electronic kinetic energy as a function of the density $\rho(r)$, the second term is the electron-nucleus attraction energy and the third term is the electron-electron repulsion energy. The second and third terms are the classical electrostatic energies without any exchange or correlation contributions.

Now to minimize the energy functional with respect to the density, the constraint N needs to be incorporated by the method of Lagrange undetermined multipliers, where N is the total number of electrons present in the atom and can be written as,

$$N = N[\rho(r)] = \int \rho(r) dr \qquad (2.6)$$

The constrained variation method for the minimization of the Thomas-Fermi kinetic energy by the method of Lagrange undetermined multipliers can be written as Equation 2.7, followed by the Euler-Lagrange Equation 2.8 to calculate the constant μ_{TF} where $\phi(r)$ is the electrostatic potential at point 'r' due to the nucleus and the entire electron distribution.

$$\delta\left\{E_{TF}[\rho] - \mu_{TF}\left(\int \rho(r) dr - N\right)\right\} = 0 \qquad (2.7)$$

$$\mu_{TF} = \frac{\delta E_{TF}[\rho]}{\delta \rho(r)} = \frac{5}{3} C_F \rho^{2/3}(r) - \phi(r) \qquad (2.8)$$

$$\phi(r) = \frac{Z}{r} - \int \frac{\rho(r_2)}{|r - r_2|} dr_2 \qquad (2.9)$$

The electron density obtained by solving the Euler-Lagrange Equation 2.8 in conjunction with the constraint Equation 2.6 can be put into the main Equation 2.5 of the energy functional to get the total kinetic energy for the atom. However, the Thomas-Fermi model failed to predict the kinetic energy for the molecule. Furthermore, the oversimplified approximation caused low accuracy even for the atoms with respect to the other methods.

2.2.2 Hohenberg-Kohn Theorem

In the year 1964, Hohenberg and Kohn postulated a landmark theorem where they proposed that the Thomas-Fermi model can be an approximation of the exact density functional theory for the ground state. The two Hohenberg-Kohn theorems[10] are regarded as the beginning of modern density functional theory.

Hohenberg and Kohn have postulated the first theorem as "the external potential is determined, within a trivial additive constant, by the electron density $\rho(r)$". The electron density is related to the total number of electrons. Hence, the ground state wave function

and other electronic properties can be easily determined by the electron density $\rho(r)$. This theorem demonstrates that there cannot be two different external potential which give the same density for the ground state. Thus, according to this theorem, the nuclear electron attraction term can be rewritten as a function of density with the external potential[6].

Hence, the total energy equation can be expressed as

$$E_{\upsilon}[\rho] = T[\rho] + V_{ne}[\rho] + V_{ee}[\rho] = \int \rho(r)\upsilon(r)dr + F_{HK}[\rho] \tag{2.10}$$

Where $$F_{HK}[\rho] = T[\rho] + V_{ee}[\rho] \tag{2.11}$$

The last term i.e. the electrostatic repulsion term in Equation 2.11 can be written as the summation of the classical repulsion term and the nonclassical term. The exchange-correlation energy is mainly involved in the nonclassical term.

$$V_{ee}[\rho] = J[\rho] + \text{nonclassical term} \tag{2.12}$$

The second Hohenberg-Kohn theorem is very similar to the conventional variation principle[6]. They postulated it as, "for a trial density $\tilde{\rho}(r)$, such that $\tilde{\rho}(r) \geq 0$ and $\int \tilde{\rho}(r)dr = N$",

$$E_0 \leq E_{\nu}[\tilde{\rho}] \tag{2.13}$$

where E_0 is the ground state exact energy and $E_{\nu}[\tilde{\rho}]$ is the energy functional.

Now, again, the constrained minimization process for the ground state energy equation by the method of the Lagrange undetermined multipliers forms

$$\delta\left\{E_{\upsilon}[\rho] - \mu\left[\int \rho(r)dr - N\right]\right\} = 0 \tag{2.14}$$

$$\mu = \frac{\delta E_{\upsilon}[\rho]}{\delta\rho(r)} = \upsilon(r) + \frac{\delta F_{HK}[\rho]}{\delta\rho(r)} \tag{2.15}$$

where μ is the chemical potential and $F_{HK}[\rho]$ is an universal functional of $\rho(r)$. It is very difficult to get an explicit form for the $F_{HK}[\rho]$ functional. Thus, the best possible solution of Equation 2.15 for energy minimization is very important towards the ground state energy of a system.

2.2.3 Kohn-Sham Equations

As in the above section, we have seen that the Thomas-Fermi model is an approximation for the kinetic energy $T[\rho]$ and the electron-electron repulsion potential $V_{ee}[\rho]$. However, to overcome the difficulties of the oversimplified model, the kinetic energy part must be taken care of carefully. Kohn and Sham[11], in this regard, introduced the orbitals in such a way that the kinetic energy can be computed with good accuracy.

Kohn and Sham invoked the noninteracting reference system moving in an effective potential $\upsilon(r)$ for every interacting problem of interest. The Hamiltonian of such systems bears no electron-electron repulsion terms and the ground state electron density is exactly equal to the ρ.

The kinetic energy and the electron density for a non-interacting electronic system can be written as the following equations[6],

$$T_s[\rho] = \sum_i^N \langle \psi_i | -\tfrac{1}{2}\Delta^2 | \psi_i \rangle \tag{2.16}$$

$$\rho(r) = \sum_i^N \sum_s |\psi_i(r,s)|^2 \tag{2.17}$$

The energy functional can be written as Equation 2.18 and by introducing the *N* orbitals it can be rewritten as Equation 2.19 below. The term $T_s[\rho]$ is not the exact kinetic energy functional but its component.

$$E[\rho] = T_s[\rho] + J[\rho] + E_{xc}[\rho] + \int \upsilon(r)\rho(r)dr \tag{2.18}$$

$$= \sum_i^N \sum_s \int \psi_i^*(x)(-\tfrac{1}{2}\Delta^2)\psi_i(x)dr + J[\rho] + E_{xc}[\rho] + \int \upsilon(r)\rho(r)dr \tag{2.19}$$

The first term in Equation 2.19 is the kinetic energy of electrons for the model for a non-interacting system. The second term is the classical Coulomb interaction between the electrons and the third term is the exchange-correlation energy. This exchange-correlation energy also takes care of the difference in the kinetic energy between the noninteracting and the interacting systems ($T[\rho]-T_s[\rho]$) and the nonclassical part, i.e. $V_{ee}[\rho]$. The fourth term represents the electron-nucleus attraction energy. Thus, for a known external potential [$\upsilon_{eff}(r)$], N one electron equations can be constructed (see Equation 2.20, where ε_i are eigenvalues, ψ_i are the Kohn Sham (KS) orbitals). Then, the density $\rho(r)$ will be obtained from the Equation 2.21.

$$[-\tfrac{1}{2}\nabla^2+\upsilon_{eff}]\psi_i=\varepsilon_i\psi_i \tag{2.20}$$

$$\rho(r)=\sum_i^N\sum_s|\psi_i(r,s)|^2 \tag{2.21}$$

The term, $\upsilon_{eff}(r)$, i.e. the KS effective potential can be defined as shown in Equation 2.22 and 2.23 below. The third term, $\upsilon_{xc}(r)$ in Equation 2.23 is the exchange-correlation potential. Thus. the KS non-linear equations have to be solved iteratively. This process is called the self consistent field (SCF) method.

$$\upsilon_{eff}(r)=\upsilon(r)+\frac{\delta J[\rho]}{\delta\rho(r)}+\frac{\delta E_{xc}[\rho]}{\delta\rho(r)} \tag{2.22}$$

$$=\upsilon(r)+\int\frac{\rho(r')}{|r-r'|}dr'+\upsilon_{xc}(r) \tag{2.23}$$

The total energy that is not equal to the sum of the orbital energies can be expressed as Equation 2.24 below.

$$E=\sum_i^N\varepsilon_i-\frac{1}{2}\int\frac{\rho(r)\rho(r')}{|r-r'|}drdr'+E_{xc}[\rho]+\int\upsilon_{xc}(r)\rho(r)dr \tag{2.24}$$

Better approximations to $E_{xc}[\rho]$ would give better values for ρ and E.

2.2.4 Exchange-Correlation Functional

As shown in the previous section, the total energy depends on the exchange-correlation functional ($E_{xc}[\rho]$). The better approximation of the E_{xc}, the better will be the energy. However, the great challenge is to make an accurate estimation of E_{xc}. In this regard, the local density approximation (LDA) is the best for estimating the exchange-correlation energy. The energy functional for the exchange-correlation contribution is easily computed by the assumption of the homogeneous electron gas, by which one can obtain the exchange-correlation energy for a non-uniform system by simply applying the uniform electron gas model. Thus, the local exchange-correlation energy can be written as,

$$E_{xc}^{LDA}[\rho] = \int \rho(r)\varepsilon_{xc}[\rho(r)]dr \tag{2.25}$$

where $\varepsilon_{xc}(\rho)$ is the exchange and correlation energy per particle of a uniform electron gas of density$[\rho(r)]$. Now, knowing the exchange-correlation energy contribution, one can easily construct the corresponding exchange-correlation potential and the KS equations to estimate the exchange-correlation included energy value[6].

$$\upsilon_{xc}^{LDA}(r) = \frac{\delta E_{xc}^{LDA}}{\delta\rho(r)} = \varepsilon_{xc}(\rho(r)) + \rho(r)\frac{\delta\varepsilon_{xc}(\rho)}{\delta\rho} \tag{2.26}$$

$$\left[-\frac{1}{2}\Delta^2 + \upsilon(r) + \int \frac{\rho(r')}{|r-r'|}dr' + \upsilon_{xc}^{LDA}(r)\right]\psi_i = \varepsilon_i\psi_i \tag{2.27}$$

Thus, again Equation 2.27 has to be solved iteratively by the SCF method to provide the Kohn Sham-local density approximation (LDA method). This method is well defined for the system with slowly varying densities, but is inaccurately described for the highly inhomogeneous systems such as atoms and molecules. Further modification is needed to compute the exchange energy accurately because it is the most difficult part of the total energy expression. The generalized gradient approximation (GGA) provides a modified model to improve the accuracy of the exchange and correlation functional. In this model,

the gradient of the electron density is used in place of the density. Thus, the exchange-correlation energy functional in GGA[6] can be expressed as,

$$E_{xc}^{GGA}[\rho(r)] = \int \rho(r) F[\rho(r), \nabla\rho(r)] dr \qquad (2.28)$$

Thus, the challenge is to estimate the exchange-correlation energy contribution accurately. In this regard, several functionals with different approximations have been developed to calculate the exchange- correlation energy.

In 1986, Perdew (P86)[12] proposed the correlation contribution for the gradient corrections approach and in 1988, Becke (B88)[13] proposed the exchange part of $E_{xc}^{GGA}[\rho(r)]$ by involving the gradient of the density along with the Slater exchange. The functional composed of the Becke exchange and the Perdew correlation contribution is called BP86 functional. Later, Lee, Yang and Parr (LYP)[14] in 1988 came up with a correlation functional which involved both the local and non-local parts. In 1991, Perdew and Wang (PW91)[15] and in 1996 Perdew, Burke and Ernzerhof (PBE)[16] have proposed another gradient-corrected correlation energy functional.

Another type of functional is the hybrid functional, where the exact exchange energy from the Hartree-Fock method mixes with that obtained from the DFT. B3LYP[17] is one of the well known hydrid functionals, which consists of a mixture of exchange energy with Becke exchange and Lee, Yang and Parr (LYP) correlation functional. The form of the exchange-correlation functional can be written as

EXC = 0.2*EX(HF) + 0.8*EX(LSDA) + 0.72*DEX(B88) + 0.81*EC(LYP) + 0.19*EC(VWN) (2.29)

The group of Prof. Donald Truhlar at the University of Minnesota has developed another very popular family of functionals, which are called the Minnesota Functionals (Myz)[18]. These functionals follow the hybrid generalized gradient approximation where the electron spin density, density gradient, kinetic energy density and the Hartree-Fock exchange are involved. For example, the M06-2X functional has 54% HF exchange. This functional is very useful for predicting the thermochemistry, kinetics and the non-covalent interactions for main group systems.

2.3 Møller–Plesset Perturbation Theory

The concept of the perturbation theory is to transform the exact Hamiltonian of the Schrödinger equation to an effective Hamiltonian where an external perturbation is added. The effective Hamiltonian H_{eff} can be written as,

$$H = H_0 + \lambda V \tag{2.30}$$

Where, V is the external perturbation and λ is the arbitrary perturbation parameter. In the Møller–Plesset perturbation theory[5] what is considered is the Hartree-Fock Hamiltonian as the zeroth order Hamiltonian that can be written as,

$$H_0 = \sum_i f(i) = \sum_i [h(i) + \upsilon^{HF}(i)] \tag{2.31}$$

$$V = \sum_{i<j} r_{ij}^{-1} - V^{HF} = \sum_{i<j} r_{ij}^{-1} - \sum_i \upsilon^{HF}(i) \tag{2.32}$$

The perturbation here comes from the correlation potential where the perturbation operator can be expressed as,

$$V = H - H_0 \tag{2.33}$$

Thus, by applying the correlation perturbation, the first order energy correction is

$$E_o^{(1)} = \langle \Psi_0 | V | \Psi_0 \rangle = \langle \Psi_0 \left| \sum_{i<j} r_{ij}^{-1} \right| \Psi_0 \rangle - \langle \Psi_0 \left| \sum_i \upsilon^{HF}(i) \right| \Psi_0 \rangle = \frac{1}{2} \sum_{ab} \langle ab || ab \rangle - \sum_a \langle a | \upsilon^{HF} | a \rangle = -\frac{1}{2} \sum_{ab} \langle ab || ab \rangle \tag{2.34}$$

which suggests that the MP1 energy is equal to the Hartree-Fock energy. Thus, the second order energy correction is the first energy correction to the Hartree-Fock energy[6]. The second order MP2 energy can be written as,

$$E_0^{(2)} = \sum_n \frac{|\langle 0 | V | n \rangle|^2}{E_0^{(0)} - E_n^{(0)}} \tag{2.35}$$

Due to Brillouin's theorem and the two particle nature of the perturbation, the double excitation only contributes to the energy correction. Therfore, the second order energy can be expressed as

$$E_0^{(2)} = \sum_{\substack{a<b \\ r<s}} \frac{\left| \left\langle \Psi_0 \left| \sum_{i<j} r_{ij}^{-1} \right| \Psi_{ab}^{rs} \right\rangle \right|^2}{\varepsilon_a + \varepsilon_b - \varepsilon_r - \varepsilon_s} = \sum_{\substack{a<b \\ r<s}} \frac{\left| \langle ab || rs \rangle \right|^2}{\varepsilon_a + \varepsilon_b - \varepsilon_r - \varepsilon_s} \qquad (2.36)$$

where the "ab" represents the occupied orbitals and the "rs" represents the unoccupied orbitals. Therefore, for the ground state problems, the second order Møller–Plesset perturbation theory predicts more accurate geometries and energies.

In this regard, the spin component scaled MP2 method (SCS-MP2)[19-21] is another correction to the MP2 energy. In the MP2 method, both the parallel and the anti-parallel spin contribute equally to the energy. However, by applying different contributions for the parallel and the antiparallel spin, better performance can be achieved from the MP2 calculations. Although the scaling components are optional, Grimme and co-workers have recommended the scaling factors for parallel and antiparallel spins as 6/5 (p_s) and 1/3 (p_t). Thus, the electronic correlation energy can be written as, $E_c = p_s E_s + p_t E_t$.

2.4 RI-J and MARI-J Approximation

Other approximations to reduce the computational costs and accelerate the computational process are the RI-J[22-27] (resolution of identity) and MARI-J[28] (multipole accelerated resolution of identity) approximations. The use of auxiliary basis functions helps to reduce the conventional computation time. The MARI-J method divides the Coulomb interaction into two components; the near field and the far field parts. The near field part includes the four-centre electron repulsion integrals and the long range interactions that are expressed by the multipole expansions that represent the far field component. The RI approximation reduces the four centre electron repulsion integrals into the three centre integrals by using the density fitting method, where the electron density ρ can be expressed as a linear combination of auxiliary basis functions α,

$$\rho(r) \approx \tilde{\rho}(r) = \sum_{\alpha} c_{\alpha}\alpha(r) \tag{2.37}$$

The c_α is the expansion coefficient, which can be calculated by the expression,

$$c_{\alpha} = \iint [\rho(r) - \tilde{\rho}(r)]g(r,r')[\rho(r') - \tilde{\rho}(r')]drdr' \tag{2.38}$$

Where, '*g*' is the positive definite two-electron operator. Thus, by using the particular value of '*g*' the convergence can be obtained for the Coulomb integrals.

2.5 Solvent Correction

Like other approximations, which have been taken care of during the geometry optimization process, the solvent effects have also been included through the calculations with the Conductor Like Screening Model (COSMO)[29,30]. The model is called continuum solvation model (CSM), where the solvent is represented by the dielectric continuum with the permittivity ε, by which the solute molecules are surrounded. Therefore, the charge distribution of the solute and the polarization of the dielectric medium generate the screening charges on the solute cavity surface. For an ideal solution ($\varepsilon = \infty$), the screening charges vanish at the cavity surface. However, for a solvent with a finite dielectric constant, the screening charges can be represented as,

$$\mathrm{q}^{*} = f(\varepsilon)\,\mathrm{q} \tag{2.39}$$

$$f(\varepsilon) = \frac{\varepsilon - 1}{\varepsilon + \frac{1}{2}} \tag{2.40}$$

where the screening charges are scaled by the factor. The dielectric energy can be calculated easily from the interaction at the cavity surface as it is half of the solute-solvent energy. Thus, for the solvated molecule, the absolute free energy can be calculated by the summation of the energy that is obtained from the solvated wave function and the dielectric energy.

$$E = E(\psi^{solv}) + E_{diel} \tag{2.41}$$

2.6 References

(1) E. Schrödinger, *Ann. Phys.*, 1926, 384, 361-376.
(2) M. Born, R. Oppenheimer, *Ann. Phys.*, 1927, 389, 457-484.
(3) C. David Sherrill, H. F. Schaefer, *Adv. Quantum Chem.;* Academic Press: 1999, 34, 143-269.
(4) R. J. Bartlett, *J. Phys. Chem.*, 1989, 93, 1697-1708.
(5) C. Møller, M. S. Plesset, *Phys. Rev.*, 1934, 46, 618-622.
(6) R. G. Parr, W. Yang, *Density-Functional Theory of Atoms and Molecules*; Oxford University Press, USA, 1989.
(7) L. H. Thomas, *Mathematical Proceedings of the Cambridge Philosophical Society*, 1927, 23, 542-548.
(8) E. Fermi, *Zs. f. Phys.*, 1926, 36, 902.
(9) E. Fermi, *Rendiconti Lincei*, 1927, 6, 602-607.
(10) P. Hohenberg, W. Kohn, *Phys. Rev.*, 1964, 136, B864-B871.
(11) W. Kohn, L. J. Sham, *Phys. Rev.*, 1965, 140, A1133-A1138.
(12) J. P. Perdew, *Phys. Rev. B*, 1986, 33, 8822-8824.
(13) A. D. Becke, *Phys. Rev. A*, 1988, 38, 3098-3100.
(14) C. Lee, W. Yang, R. G. Parr, *Phys. Rev.*, B 1988, 37, 785.
(15) J. P. Perdew, Y. Wang, *Phys. Rev. B*, 1992, 45, 13244-13249.
(16) J. P. Perdew, K. Burke, M. Ernzerhof, *Phys. Rev. Lett.*, 1996, 77, 3865-3868.
(17) A. D. Becke, *J. Chem. Phys.*, 1993, 98, 5648-5652.
(18) Y. Zhao, D. G. Truhlar, *Theor.Chem. Acc.*, 2008, 120, 215-241.
(19) A. Hellweg, S. A. Grun, C. Hattig, *Phys. Chem. Chem. Phys.*, 2008, 10, 4119-4127.
(20) T. P. M. Goumans, A. W. Ehlers, K. Lammertsma, E.-U. Würthwein, S. Grimme, *Chem. –Eur. J.*, 2004, 10, 6468-6475.
(21) S. Grimme, *J. Chem. Phys.*, 2003, 118, 9095-9102.
(22) K. Eichkorn, O. Treutler, H. Öhm, M. Häser, R. Ahlrichs, *Chem. Phys. Lett.*, 1995, 240, 283-290.
(23) A. M. Burow, M. Sierka, F. Mohamed, *J. Chem. Phys.*, 2009, 131, 214101.
(24) J. L. Whitten, *J. Chem. Phys.*, 1973, 58, 4496-4501.
(25) O. Vahtras, J. Almlöf, M. W. Feyereisen, *Chem. Phys. Lett.*, 1993, 213, 514-518.
(26) B. I. Dunlap, J. W. D. Connolly, J. R. Sabin, *J. Chem. Phys.*, 1979, 71, 3396-3402.
(27) K. Eichkorn, F. Weigend, O. Treutler, R. Ahlrichs, *Theor. Chem. Acc.*, 1997, 97, 119-124.
(28) M. Sierka, A. Hogekamp, R. Ahlrichs, *J. Chem. Phys.*, 2003, 118, 9136-9148.
(29) A. Klamt, G. Schuurmann, *J. Chem. Soc. Perkin Trans.*, 2 1993, 799-805.
(30) User's Manual, *Turbomole* Version 6.4 2012.

Chapter 3

Proposing Late Transition Metal Complexes as Frustrated Lewis Pairs

Abstract

There has been considerable interest in recent times to develop transition metal complex systems that can demonstrate metal-ligand cooperativity. It has recently been shown (Wass *et al.J. Am. Chem. Soc*., 2011, 133, 18463) that early transition metals can cooperate with ligands carrying phosphines as pendant groups, working as metal analogues to frustrated Lewis pairs (FLPs) to mediate in a variety of important reactions. What the current work attempts to do is to show how this concept of metal containing FLPs can be expanded to include late transition metal complexes as well: complexes that have been modified from existing systems that serve as efficient catalysts for homogeneous polymerization. A modified palladium complex has been considered in this regard as an example of a potential late transition metal FLP and studied with full quantum mechanical calculations. The calculations indicate that this complex would be effective at catalyzing ammonia borane dehydrogenation. The possibility of competing side reactions such as reductive elimination have also been considered, and it has been found that such processes would also yield stable products which could act as an FLP in catalyzing reactions such as the dehydrogenation of ammonia borane. The current work therefore expands the scope of metal containing FLPs to include late transition metals and demonstrates computationally the potential of such complexes for exhibiting metal-ligand cooperativity.

3.1 Introduction

Non-metal complexes possessing a combination of sterically separated Lewis acidic and Lewis basic sites, termed as "frustrated lewis pairs" (FLPs), have recently become a subject of much research owing to their ability to perform interesting solution phase chemistry in a catalytic[1, 2], as well as in a stoichiometric fashion[3-5]. FLPs have been found to mediate successfully in a variety of different chemical transformations, including the reversible activation of dihydrogen[5], reactivity towards alkenes[6] as well as to alkynes[7] and imines[8], enamines[1] and nitriles[8, 9]. Diverse intermolecular and intramolecular combinations have been made in order to expand the concept of FLPs into the domain of small molecule activation, with boron/carbene[10, 11], boron/amine[12] and phosphorus/nitrogen[13] pairs proving to be particularly effective. Theoretical studies have also contributed to the understanding of FLP chemistry[14-18].

Thus, the discovery of FLPs has opened up the door to cooperativity in non-metal systems. Recently, Douglas Stephan's group[7] has shown how the concept can be extended to include metal systems, employing an aluminium-phosphorus system as a frustrated Lewis pair. This has been further extended recently by Duncan Wass and co-workers[19, 20] to include transition metal systems, by making FLPs with cationic zirconocene-phosphinoaryloxide complexes. These complexes were found to exhibit the same ditopic activation that is present in the main-group FLPs but had the advantage of exhibiting significantly higher reactivity than their non-metal counterparts. Moreover, the zirconium based FLPs also showed the ability to mediate in reactions for which main group FLPs have been ineffective[19]. Their work therefore demonstrates that the concept of FLPs can be employed as a means of developing new avenues for metal-ligand cooperativity. Other zirconium based FLP systems have also been developed[2,21]. New developments in metal-ligand cooperativity hold great significance[22], since this has led to the facilitation, under mild conditions, of the catalysis of an array of important reactions. The group of David Milstein, for instance, has exploited metal-ligand cooperativity *via* aromatization-dearomatization of pincer type pyridinic or acridinic moieties with several transition metals[23]. These complexes can readily cleave the O-H bond in water as well as

the N-H bond in amines at room temperature[24]. Several types of hybrid[25], hemi-labile[25] or non-innocent[25] ligands have "cooperated" with metals in mediating in a variety of different reactions. Cooperation between ruthenium and nitrogen of the coordinated pincer ligand, for instance, has been found to lead to the very efficient catalysis of important reactions such as the dehydrogenation of ammonia borane[26]. Hence, given the importance of the field of metal-ligand cooperativity, the true significance of the work of Duncan Wass's group in designing a system exploiting metal-ligand cooperativity through a metal-nonmetal FLP combination (zirconium and phosphorus[19, 20], mentioned earlier), may lie in its showcasing of the possibilities of designing new metal-nonmetal FLP combinations that can exhibit interesting chemical reactivity, especially for catalytic transformations.

In this context, it is interesting to note that the cationic active species in the Wass FLP complexes bear a resemblance to the active species employed in the solution phase homogeneous olefin polymerization catalysts[27, 28]. The cationic zirconocene-phosphinoaryloxide species prepared by Wass and co-workers can be considered a modification of the cationic zirconocene complex (known to be an active olefin polymerization catalyst[27, 28]), with the addition of a phosphine group that can bind weakly to the metal (see Figure 1 below). It is therefore pertinent to consider the possibility of other transition metal systems also having the potential to act as FLPs, if they can be modified from analogous complexes that have been found to be efficient homogeneous olefin polymerization catalysts. This idea has significance because one could then conceivably expand the concept of highly efficient FLPs to late transition metal complex systems, since late transition metal complexes have been known to be good catalysts for homogeneous olefin polymerization catalysis. In this regards, another example of a late transition metal complex that could function as an FLP is a ruthenium based complex employed by Douglas Stephan's group[29].

With regard to the idea proposed above, of designing late transition metal FLPs based on a comparison to effective, existing homogeneous olefin polymerization catalyst, one potential candidate is the diimine ligand-based palladium complex[30], denoted as **I** in

Figure 1 below. There are several examples known of labile bonds between phosphines (both aromatic and aliphatic) and late transition metals[31-34]. One can envisage a cationic palladium species with a weak metal-phosphorus linkage (denoted as **II**), which is a modification of **I**. It is likely that the Pd-P bond in **II** would be labile, since the complex is isolobal to the neutral, square planar rhodium complex,[$(PEt_3)_3Rh(NHAr)$ (Ar=*p*-tolyl)] which is known to have a labile rhodium-phosphorus bond[35]. Calculations comparing the ease of separation of the rhodium phosphorus bond in $(PEt_3)_3Rh(NHAr)$ (Ar=*p*-tolyl) with that of the palladium phosphorus bond in **II**, shown in Figure 2, indicate that the energy of metal-P separation in the two cases is quite comparable.

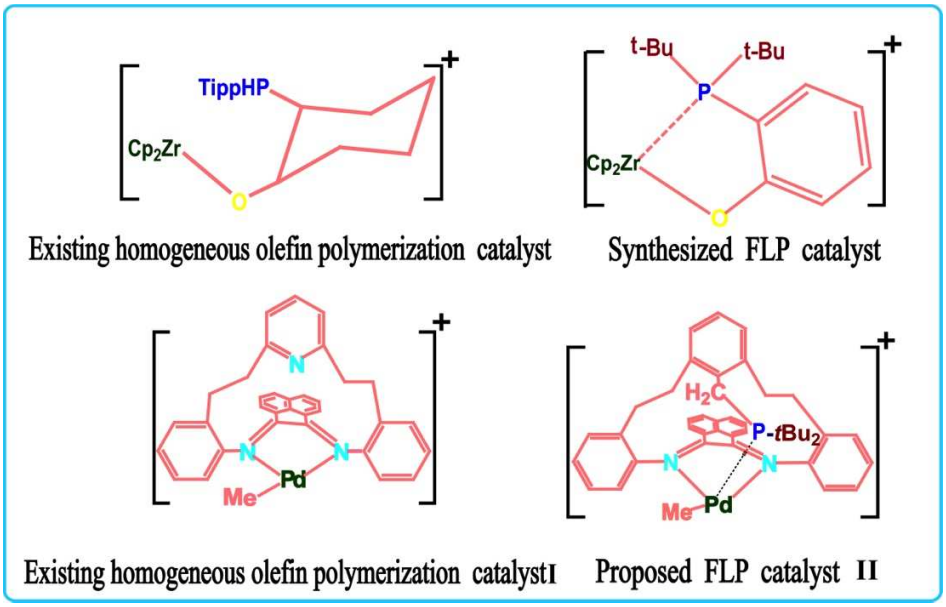

Figure 1. The concept behind the proposed palladium based frustrated Lewis pair: analogy to olefin polymerization catalysts; the colour scheme is as follows: carbon – pink, nitrogen – light blue, palladium, zirconium (TM center) – green, phosphorus – blue, oxygen – yellow, the tertiary butyl groups – red.

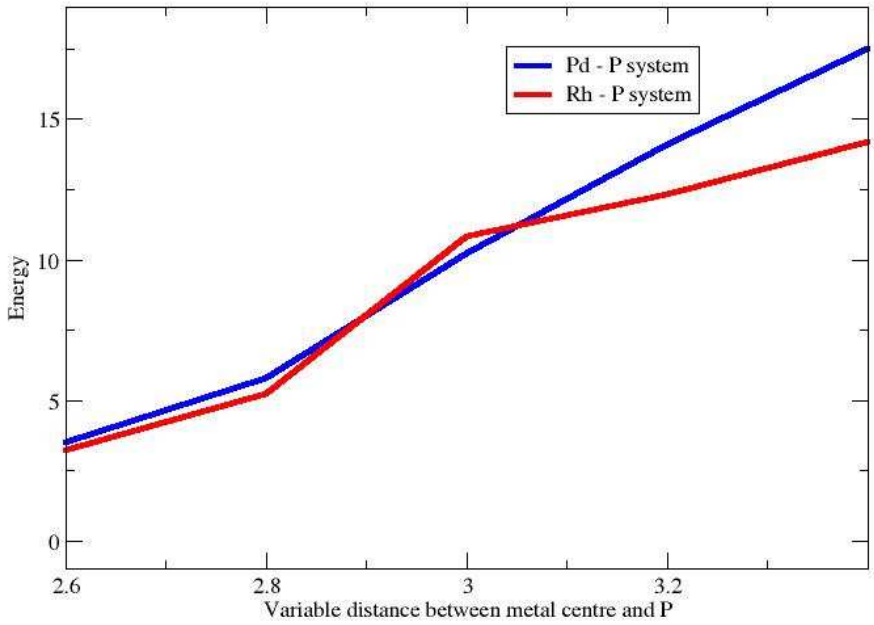

Figure 2. Comparison of the energy required to displace the phosphorus atom from the metal centre for the Rh,[$(PEt_3)_3$Rh(NHAr) (Ar=*p*-*t*olyl)] and the proposed palladium based FLP complex **II**, discussed in the manuscript (see Figure 1); the values along the X axis are in A^0, and along the Y axis are in kcal/mol.

Hence, based on the ideas discussed here, we postulate that a cationic palladium species of the type **II** shown in Figure 1 can serve as an example of a very effective late-transition metal containing FLP. This will be demonstrated by full quantum chemical calculations with density functional theory (DFT) calculations, exploring the FLP behaviour of **II** for the dehydrogenation of ammonia borane (AB), an important candidate for the chemical storage of hydrogen. It is noted here that **II** is used primarily as an example to highlight how the concept of FLPs can be extended to late transition metals. Since palladium complexes are easy to handle and do bench-top chemistry with[36], the work discussed here opens up new possibilities in the field of metal-ligand cooperativity using late transition metal based FLPs.

3.2 Computational Details

The DFT calculations have been done with the Turbomole suite of programs, using Turbomole 6.0[37]. The TZVP basis set[38-40](triple-z basis set augmented by a polarization function) and the PBE functional[41-44] have been employed in all the calculations. The resolution of identity (RI)[45], along with the multipole accelerated resolution of identity (marij)[46] approximations were employed for an accurate and efficient treatment of the electronic Coulomb term in the DFT calculations. Furthermore, single point MP2[47-50] calculations (also with the RI approximation) have been done with the optimized minima and transition state structures for all the species along the potential energy surface for the catalytic pathways for AB dehydrogenation. Solvent effects have been included for the solvent dichloromethane ($\varepsilon = 9.08$) through single point calculations with the Conductor Like Screening Model – COSMO[51]. Frequency calculations have been done at the DFT level in order to obtain the zero point energy, the internal energy and entropic contributions (calculated at 298.15 K). Care was taken to ensure that the obtained transition state structures possessed only one imaginary frequency corresponding to the correct normal mode. Hence the numbers reported are ΔG values.

3.3 Results and Discussion

The proposed precursor to the cationic diimine palladium complex **II**, shown in Figure 1, is likely to be easily synthesized by following the same route[30] as that employed experimentally to synthesize the analogous α-diimine ligand-Pd (II) system **I**. The diimine cationic complex **II** can then be formed *in situ* in solution by the addition of a co-catalyst such as MAO, as is commonly done in homogeneous olefin polymerization catalysts[52]. Shown in Figure 3 is the reaction pathway for the dehydrogenation of ammonia borane (AB) using complex **II**. Ammonia borane (AB), it is noted, is one of the most promising compounds for the chemical storage of hydrogen[53,54], and the efficient catalysis of its dehydrogenation has been an important area of work in the field of hydrogen storage research[55]. The three barriers involved in dehydrogenating AB are calculated to lie in the range 4.0-25.0 kcal/mol (first barrier = 25.0 kcal/mol, second

barrier = 7.3 kcal/mol and third barrier = 4.0 kcal/mol, all values are solvent corrected ΔG values; see Figure 3), which is comparable to barriers obtained for existing, state-of-the-art AB dehydrogenation catalyst systems[56]. The first, rate determining step, involves the dissociation of the phosphorus from the palladium centre, as well as the extraction of two hydrogens from AB: the hydridic hydrogen, coordinated to boron being taken by the palladium centre in the catalyst and the protic hydrogen, coordinated to the nitrogen, being extracted by the phosphorus atom (see Figure 3). This would lead to a phosphonium cationic species that can coordinate to the metal center. Examples of complexes where a phosphonium cation coordinates to the metal center are known[57-59]. Thus, the metal-phosphorus bond distance is increased in this transition state. This leads to the intermediate, indicated as **II-H_2** in Figure 3. It is to be noted that the competing alternate possibility: the oxidative addition of two hydrogens directly to the palladium (II) center, is unlikely. This is because the product for this competing process has been calculated to be 6.2 kcal/mol higher in energy than **II-H_2**.

After the formation of **II-H_2**, the next step involves the transfer of the phosphorus bound hydrogen to the palladium center *via* a three-membered transition state involving palladium, phosphorus and hydrogen, followed by the removal of H_2 from the metal, thus completing the cycle. Like rhodium in hydroformylation[60], palladium shows here the ability to increase its coordination number by two units. The angle between the two hydrogen atoms with palladium (81.2°) is comparable with the $P(OPh)_3$ modified rhodium hydroformylation catalyst (79.2°) described by Sparta *et al*[60]. The low barriers for the successive steps indicate that the cycle would be catalytic, since the intermediates formed would proceed to yield the products. Also, the value of the barriers obtained suggests that the catalysis would be possible at room temperature.

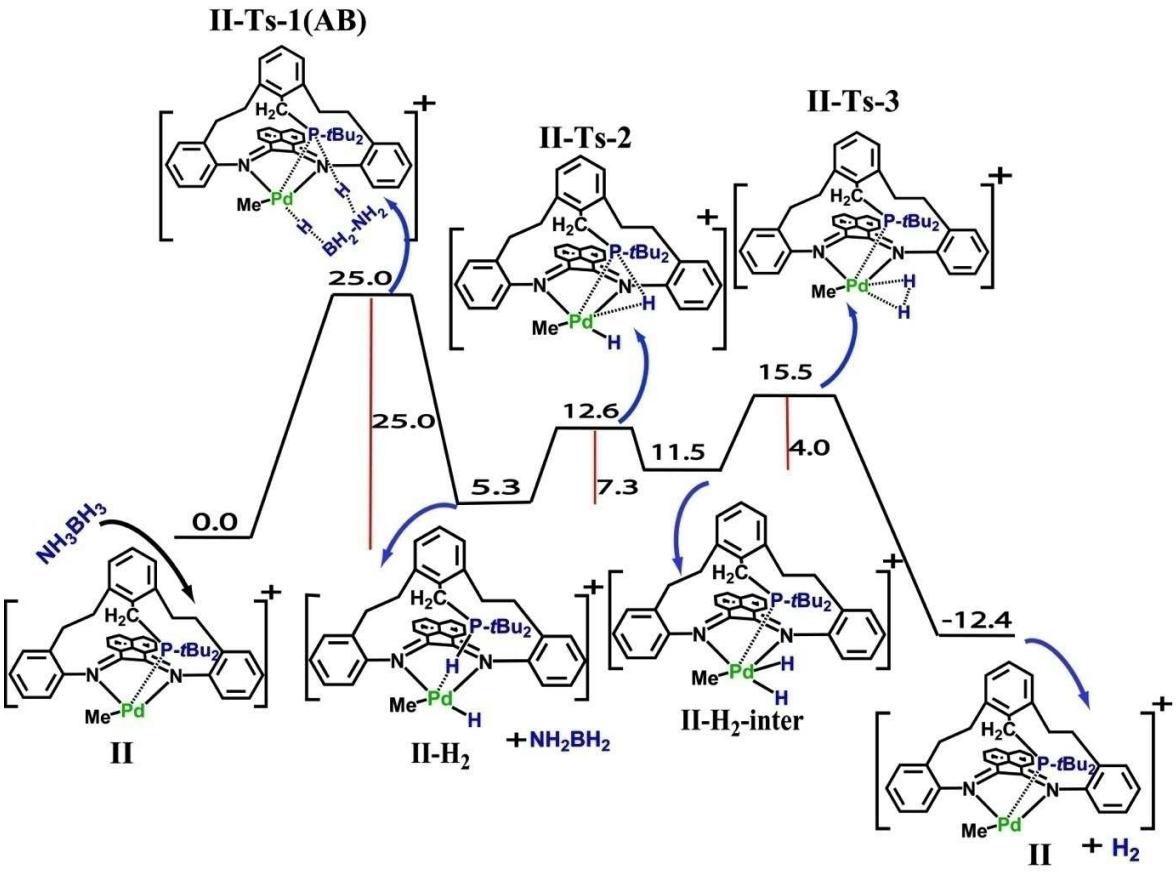

Figure 3. The schematic representation of the free energy surface for the catalysis of the dehydrogenation of ammonia borane (AB) using the proposed palladium based FLP; only the hydrogens of AB are shown, the rest have been removed for the purpose of clarity; all the values are in kcal/mol.

Figure 3 discuss the free energy (ΔG) values for the catalytic pathway for the AB dehydrogenation process. The corresponding enthalpy (ΔH) values have also been shown, in Figure 4 below. (However, all the other reaction pathway figures shown below in the chapter indicate the free energy surface.) A perusal of the corresponding ΔH values shows that the barrier heights are not different: the slowest (first) step of the reaction has a ΔG barrier of 25.0 kcal/mol (see Figure 3), while the ΔH value for this step is 23.9 kcal/mol (see Figure 4). The chief difference occurs in the overall thermodynamics of the reaction: while the calculated free energy surface, indicated above, is shown to be

exergonic by 12.4 kcal/mol, (see Figure 3), it is calculated to be endergonic by 6.7 kcal/mol when ΔH is considered (see Figure 4). This indicates that there is significant entropic gain in the elimination of dihydrogen from the vicinity of the catalyst, which makes the overall reaction exergonic in ΔG. A similar trend is observed in the case of all the free energy and enthalpy surfaces that have been discussed in the other reactions pathways below: the barrier heights calculated are about the same in both ΔG and ΔH, but the overall exergonicity of the reaction is significantly helped by the inclusion of entropy (in the ΔG values).

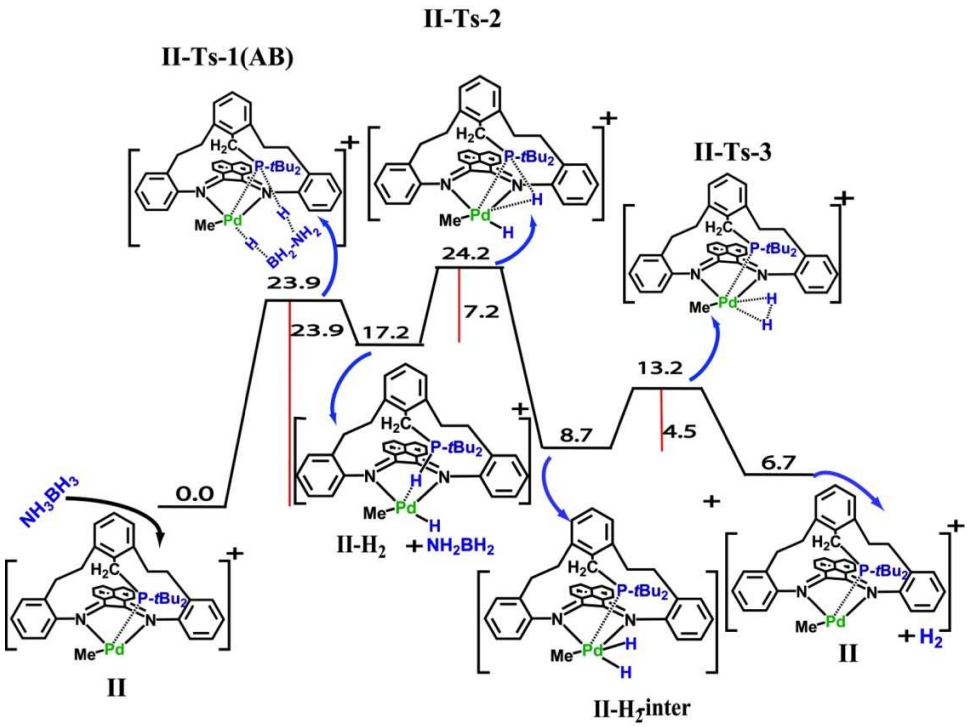

Figure 4. The schematic representation of the reaction enthalpy (ΔH) surface for the catalysis of the dehydrogenation of ammonia borane (AB) using the proposed palladium based FLP; all the values are in kcal/mol.

While the reaction shown in Figure 4 indicates the reaction to be favourable, it is to be noted that there is a competing reaction to this catalysis pathway. This is outlined in Figure 5 below: after the formation of the **II-H$_2$** species, it is possible that the methyl group attached to the palladium center can combine with the hydride that is now present

at the metal center, thereby forming methane, CH_4, and leading to a new complex denoted as **III** in Figure 5 below. Palladium complexes have shown the propensity to undergo such a reductive elimination process[61]. The energetics of this process is indicated to be quite favourable: both kinetically and thermodynamically. While the slowest step for the pathway from **II-H$_2$** to **II** is 7.3 kcal/mol, the reductive elimination step from **II-H$_2$** to **III** is 4.9 kcal/mol. Moreover, while the final product complex is found to be stable by 12.4 kcal/mol in the catalysis pathway, it is stable by 36.3 kcal/mol in the reductive elimination pathway. These results indicate that while the palladium complex **II** might be successful at catalyzing the dehydrogenation of ammonia borane, it is more likely that ammonia borane would serve to provide **II** with hydrogens to convert it to the reduced complex **III**.

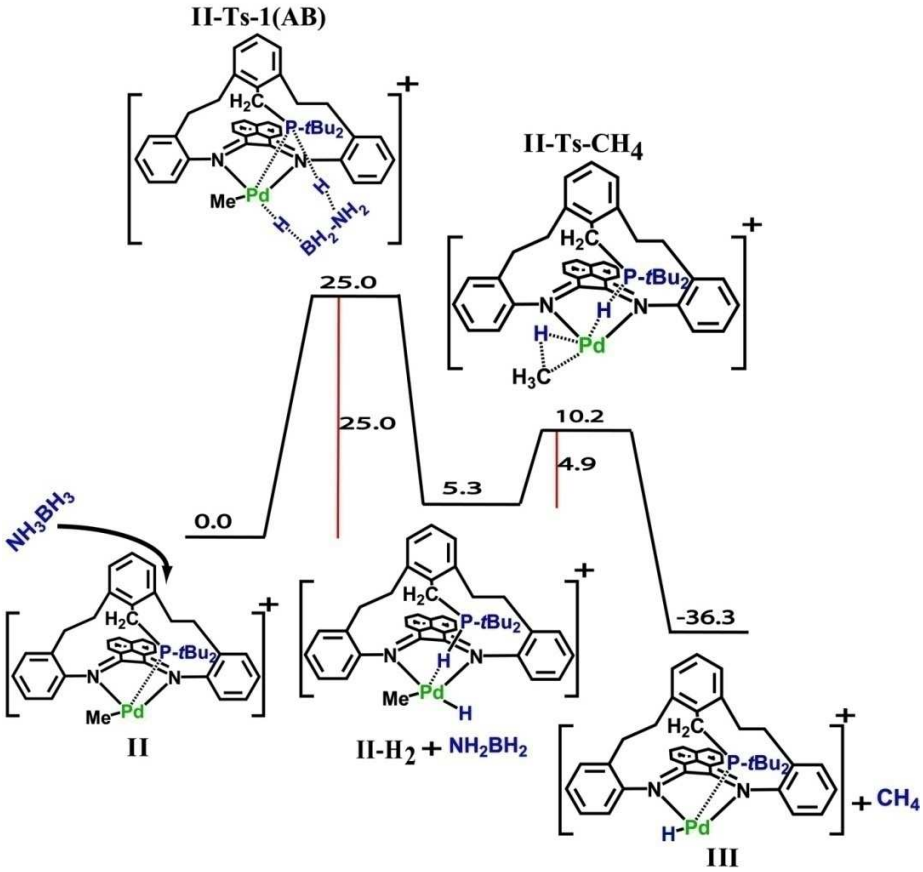

Figure 5. The schematic representation of the free energy surface showing the possibility of dehydrogenation of ammonia borane followed by a reductive elimination step leading

to the loss of methane from the palladium complex; only the hydrogens of AB are shown, the rest have been removed for the purpose of clarity; all the values are in kcal/mol.

However, the fact that this reductive elimination reaction is so thermodynamically favorable also indicates that the resultant complex would be a very stable species, and therefore likely to exist for a long time in the reaction mixture. Since **II** would only be present in catalytic amounts in comparison to the substrate AB, only a small amount of AB would have been expended in order to create the complex **III**. Since **III** also possesses a labile palladium-phosphorus bond (see Figures 5 and 6), it can also act as an FLP. This possibility has been investigated, with the results being indicated in Figure 6 below. It is seen that **III** would also be a very effective catalyst for the dehydrogenation of ammonia borane: the slowest step of the reaction has a barrier of 27.5 kcal/mol. It is to be noted that the reactant in this case lies 36.3 kcal/mol lower in energy than the beginning reactant species, as seen from the previous Figure 5. Hence, the process yielding the final, regenerated species **III**, with the elimination of H_2, is seen to be highly exergonic, by 57.1 kcal/mol (see Figure 6 below). Similar exergonic profiles will also be observed for other processes that will be described subsequently.

As opposed to the three step AB dehydrogenation catalysis by **II**, **III** achieves the AB dehydrogenation catalysis in only two steps, with the second step having a barrier of only 2.1 kcal/mol. Hence, it is quite possible that, were **II** to be employed as a potential catalyst for AB dehydrogenation, it would serve primarily as a pre-catalyst, creating the FLP **III**, which would act as the actual active catalyst in solution.

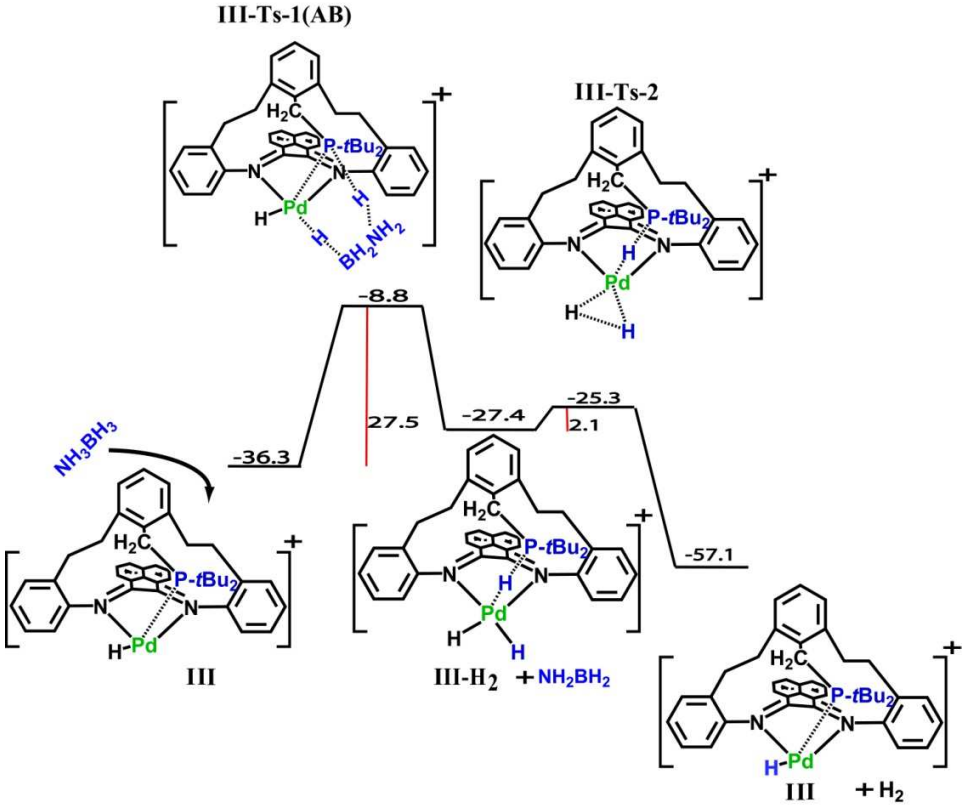

Figure 6. The schematic representation of the free energy surface for the catalysis of the dehydrogenation of ammonia borane (AB) using FLP (**III**) formed during the catalysis; only the hydrogens of AB are shown, the rest have been removed for the purpose of clarity; the colour scheme is the same as used in Figure 1; all the values are in kcal/mol.

It is to be noted that AB dehydrogenation catalysis has been demonstrated in the past with cationic palladium complexes[62]. The novelty in the current approach lies in the exploitation of metal ligand cooperativity between the palladium and the phosphorus atom in the original FLP**II**, as well as in the FLP formed *in situ*, **III**, in order to effect the catalysis.

A further reaction that has been considered is the hydrogenation of alkenes such as ethylene. This would occur if ethylene were to be present in the reaction vessel in high concentrations, allowing the species **II-H2**, formed as the intermediate in the dehydrogenation processes discussed above, to transfer the hydrogens to the alkene, thereby forming the corresponding alkane. This is illustrated in Figure 7 below. The ΔG

value for the transfer process was found to be 32.8 kcal/mol. While this barrier is higher than the AB dehydrogenation barriers discussed earlier, it is likely that the process could occur at elevated temperatures. Reactions having a barrier of 35.0-40.0 kcal/mol have been known to occur at temperatures of about 50°C[63-66].

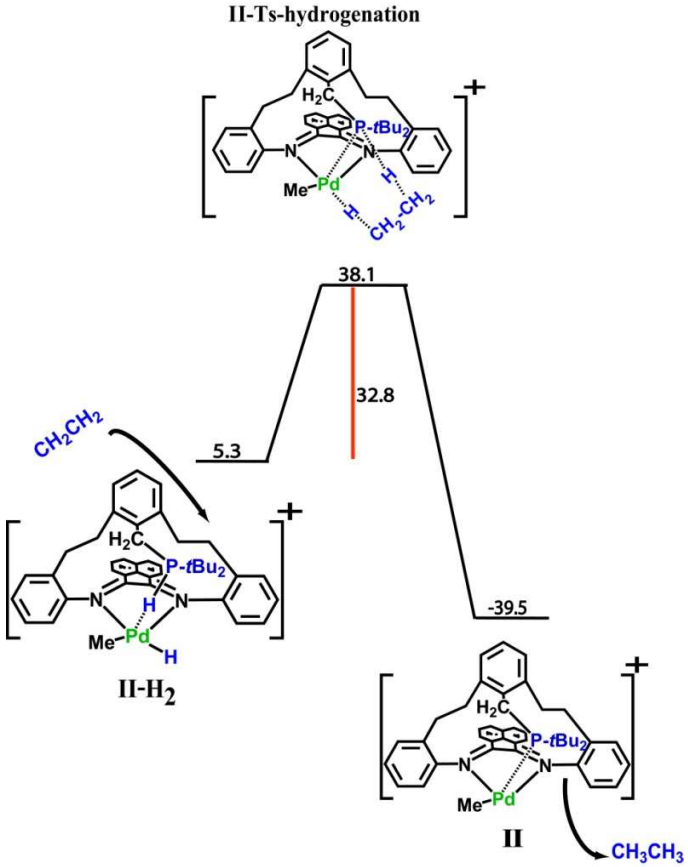

Figure 7. The schematic representation of the free energy surface for the hydrogenation of ethylene with the hydrated palladium based FLP-**II-H_2**; all the values are in kcal/mol.

Furthermore, as discussed above, since **II** would be likely to yield the new FLP **III** in solution, the possibility of **III** effecting the hydrogenation of alkenes has also been considered. As shown in Figure 8 below, this, too, is a process that would be favourable at temperatures slightly higher than ambient temperatures, having a barrier of 31.5 kcal/mol, with the product laying a very stable 74.3 kcal/mol on the free energy surface.

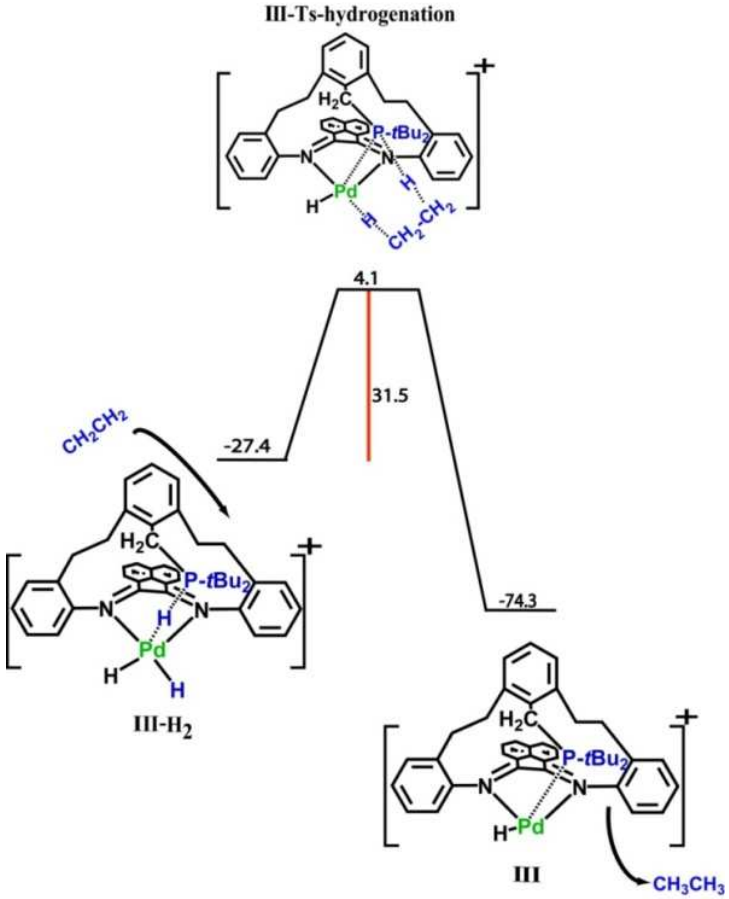

Figure 8. The schematic representation of the free energy surface for the hydrogenation of ethylene with the hydrated palladium based FLP-**III-H$_2$** formed during the catalysis; all the values are in kcal/mol.

One can also imagine variations to the proposed palladium based FLP complex **II**. As shown in Figure 9, a simpler system can be envisaged, with a palladium phosphorus bond, but with no connection between the phosphorus and the diimine ligand system.

Such a complex can also act to dehydrogenate ammonia borane (Figure 9), hydrogenate ethylene (Figure 12) with barriers comparable to the analogous reactions with **II**. The possibility that the new FLP, **III-s**, would be formed *in situ*, and also serve as a catalyst has also been studied. The results, indicated in Figure 9 and 10 below, show that **III-s**, too, would be quite effective as an FLP.

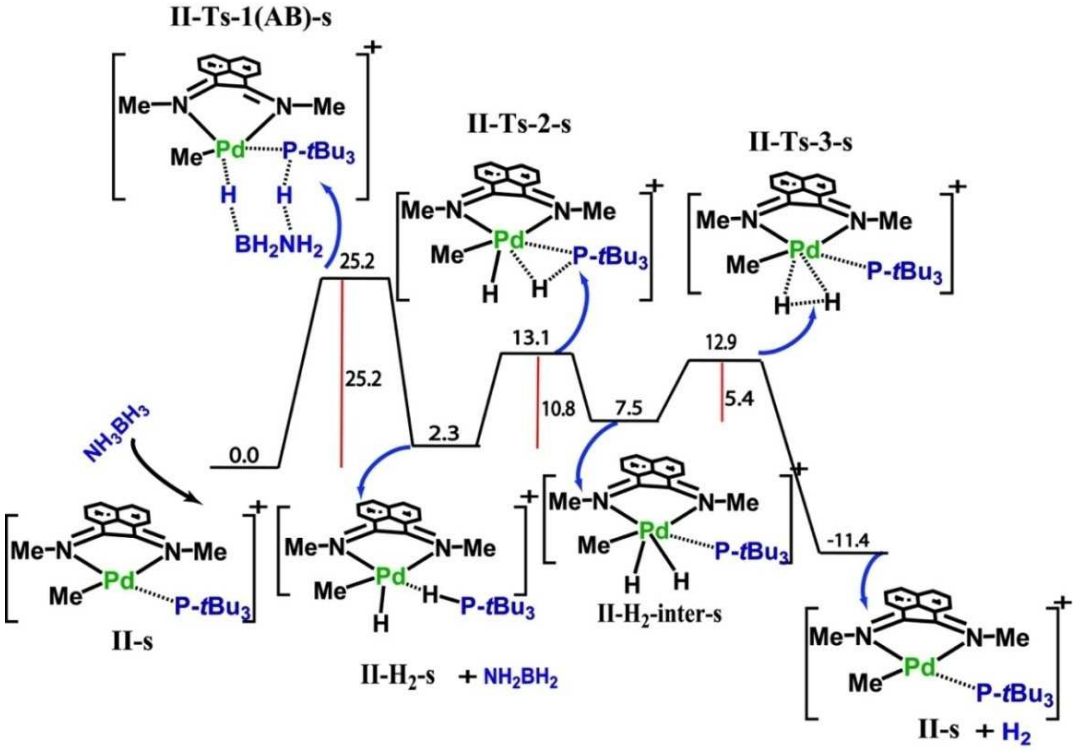

Figure 9. A simpler palladium based FLP system: no linkage between the phosphorus and the diimine ligand; shown above is the free energy surface for the catalysis of the dehydrogenation of ammonia borane; all the values are in kcal/mol.

The only potential drawback in employing simpler FLP analogues to **II** is that the possibility exists that the coordinating phosphine, not being bound to the diimine ligand, can be completely displaced from the metal coordination sphere by solvent molecules, or other species in solution, thereby not allowing the metal-ligand cooperativity to occur effectively. Nevertheless, in the presence of phosphine as an extra reagent in the reaction mixture, FLPs of the type shown in the Figures 9 to 13 may also be effective at small molecule activation and catalysis.

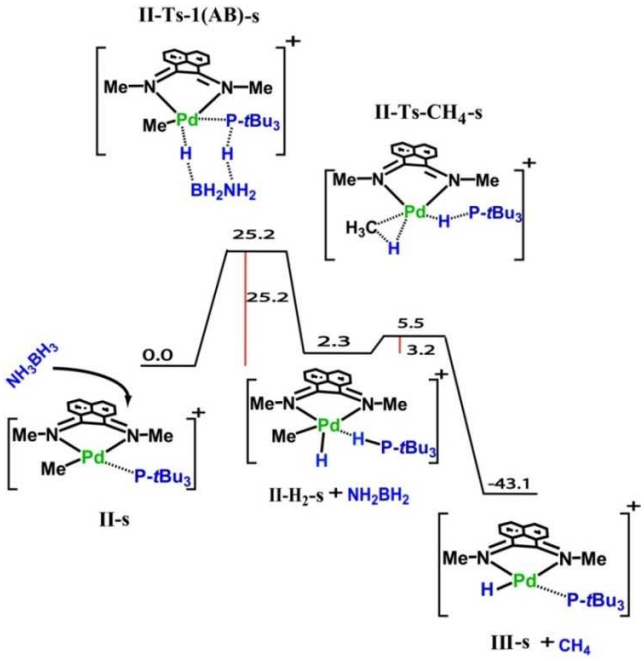

Figure 10. The schematic representation of the free energy surface showing the possibility of dehydrogenation of ammonia borane followed by a reductive elimination step leading to the loss of methane from the simple palladium complex; only the hydrogens of AB are shown, the rest have been removed for the purpose of clarity; all the values are in kcal/mol.

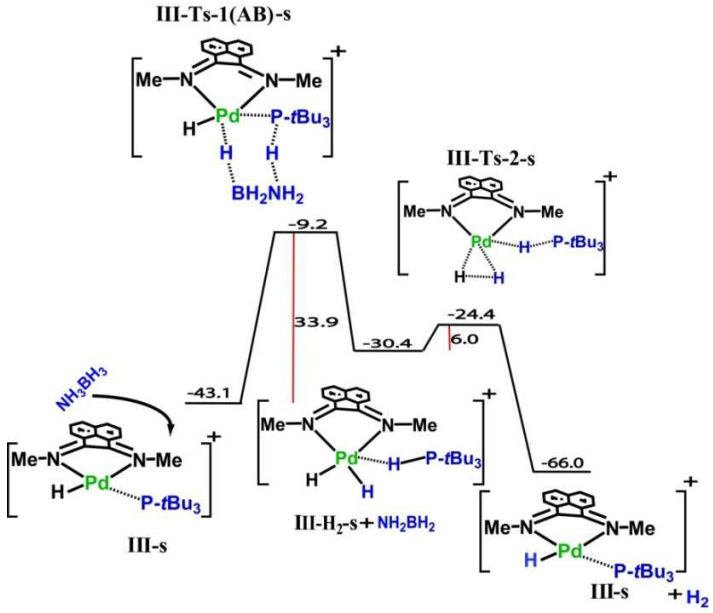

Figure 11. The schematic representation of the free energy surface for the catalysis of the dehydrogenation of ammonia borane (AB) using FLP (**III-s**) formed during the catalysis; with the simple palladium based FLP; all the values are in kcal/mol.

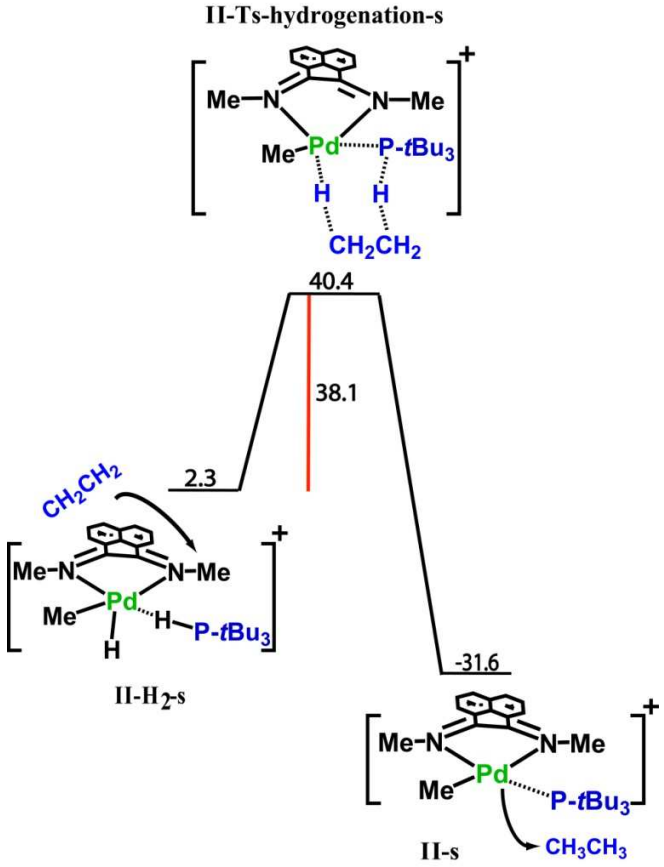

Figure 12. The schematic representation of the free energy surface for the hydrogenation of ethylene to ethane with the hydrogenated simple palladium based FLP; all the values are in kcal/mol.

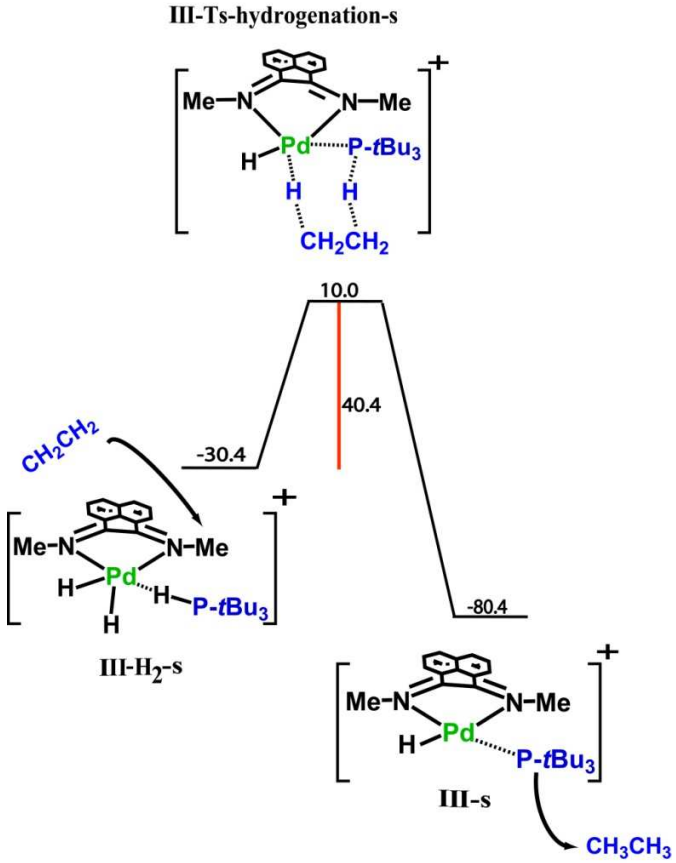

Figure 13. The schematic representation of the free energy surface for the hydrogenation of ethylene with the hydrated simple palladium based FLP-**III-H_2-s**formed during the catalysis; all the values are in kcal/mol.

3.4 Conclusions

In summary, by analogy to homogeneous olefin polymerization catalysts, late transition metal frustrated Lewis pairs (FLPs) have been proposed, based on the design of an α diimine ligand having a labile phosphorus bond with the metal (palladium) centre.This complex has been investigated as an example to illustrate the potential of late transition metal containing FLPs at mediating in important chemical transformations. Calculations with DFT/MP2 methods indicate that such late transition metal containing FLPs would be effective at catalyzing the dehydrogenation of ammonia borane (AB), as well as facilitating the hydrogenation of ethylene at high concentrations of the substrate. The possibility of side reactions occurring during the catalysis has been investigated, and it

has been found that, while competing reactions such as the reductive elimination of alkanes, would be possible, the resulting products can also serve as equally effective or even better FLPs for catalysis processes. As such, the current work opens up exciting new possibilities in the area of metal-ligand cooperativity and small molecule activation.

3.5 References

1. P. Spies, S. Schwendemann, S. Lange, G. Kehr, R. Fröhlich, G. Erker, *Angew. Chem., Int. Ed.,* 2008, 47, 7543–7546.

2. K. V. Axenov, G. Kehr, R. Fröhlich, G. Erker, *Organometallics*, 2009, 28, 5148–5158.

3. G. Ménard, D. W. Stephan, *J. Am. Chem. Soc.*, 2010, 132, 1796–1797.

4. C. M. Mömming, E. Otten, G. Kehr, R. Fröhlich, S. Grimme, D. W. Stephan, G. Erker, *Angew. Chem., Int. Ed.,* 2009, 48, 6643–6646.

5. D. W. Stephan, G. Erker, *Angew. Chem., Int. Ed.,* 2010, 49,46–76.

6. J. S. J. McCahill, G. C. Welch, D. W. Stephan, *Angew. Chem., Int. Ed.*, 2007, 46, 4968–4971.

7. M. A. Dureen, D. W. Stephan, *J. Am. Chem. Soc.*, 2009, 131, 8396–8397.

8. P. A. Chase, T. Jurca, D. W. Stephan, *Chem. Commun.*, 2008, 1701–1703.

9. P. A. Chase, G. C. Welch, T. Jurca, D. W. Stephan, *Angew. Chem., Int. Ed.*, 2007, 46, 8050–8053.

10. P. A. Chase, D. W. Stephan, *Angew. Chem., Int. Ed.*,2008, 47, 7433–7437.

11. D. Holschumacher, T. Bannenberg, C. G. Hrib, P. G. Jones, M. Tamm, *Angew. Chem., Int. Ed.*, 2008, 47, 7428–7432.

12. V. Sumerin, F. Schulz, M. Atsumi, C. Wang, M. Nieger, M. Leskelä, T. Repo, P. Pyykkö, B. Rieger, J. Am. Chem. Soc., 2008, 130, 14117–14119.

13. L. J. Hounjet, C. B. Caputo, D. W. Stephan, *Angew. Chem., Int. Ed.*, 2012, 51, 4714–4717.

14. T. A. Rokob, A. Hamza, A. Stirling, T. Soós, I. Pápai, *Angew. Chem.*, 2008, 120, 2469–2472.

15. S. Grimme, H. Kruse, L. Goerigk, G. Erker, *Angew. Chem., Int. Ed.*, 2010, 49, 1402–1405.

16. G. Lu, H. Li, L. Zhao, F. Huang, Z.-X. Wang, *Inorg. Chem*., 2009, 49, 295–301.

17. Y. Guo, X. He, Z. Li, Z. Zou, *Inorg. Chem.*, 2010, 49, 3419–3423.

18. A. Pal, K. Vanka, *Chem. Commun.*, 2011, 47, 11417– 11419.

19. A. M. Chapman, M. F. Haddow, D. F. Wass, *J. Am. Chem. Soc*., 2011, 133, 18463–18478.

20. A. M. Chapman, M. F. Haddow, D. F. Wass, *J. Am. Chem. Soc.*, 2011, 133, 8826–8829.

21. G. Bender, T. Wiegand, H. Eckert, R. Fröhlich, C. G. Daniliuc, C. Mück-Lichtenfeld, S. Ndambuki, T. Ziegler, G. Kehr, G. Erker, *Angew. Chem., Int. Ed.*,2012, 51, 8846–8849.

22. C. Gunanathan, D. Milstein, *Acc. Chem. Res*., 2011, 44, 588–602.

23. S. W. Kohl, L. Weiner, L. Schwartsburd, L. Konstantinovski, L. J. W. Shimon, Y. Ben-David, M. A. Iron, D. Milstein, *Science*, 2009, 324,74–77.

24. E. Khaskin, M. A. Iron, L. J. W. Shimon, J. Zhang, D. Milstein, *J. Am. Chem. Soc.*, 2010, 132, 8542–8543.

25. H. Grützmacher, *Angew. Chem., Int. Ed*.,2008, 47, 1814– 1818.

26. N. Blaquiere, S. Diallo-Garcia, S. I. Gorelsky, D. A. Black, K. Fagnou, *J. Am. Chem. Soc*., 2008, 130, 14034– 14035.

27. T. Koch, S. Blaurock, E. Hey-Hawkins, M. Galan-Fereres, D. Plat, M. S. Eisen, *J. Organomet. Chem.*, 2000, 595, 126–133.

28. A. V. Firth, J. C. Stewart, A. J. Hoskin, D. W. Stephan, *J. Organomet. Chem.*, 1999, 591, 185–193.

29. M. J. Sgro, D. W. Stephan, *Angew. Chem., Int. Ed*., 2012, 51, 11343–11345.

30. D. H. Leung, J. W. Ziller, Z. Guan, *J. Am. Chem. Soc*., 2008, 130, 7538–7539.

31. A. W. Holland, R. G. Bergman, *J. Am. Chem. Soc*., 2002, 124, 14684–14695.

32. J. K. MacDougall, D. J. Cole-Hamilton, *J. Chem. Soc., Chem. Commun*., 1990, 165–167.

33. J. K. MacDougall, M. C. Simpson, M. J. Green, D. J. Cole-Hamilton, *J. Chem. Soc., Dalton Trans.*, 1996, 1161–1172.

34. P. Cheliatsidou, D. F. S. White, D. J. Cole-Hamilton, *Dalton Trans.*, 2004, 3425–3427.

35. P. Zhao, C. Krug, J. F. Hartwig, *J. Am. Chem. Soc*., 2005, 127, 12066–12073.

36. S. E. Denmark, R. A. Stavenger, A.-M. Faucher, J. P. Edwards, *J. Org. Chem*., 1997, 62, 3375–3389.

37. R. Ahlrichs, M. Bär, M. Häser, H. Horn, C. Kölmel, *Chem. Phys. Lett*., 1989, 162, 165–169.

38. F. Weigend, *Phys. Chem. Chem. Phys*., 2002, 4, 4285–4291.

39. F. Weigend, R. Ahlrichs, *Phys. Chem. Chem. Phys*., 2005, 7, 3297–3305.

40. A. Schafer, H. Horn, R. Ahlrichs, *J. Chem. Phys*., 1992, 97, 2571–2577.

41. P. A. M. Dirac, *Proc. R. Soc. London, Ser. A*, 1929, 123, 714–733.

42. J. C. Slater, *Phys. Rev*., 1951, 81, 385–390.

43. J. P. Perdew, K. Burke, M. Ernzerhof, *Phys. Rev. Lett*., 1996, 77, 3865–3868.

44. J. P. Perdew, Y. Wang, *Phys. Rev. B: Condens. Matter*, 1992, 45, 13244–13249.

45. K. Eichkorn, O. Treutler, H. Öhm, M. Häser, R. Ahlrichs, *Chem. Phys. Lett.*, 1995, 240, 283–290.

46. M. Sierka, A. Hogekamp, R. Ahlrichs, *J. Chem. Phys*., 2003, 118, 9136–9148.

47. C. Hattig, *J. Chem. Phys*., 2003, 118, 7751–7761.

48. C. Hattig, K. Hald, *Phys. Chem. Chem. Phys*., 2002, 4, 2111–2118.

49. C. Hattig, A. Kohn, K. Hald, *J. Chem. Phys*., 2002, 116, 5401–5410.

50. C. Hattig, F. Weigend, *J. Chem. Phys*., 2000, 113, 5154– 5161.

51. A. Klamt, G. Schuurmann, *J. Chem. Soc., Perkin Trans. 2*, 1993, 799–805.

52. S. D. Ittel, L. K. Johnson, M. Brookhart, *Chem. Rev*., 2000, 100, 1169–1204.

53. A. Staubitz, A. P. M. Robertson, I. Manners, *Chem. Rev*., 2010, 110, 4079–4124.

54. M. C. Denney, V. Pons, T. J. Hebden, D. M. Heinekey, K. I. Goldberg, *J. Am. Chem. Soc*., 2006, 128, 12048– 12049.

55. T. B. Marder, *Angew. Chem., Int. Ed*.,2007, 46,8116– 8118.

56. Y. Luo, K. Ohno, *Organometallics*, 2007, 26, 3597– 3600.

57. N. Kuhn, G. Henkel, M. Göhner, *Z. Anorg. Allg. Chem*., 1999, 625, 1415–1416.

58. J.,rieu, M. Azouri, P. Richard, *Inorg. Chem. Commun*., 2008, 11, 1401–1404.

59. I. Abdellah, C. Lepetit, Y. Canac, C. Duhayon, R. Chauvin, *Chem. Eur. J*., 2010, 16, 13095–13108.

60. M. Sparta, K. J. Børve, V. R. Jensen, *J. Am. Chem. Soc*., 2007, 129, 8487–8499.

61. B. Kellenberger, S. J. Young, J. K. Stille, *J. Am. Chem. Soc*., 1985, 107, 6105–6107.

62. S.-K. Kim, W.-S. Han, T.-J. Kim, T.-Y. Kim, S. W. Nam, M. Mitoraj, Ł. Piekoś, A. Michalak, S.-J. Hwang, S. O. Kang, *J. Am. Chem. Soc*., 2010, 132, 9954–9955.

63. A. Berkessel, J. A. Adrio, *J. Am. Chem. Soc*., 2006, 128, 13412–13420.

64. W. J. Shaw, J. C. Linehan, N. K. Szymczak, D. J. Heldebrant, C. Yonker, D. M. Camaioni, R. T. Baker, T. Autrey, *Angew. Chem., Int. Ed.*, 2008, 47, 7493–7496.

65. P. M. Zimmerman, A. Paul, Z. Zhang, C. B. Musgrave, *Inorg. Chem.*, 2009, 48, 1069–1081.

66. M. T. Nguyen, V. S. Nguyen, M. H. Matus, G. Gopakumar, D. A. Dixon, *J. Phys. Chem. A*, 2007, 111, 679–690.

Chapter 4

The Potentially Effective Porous Organic Cages With Different Lewis Pair Combinations For The Organocatalysis Of Ammonia Borane

Abstract

Zero Dimensional cage structure containing four phenyl rings separated by imine linkers have recently been synthesized. In the current work, a computational investigation using density functional theory (DFT), we demonstrate that modifying such cages by replacing the 2, 4, 6 carbon atoms in the phenyl rings to yield new rings, as well as replacing the imine moiety in the linker by other electronegative atoms, can yield interesting new cages that can be reactive in catalysing reactions such as the dehydrogenation of ammonia borane – an important reaction in hydrogen storage research. Specifically, it is predicted that phosphorus-nitrogen pairs (phosphorus in the 2, 4, 6 positions in the ring, nitrogen in the linker position), germanium-nitrogen and germanium-phosphorus pair combinations would lead to effective Lewis pairs that can work in tandem to dehydrogenate ammonia borane efficiently under room temperature conditions.

4.1 Introduction

The possibility of using hydrogen (H_2) as a fuel for transportation purpose has been receiving considerable attention in the last decade. The energy content of hydrogen per unit mass (120 $MJkg^{-1}$) is more than double compared to the conventionally used petroleum based fuels (ca. 44 $MJkg^{-1}$). Moreover, the potential environmental benefits of using hydrogen as a green fuel is the water, which is only the by product. However, a major bottleneck for its utilization is the current lack of a safe and practical method for the on-board storage of hydrogen. Hydrogen remains gaseous over a large range of temperatures and thus poses a hazard to its transportation in cylinders due to large volume. One possible solution involves storage of hydrogen in a chemical compound through a reversible chemical reaction[1-5]. In this respect, ammonia borane (NH_3BH_3, AB, solid at room temperature) and related amine boranes have emerged as attractive candidates for hydrogen storage materials. On account of their high percentage by weight (19.6 wt%) of available hydrogen, ammonia borane has been identified as a highly promising candidate for the chemical storage of hydrogen via the potential reversibility of the dehydrogenation reactions[6, 7]. However, such dehydrogenation reaction involves use of a catalyst, and till date there have been several potential transition metal catalysts are known which can effectively dehydrogenate ammonia borane[8, 9].

One approach to improve on the catalyst systems would be the use of efficient organocatalysts in place of the transition metal catalysts for AB dehydrogenation.The potential advantages of main-group catalysts over transition metal systems are many; the possibility of them being cheaper and more environmentally friendly makes the search worthwhile for the new main-group complexes that can catalyze important reactions such as AB dehydrogenation. Indeed, such a substitution may become necessary for ammonia borane, which is the large scale primary hydrogen storage material. In order to avoid dependence on expensive and non-renewable transition metals, strategies towards using organocatalysts with respect to hydrogen activation and storage have been explored in the literature[10-15].

The “frustrated Lewis pair” (FLP) concept, recently developed by Douglas Stephan’s group[16, 17] involves the cooperation between two main group elements with differing

electronegativity, lying in close proximity in the same molecule[17] or different molecules[18]. Such a pair of main-group elements contain latent Lewis acidity and basicity, because they are not able to bond together due to steric reasons – hence the term "frustrated" Lewis pairs (FLPs). Such FLPs can be exploited for the ditopic activation of different bonds. Frustrated Lewis pairs, such as the boron-phosphorus compound: $(C_6H_2Me_3)_2P(C_6F_4)B(C_6F_5)_2$ and $P(^tBu)_3$ with $B(C_6F_5)_2R$ (where R is an alkyl group), have been employed to do solution phase chemistry in a stoichiometric[18-21] as well as a catalytic fashion[22, 23]. To date, FLPs have been successfully employed for the C-C, C-O, C-H and N-O bond activations in small molecules[18, 22, 24, 25].

Miller *et al.*[26] have used the aforementioned concept to catalyze amine-borane dehydrogenation using a tertiary phosphine borane Lewis pair. On the other hand, Guo *et al.*[27] have shown through DFT calculations that FLPs can serve as an efficient organocatalysts for AB dehydrogenation reaction. In recent years, zero dimensional porous cage molecules have appeared as a new generation materials. In this regard, porous covalent organic cage molecule is shown in Figure 1, designed and experimentally synthesized by Tozawa *et al.* appears to hold considerable promise[28]. This is because the caged structure contains electronegative nitrogen atoms in close proximity to C-H bonds that can act as a potential "frustrated" Lewis pairs. Since AB (NH_3BH_3), unlike its iso-electronic counterpart CH_3CH_3, contains a protic N-H hydrogen and a hydridic B-H hydrogen, it is to be expected that the nitrogen and the proximal carbon atoms in the 0D cage molecule shown in Figure 1 can effectively extract the protic and hydridic hydrogens respectively from AB to give rise to N-H and C-H bonds and form NH_2BH_2: the first step to AB dehydrogenation. Furthermore, since such an extraction would distort the cage structure, an incentive would exist for the newly formed proximal N-H and C-H bonds to break and yield H_2, thereby reconverting to the original undistorted, stable cage. This would complete the catalytic cycle and dehydrogenate AB. Now, since there are twelve nitrogen atoms in each cage, *there is the possibility of several dehydrogenation reactions taking place at the same time, for each cage molecule*, which would make for an efficient organocatalyst[29].

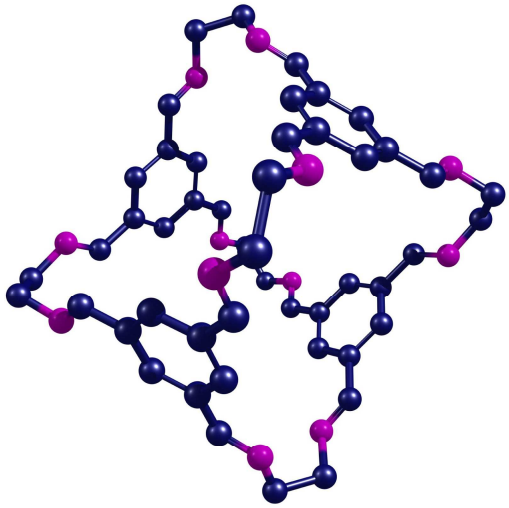

N-C-cage Ia

Figure 1. The porous, organic cage structure synthesized by Tozawa and coworkers; the colour scheme is as follows: dark blue: carbon, violet: nitrogen; the hydrogens have been removed for the sake of clarity.

The reported work therefore suggested that main-group FLPs could be designed that would be effective at catalyzing AB dehydrogenation. However, it was also clear from the work that the potential of the cages required further exploration, as new FLP combinations could be envisaged that could possibly be comparable or even better catalysts than the N-C cage. Shown in Figure 2 are other combinations that are possible: P-C (substitution of the nitrogens in N-C cage by the phosphorus), C-P (each of the imine nitrogens replaced by a carbon and the three carbons in each of the phenyl rings – in the 2, 4 and 6 positions, replaced by phosphorus atoms), N-P, N-Ge and P-Ge cages. Like in the N-C and P-C cages studied earlier, these newly proposed cages would also contain twelve Lewis pairs and hence could potentially perform as multi-site catalysts for reactions such as AB dehydrogenation.

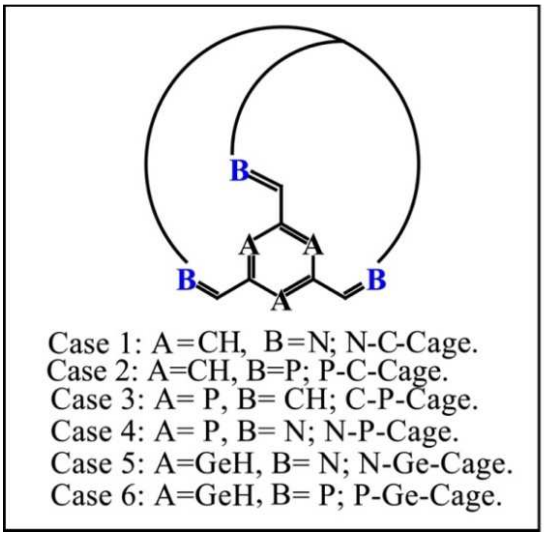

Figure 2. Different possibilities for Lewis pair combinations in porous zero dimensional cages.

The current chapter attempts to study the possibility of the four proposed porous cage cases: the “C-P”, “N-P”, “N-Ge” and “P-Ge”cages, for catalyzing the dehydrogenation of AB, and compare them to the “N-C” and the “P-C” cages. The complete reaction cycles for the dehydrogenation have been considered for each case. Furthermore, alternative, undesired, reaction pathways that can occur during the dehydrogenation, such as the attack of the N-H and B-H bonds of AB on the double bond outside of the ring in the cages (shown as “Possibility 2” in Figure 3 below), instead of the preferred reaction with the Lewis pair (shown as “Possibility 1” in Figure 3), which would lead to a dormant species, have also been considered. Indeed, it has been shown that the newly proposed cages fare significantly better than the previously proposed caged structures, because such undesired side reactions are found to be the dominant pathways for the N-C and P-C caged complexes. Hence the current calculations provide a complete picture of the possibilities that would exist if AB were to approach and react with a cage containing FLPs, and makes predictions with regard to which Lewis pair combinations would be the most effective at catalyzing AB dehydrogenation.

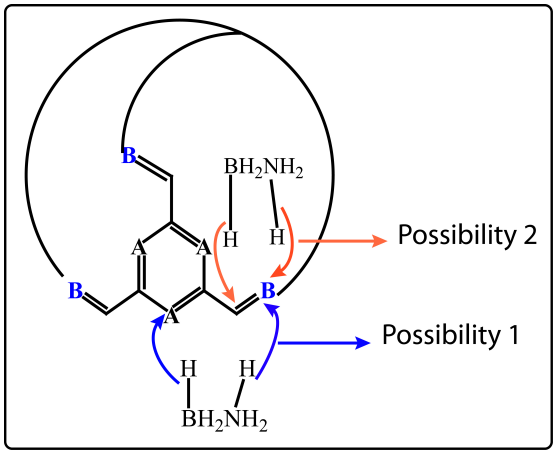

Figure 3. Competing pathways for the reaction between ammonia borane and the zero dimensional cage.

4.2 Computational Details

All the reaction pathways have been investigated with full quantum mechanical (QM) density functional theory (DFT) calculations with the Turbomole software (version 6.0)[30], employing the triple-ζ basis set augmented by a polarization function - the TZVP basis set[31-33], and by employing the PBE functional[34-37]. Since it is possible that the geometry optimization procedure with DFT may be sensitive to the nature of the functional, a further test has been done to ensure the reliability of the obtained geometry optimized structures: all the minima and transition state structures were also optimized with the B-P 86[24-25] functional at the same, TZVP, basis set level. A comparison was then done between the corresponding structures obtained with the PBE and the B-P 86 functionals. The comparison showed very little difference in bond lengths, angles and dihedral values between the corresponding structures for all the cases. A further corroboration of the small difference between the structures obtained from the two functionals comes from comparison of the potential energy surfaces for the different reactions. The ΔE values obtained from the two separate set of DFT calculations are almost similar in most of the cases (see the Tables 1 below) thus providing further proof of the reliability of the PBE functional in obtaining the optimised geometries and transition states. The resolution of identity (RI)[38], along with the multipole accelerated resolution of identity

(marij)[39]approximations were employed for an accurate and efficient treatment of the electronic Coulomb term in the density functional calculations. In order to further improve the quality of the energies obtained, dispersion corrections were included through single point calcations. Furthermore, single point calculations were done with the hybrid B3-LYP functional[40, 41] on all the obtained minima and transition state structures, in order to obtain more reliable energy values for the potential energy surfaces for the different investigated reactions. Frequency calculations have been done at the DFT (PBE) level. The zero point energy, internal energy and entropy contributions were calculated following the frequency calculations, with the temperature taken to be 298.15 K. Thus, all the energies reported in the Figures of the paper are the ΔG values. The calculations were done using atom centred basis sets. This is because the structures are self-contained and zero dimensional (0D) without any framework linkages between the individual cages, thus not necessitating the use of plane wave basis sets. Care was taken to ensure that the obtained transition state structures possessed only one imaginary frequency corresponding to the correct normal mode. It is also to be noted that the caged structure that has been considered in every case has T_d symmetry. Cooper *et al.*[42] have also reported the possibility of the 0D cages having C_3 symmetry. It is possible that the C_3 symmetry cages will also display FLP type behaviour. However, the focus of the current work has been on the T_d symmetry cages. The possibilities with the C_3 symmetry cages will be taken up in a future work.

	Name of the Cages	B-P 86 functional (kcal/mol)	PBE Functional (kcal/mol)
1	P-N cage case		
	Ts-1	2.1	6.3
	Ts-2	31.0	32.2
2	P-C cage case		
	Ts-1	40.1	39.8
	Ts-2	31.0	31.4
3	Ge-N cage case		
	Ts-1	3.2	2.6
	Ts-2	31.5	31.6
4	Ge-P cage case		
	Ts-1	6.6	6.8
	Ts-2	22.8	22.8

Table1. The comparison between the ΔE values for the barrier heights corresponding to the transition states obtained with the PBE and the B-P 86 functionals; all the values are ΔE values in kcal/mol.

4.3 Results and Discussion

4.3.1 Case 1-the "N-C" Cage: Shown in Figure 4 below is the free energy surface for the dehydrogenation of AB by the N-C cage. The first step – the extraction of the protic and hydridic hydrogen atoms from the nitrogen and boron atoms respectively in AB – is found to have a barrier of 33.4 kcal/mol. It is pertinent to note, in this regard, that the reactant species considered is an adduct complex, with the AB lying in the vicinity of the N-C cage; this is also true for all the other reactant complexes that will be discussed in the subsequent sub-sections. It is to be further noted that all the reaction pathways have been determined starting with the reactants having formed a complex, instead of beginning from the separated reactant species, a procedure that has also been followed by other groups[43-49]. This has been done because the entropic term is likely to be miss-represented when the reactants are considered separately in a reaction pathway: it is well known that the translational entropy is artificially increased in such cases[50]. The subsequent barrier for the dehydrogenation step was seen to have a barrier of 37.3 kcal/mol (see Figure 4a). The height of the barriers suggests that the catalysis of the AB dehydrogenation reaction by the N-C cage would require elevated temperatures. However, a more significant issue could be the competing deactivation reaction, which, as shown in Figure 4b below, is both thermodynamically and kinetically more favorable than the desired AB dehydrogenation catalysis pathway. This intermediate is likely to be a dormant species because of two reasons: (i) the high stability of N-C-cage-H_2-C-N suggests that it would require a high barrier for dehydrogenation (second step of the cycle) in order to recover the original C-P cage catalyst and complete the cycle, and (ii) the second step involves the formation of the H-H bond between the proximal hydrogen atoms that had been extracted from AB, and this would necessitate a four membered transition state, which is a sterically constrained transition state, and would thus lead to a high barrier reaction. This result suggests that the possibility of undesired side reactions

deactivating the cage is a significant issue for cages such as the N-C cage system. In the succeeding sub-sections, these competing possibilities are also discussed for the other cage systems mentioned in the Introduction.

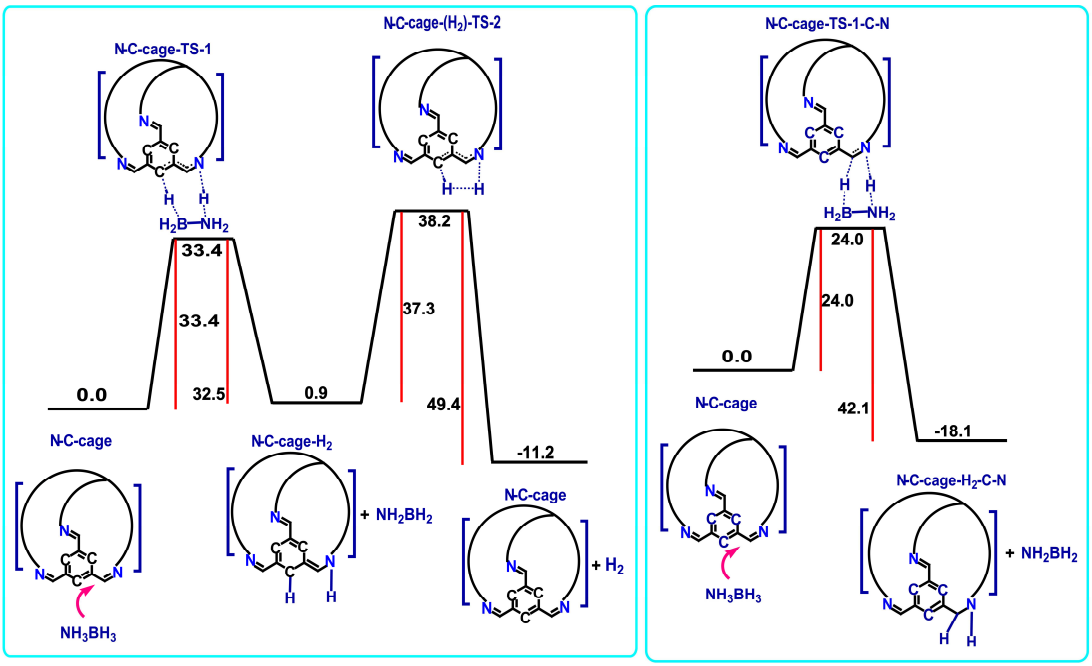

Figure 4a. The free energy surface for the dehydrogenation of ammonia borane by the N-C cage; Figure 4b. The free energy surface for the dormant species formation by attack of ammonia borane on N-C cage; all values in kcal/mol.

4.3.2 Case 2 - the "P-C" Cage: The "P-C" cage is a proposed modification to the existing "N-C" cage: where the nitrogen atoms in the linker groups have been replaced by phosphorus atoms. The possible reactions of this caged complex with AB are shown in Figure 5 below. What the results indicate is that, like in the N-C cage case, here, too, there is a likelihood of the deactivation reaction: the hydrogenation of the P-C double bond, taking precedence over the desired AB dehydrogenation pathway. Not only is the deactivation reaction much more kinetically facile (having a barrier of 23.1 kcal/mol as compared to the competing barrier of 46.5 kcal/mol), the formation of the dormant species is also a highly exergonic process, being more stable by 32.0 kcal/mol over AB

and the P-C cage complex. Hence, the current investigations indicate that this system, too, is unlikely to be a good catalyst for AB dehydrogenation.

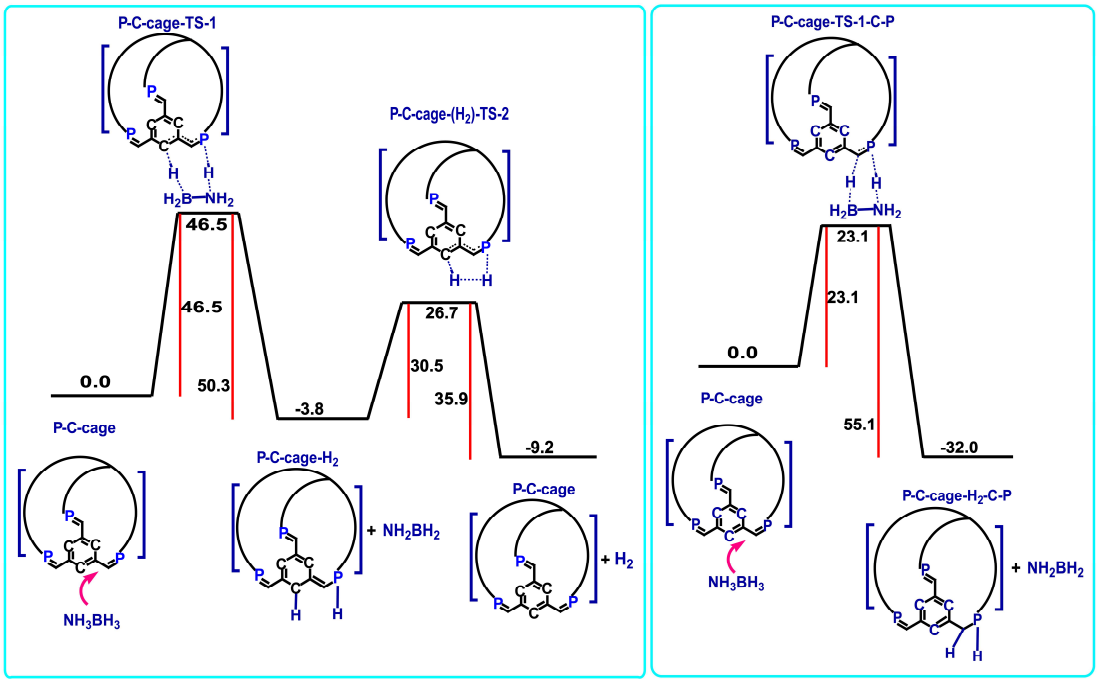

5a 5b

Figure 5a. The free energy surface for the dehydrogenation of ammonia borane by the P-C cage; Figure 5b. The free energy surface for the dormant species formation by attack of ammonia borane on the P-C cage; all values in kcal/mol.

4.3.3 Case 3 - the "C-P" Cage: The C-P cage is a proposed modification to the existing "N-C" cage[28], with carbon atoms in place of the imine nitrogens in the linkers and phosphorus atoms in the 2, 4 and 6 positions in place of the carbons of the phenyl rings of the original cages. Modified rings with hetero atoms such as phosphorus in place of carbon have been reported in the literature[51, 52].

The first step – the extraction of the protic and hydridic hydrogens from the nitrogen and boron atoms respectively in AB – is found to have a barrier of 44.1 kcal/mol. As shown in Figure 6 below, the intermediate formed after the first transition state, denoted as "C-

P-cage-H_2", is quite stable, lying 12.9 kcal/mol below the reactant species. The NH_2BH_2 that has been formed, being labile, is assumed to be removed from the system. C-P-cage-H_2, however, requires a further 35.8 kcal/mol in energy in order to convert back to the original C-P cages structure and release hydrogen, thereby completing the catalytic cycle. The entire process is exothermic, leading to a release of 13.4 kcal/mol (see Figure 6), implying that the process would be thermodynamically feasible. However, the height of both the barriers (especially the first barrier of 41.1 kcal/mol) in the dehydrogenation process shown in Figure 6 indicates that the reaction would not be a favourable one at room temperature[53-56]. The other issue is illustrated in Figure 7 below: calculations investigating the alternate possibility of the attack of the N-H and B-H bonds in AB on the double bond present outside the ring, indicate that Possibility 2 would be more highly favoured than the competing attack of the N-H and B-H bonds on the carbon and phosphorus of the Lewis pair. The barrier for this alternative possibility is 35.8 kcal/mol, as opposed to the barrier of 41.1 kcal/mol for Possibility 1. Moreover, the intermediate formed along this alternative pathway: C-P-cage-H_2-C-C (see Figure 7a), would also be highly stable: lying 28.1 kcal/mol below the reactant species (as opposed to the intermediate formed from the dehydrogenation pathway, which would lie 15.2 kcal/mol below the reactant species). Hence, from both a thermodynamic as well as a kinetic perspective, it is likely that the species, C-P-cage-H_2-C-C, would be the one more likely to be formed in the reaction vessel during the AB dehydrogenation process by the C-P cage. It should also be noted that another possible pathway for deactivating the caged system - the hydrogenation of the P=C bonds in the ring – has also been considered. The results of these investigations are shown in Figure 7b below. As Figure 7b indicates, such an attack is the most favoured kinetically, with the barrier being lower by 9.0 kcal/mol over the competing hydrogenation of the C=C bond in the linker. Hence, the results indicate that there are multiple pathways by which such cages can become deactivated, thus making them less effective as catalyst candidates for reactions such as AB dehydrogenation.

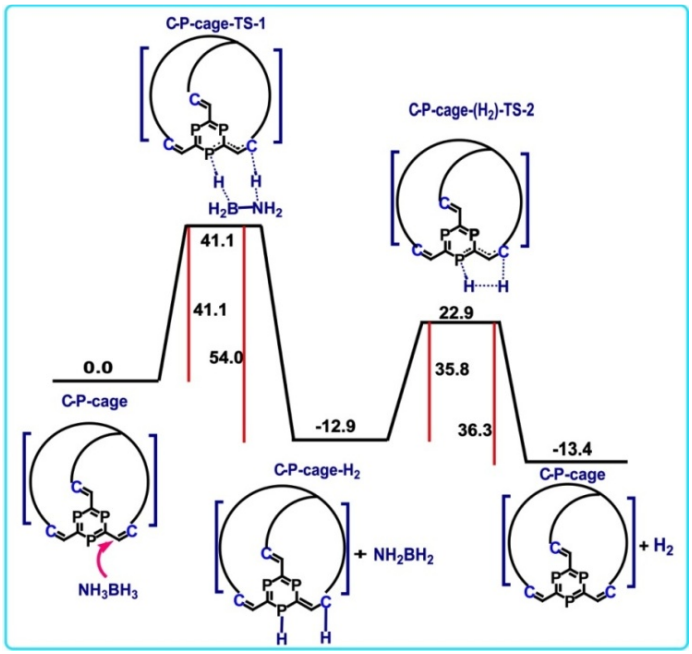

Figure 6. The free energy surface for the dehydrogenation of ammonia borane by the C-P cage; all values in kcal/mol.

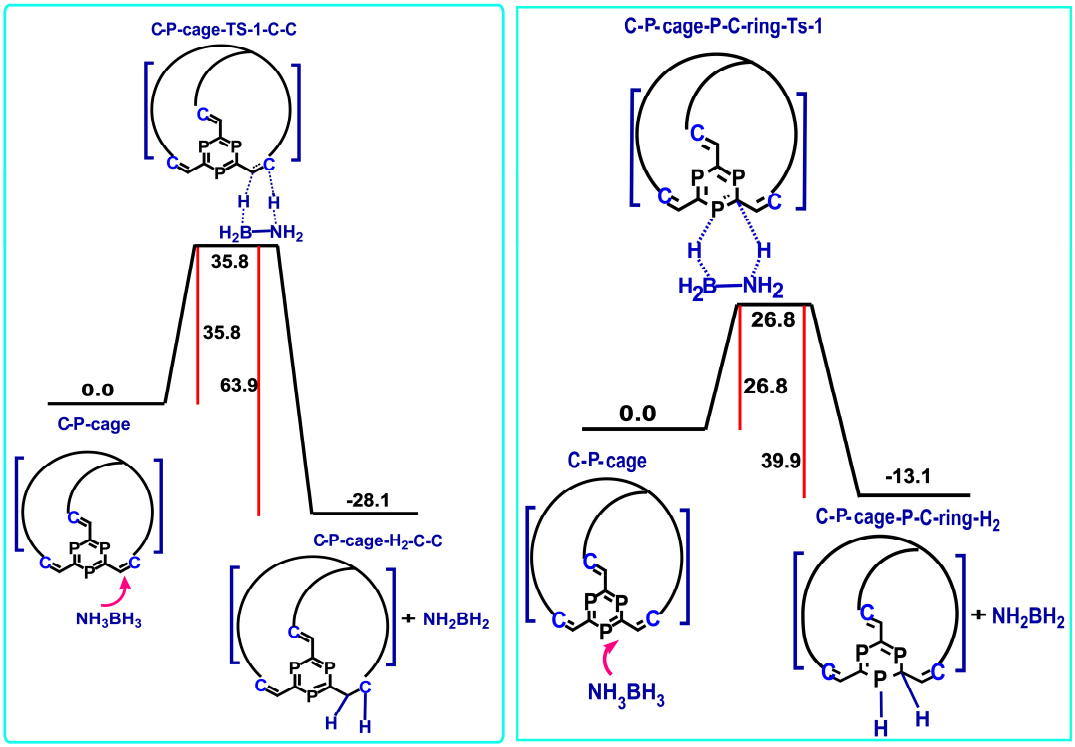

7a 7b

Figure 7a. The free energy surface for the dormant species formation by attack of ammonia borane on the C-P cage; Figure 7b. The free energy surface for the dormant species formation by attack of ammonia borane on the C-P cage leading to the hydrogenation of the P-C bond in the ring; all values in kcal/mol.

Hence, the calculations investigating the competing pathways for the C-P cage case indicate that, like the N-C and P-C cage cases discussed earlier, it, too, would be unlikely to be an effective catalyst for AB dehydrogenation. Instead, it is likely that the presence of AB in the vicinity of the cage would lead to the hydrogenation of the double bonds present in the cage. While this indicates that AB would be an effective hydrogenating agent for this cage system, this also suggests that this C-P cage contains Lewis pairs that would be unsuccessful at catalyzing the dehydrogenation of AB.

4.3.4 Case 4 - the "N-P" Cage: The C-P cage (Case 3) discussed in the previous sub-section contained two drawbacks: the first barrier in the two step process of AB dehydrogenation catalysis was high (41.1 kcal/mol), and the competing pathway that would lead to a dormant species was more favoured, having a barrier of 35.8 kcal/mol. The reason for this is likely to lie in the relative difference in electronegativity between the phosphorus and the carbon atoms in the C-P cage. It is likely that the design of a more effective Lewis pair would involve increasing the electronegativity difference between the electropositive and electronegative atoms in the pair. Since nitrogen is more electronegative than carbon, an N-P pair would be likely to show greater effectiveness in comparison to a C-P Lewis pair. Hence, the case of an N-P cage is considered next (Case 4), with the phosphorus atoms retained in the ring structure of the cage, but with nitrogens in the linker groups, that is, with the imine linkages present in the original cage structures synthesized by Tozawa *et al.*[28], reinstated. Shown in Figure 8 below is the free energy surface for the catalysis of the dehydrogenation of AB by the N-P Lewis pair. It is clear from Figure 8 that the cycle is much more catalytically feasible, from both a thermodynamic as well as a kinetic point of view. The first barrier is reduced to only 9.5 kcal/mol, and the second barrier is an acceptable 32.8 kcal/mol for this case (see Figure 8). Moreover, the intermediate species, N-P-cage-H_2, is stable by 18.1 kcal/mol in

comparison to the reactant species, which suggests that it would be long-lived in the reaction vessel, thereby making the second, cycle completing step, highly feasible. Cases in AB dehydrogenation catalysis where the first barrier was found to be significantly lower than the second have been reported earlier in the literature[57].

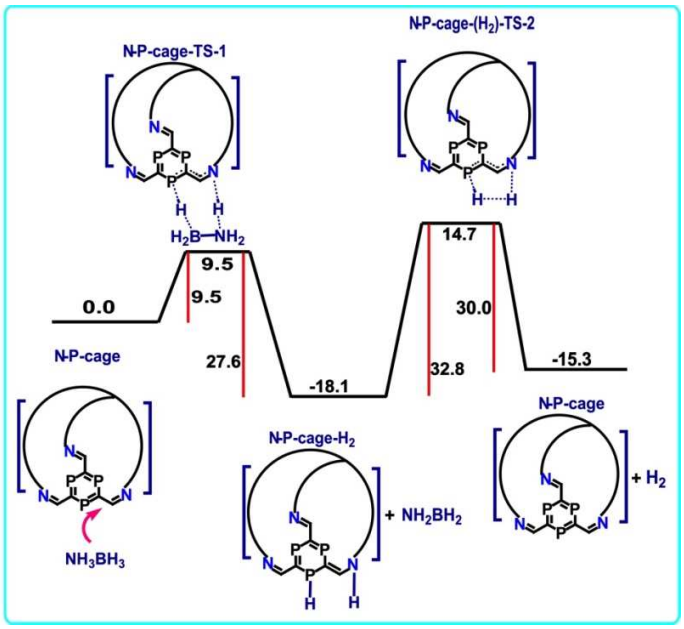

Figure 8. The free energy surface for the dehydrogenation of ammonia borane by the N-P cage; all values are in kcal/mol.

The reason the first barrier is reduced considerably in comparison to the C-P cage case is because of the facilitation of the proton transfer in the N-P cage case in comparison to the C-P cage. As illustrated in Figure 9, a comparison of the first transition states in the C-P and N-P cage cases shows that the distance between the protic hydrogen and the accepting carbon in the C-P cage is 1.39 Å, while the corresponding value in the N-P cage is 1.28 Å. This is because of the greater electronegativity of nitrogen in comparison to carbon. This, for the case of the N-P cage, leads to a lesser transfer of the hydridic hydrogen to the accepting phosphorus in the ring. The consequence of this is reduced distortion of the phosphorus containing ring in the transition state in the case of the N-P cage, and thus to a significant lowering of the barrier. For the N-P cage, the P-C-P-C

dihedral angle in the ring is only -2.6° in the first transition state, as compared to the significantly higher value of -17.4° for the C-P cage case.

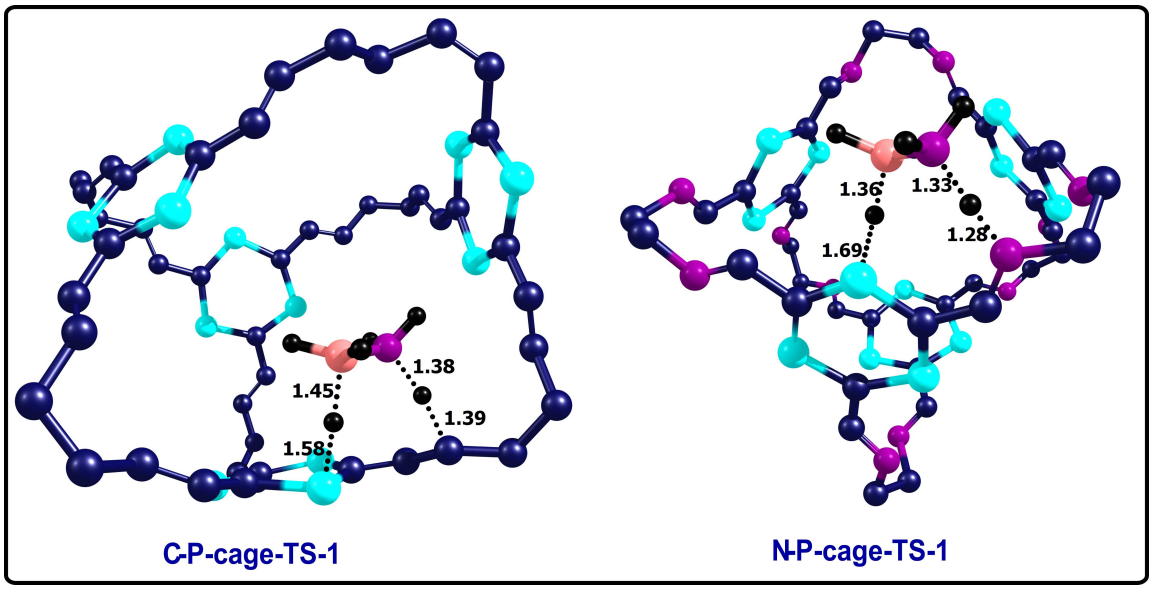

Figure 9. The optimized structures of the first transition states obtained along the ammonia borane dehydrogenation pathways, for the C-P cage and the N-P cage cases; the colour scheme is the same as in Figure 1, the additional atoms are boron: light brown and the hydrogens of ammonia borane: black.

What is also important is that the competing pathway (Possibility 2), which would lead to the hydrogenation of the double bond outside the ring and form the dormant species, has a barrier of 23.1 kcal/mol (as shown in Figure 10a below). The alternate possibility of hydrogenating the P-C bond in the ring has also been considered (see Figure 10b below) and also found to be a less favoured pathway. This suggests that in the competition between the FLP of nitrogen and phosphorus, and the double bond in the ring and in the linker, for the hydrogens of AB, the FLP would succeed, and thereby make the catalytic dehydrogenation possible. Hence, overall, the calculations suggest that the N-P cage would be a significant improvement over its C-P counterpart in terms of successfully catalyzing the dehydrogenation of AB.

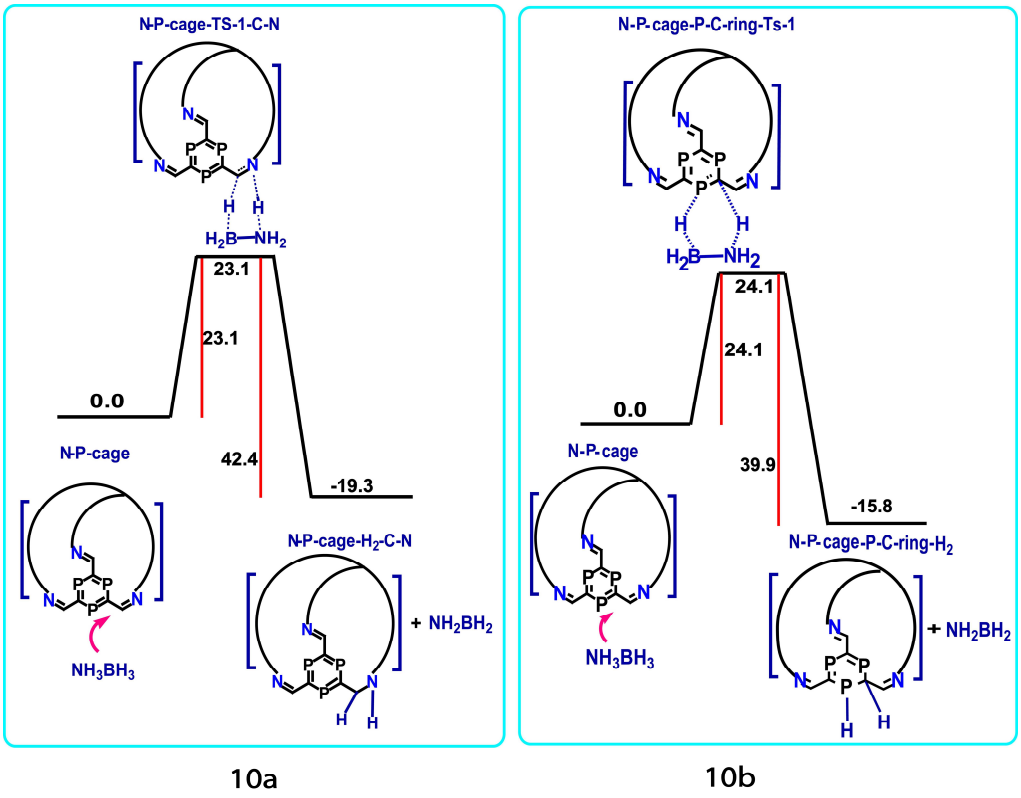

Figure 10a. The free energy surface for the dormant species formation by attack of ammonia borane on the N-P cage; Figure 10b. The free energy surface for the dormant species formation by attack of ammonia borane on the N-P cage leading to the hydrogenation of the P-C bond in the ring; all values in kcal/mol.

4.3.5 Case 5 - the "N-Ge" Cage: The next cage case that has been considered is the N-Ge cage, with the imine linkers kept intact from Case 4 - the N-P cage, but with germanium atoms in place of the phosphorus at the 2, 4, 6 positions in each ring. C-Ge bonds have been reported to have been formed in the case of non-aromatic cage structures[58]. C_5Ge aromatic structures have also been reported, with bulky substituent groups present to stabilize the complex[59-63]. Ge-C or Ge=Ge double bondedcomplexes have also been reported[59, 64, 65]. It is also noteworthy that amino-germyne complexes have been synthesized recently[66]. Aromatic rings with more than one germanium atom in the ring, however, have so far not been reported in the literature, though there are several computational studies with such complexes[67-69]. The current work can be considered a

model study to demonstrate the potential of such N-Ge caged complexes. It is possible that for N-Ge caged complexes to be stable, bulky ligands will be necessary. However, keeping the issue of computational expense in mind, bulky substituents have not been considered for the rings in these model systems, with hydrogens being employed instead.

The calculations described in Figure 11, Figure 12 and Figure 13 below have been done with the symmetric trigermabenzene complex. Other isomers of the ring structures in the N-Ge cages have been considered and found to be higher in energy, thus validating the use of the symmetric trigermabenzene ring in the N-Ge cage for the reactivity studies. Shown in Figure 11 is the free energy surface for the catalysis pathway for AB dehydrogenation using the N-Ge cage. In comparison to the case of the N-P cage, the first barrier is further reduced to only 0.3 kcal/mol. Moreover, the N-Ge-H_2 intermediate is significantly lower in energy, stabler by 22.1 kcal/mol, see Figure 11, than the reactant adduct complex. Hence, the combined high kinetic and thermodynamic favourability makes the formation of the N-Ge-H_2 intermediate a near certainty. The corresponding intermediate N-Ge-H_2-C-N – the dormant species that would be formed in the competing (Possibility 2) pathway – is more unstable than N-Ge-H_2 by 13.1 kcal/mol. The transition state for the dormant species could not, however, be determined, but the results comparing the relative stabilities of the two intermediates, as well as the very low barrier to the formation of the preferred N-Ge-H_2 intermediate, indicates that the dormant species would be unlikely to be formed, and the pathway (Possibility 2) leading to the formation of the dormant species would not be operative for the N-Ge cage case. Moreover, the possibility of the Ge-C bond in the ring getting hydrogenated by AB has also been studied and found to be an unfavourable reaction pathway (see Fig. 13 below).

The second barrier is, like in the previous case, higher, having a value of 34.4 kcal/mol, which makes the second step the rate determining step in the reaction. The value of the second barrier is higher by 2.4 kcal/mol than the corresponding value for the N-P cage case, which means that while the N-Ge cage would also be an effective catalyst for AB dehydrogenation, it would not be as effective as the N-P cage for the same. Nevertheless, given the recent interest in forming germanium analogues to carbon compounds[51, 66], this

computational investigation of the potential of the N-Ge cages for catalyzing important reactions, such as AB dehydrogenation, is of relevance. Shown in Figure 12 below are the optimized structures for all the principal species along the AB dehydrogenation pathway when using the N-Ge cage system.

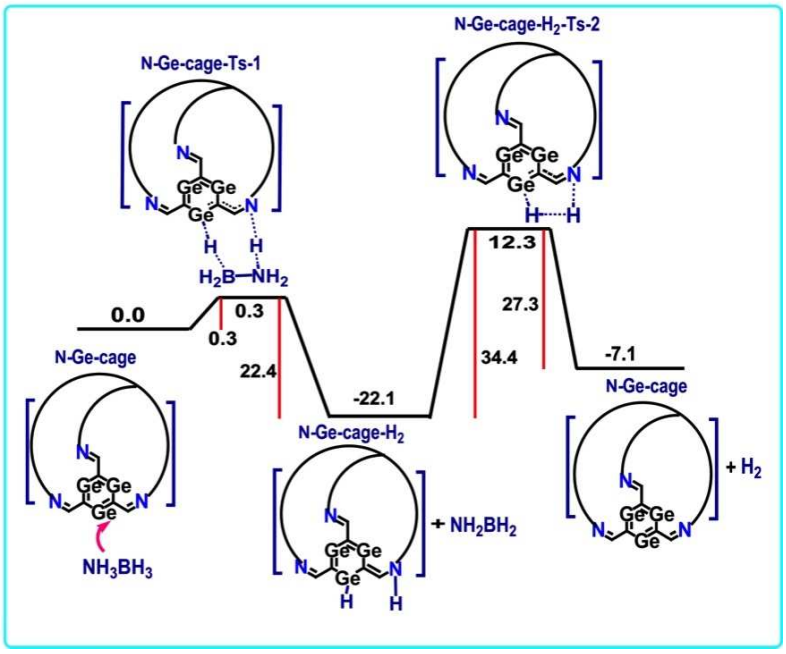

Figure 11. The free energy surface for the dehydrogenation of ammonia borane by the N-Ge cage; all values are in kcal/mol.

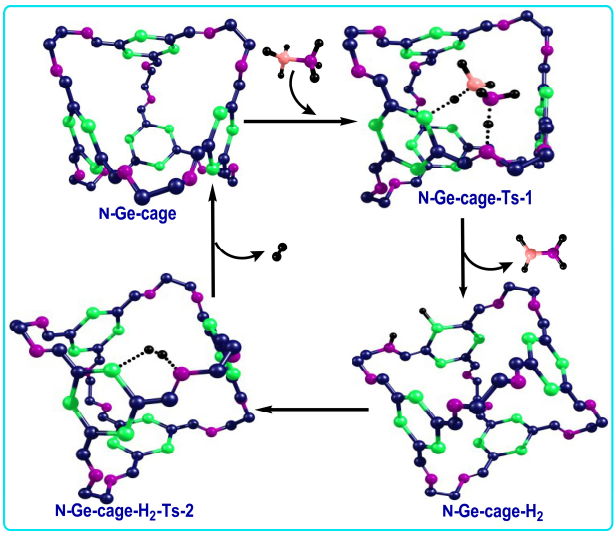

Figure 12. The optimized structures obtained for the ammonia borane dehydrogenation process with the N-Ge cage; the colour scheme is the same as in Figure 9; the additional atom is germanium (light green).

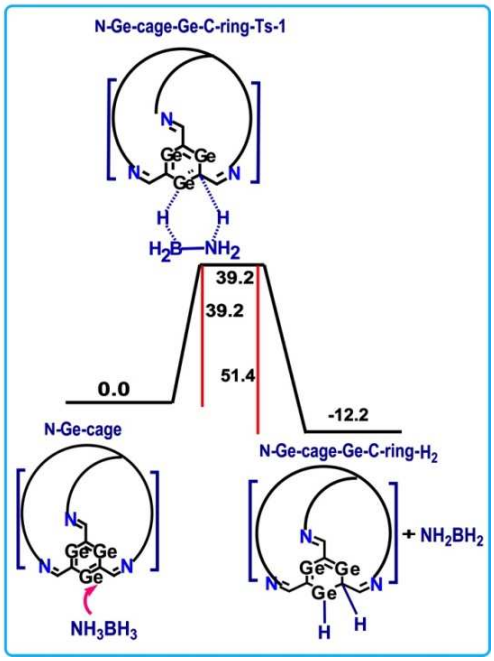

Figure 13. The free energy surface for the dormant species formation by attack of ammonia borane on the N-Ge cage leading to the hydrogenation of the Ge-C bond in the ring; all values in kcal/mol.

4.3.6 Case 6 - the "P-Ge" Cage: The last case that has been considered is the P-Ge cage, which retains the germanium atom containing rings as in the N-Ge cage discussed in the previous section, but which contains phosphorus atoms in place of nitrogens in the linkers. Caged structures containing phosphorus and germanium atoms have recently been synthesized[70]. As the free energy profile (shown in Figure 14 below) for AB dehydrogenation using the P-Ge cage indicates, such cages would be excellent catalysts for AB dehydrogenation. The first barrier is only 1.6 kcal/mol, and the intermediate species, P-Ge-H_2, lies 18.9 kcal/mol below the adduct reactant complex, making its formation a highly likely process. Moreover, the second transition state would also be easier to access than the corresponding transition states in the other three cases

considered: the second barrier is only 32.5 kcal/mol. Thus, overall the catalysis would be likely to progress in a very facile fashion if a cage such as P-Ge were to be employed. The reason for the reduction of the barrier upon replacing nitrogen atoms with phosphorus is because the germanium containing ring structure is already seen to be distorted in the reactant adduct complex before the occurrence of the first transition state. As shown in Figure 15 below, the adduct complex contains an interaction between one of the germaniums not taking part in the AB dehydrogenation catalysis process and a phosphorus atom in the adjoining linker group. This leads to the distortion of the ring in the adduct complex itself. What facilitates this interaction between the germanium and the phosphorus atoms in the adduct complex is the loss of aromaticity in the rings due to the presence of germanium in place of carbon. Now, as had been shown in the previous investigation with the P-C cage structures[29], the barrier for the first transition state for AB dehydrogenation catalysis was significantly reduced when a second P-C pair was considered. This was because of the distortion of the phenyl ring due to the AB dehydrogenation by the first P-C pair in that case, making the further distortion of the cage more facile. In the current case of the P-Ge cage, such distortion *already occurs* because of the interaction between the germaniun and phsophorus atoms in the adduct complex, thereby making the first barrier even lower than for the N-Ge cage case considered earlier.

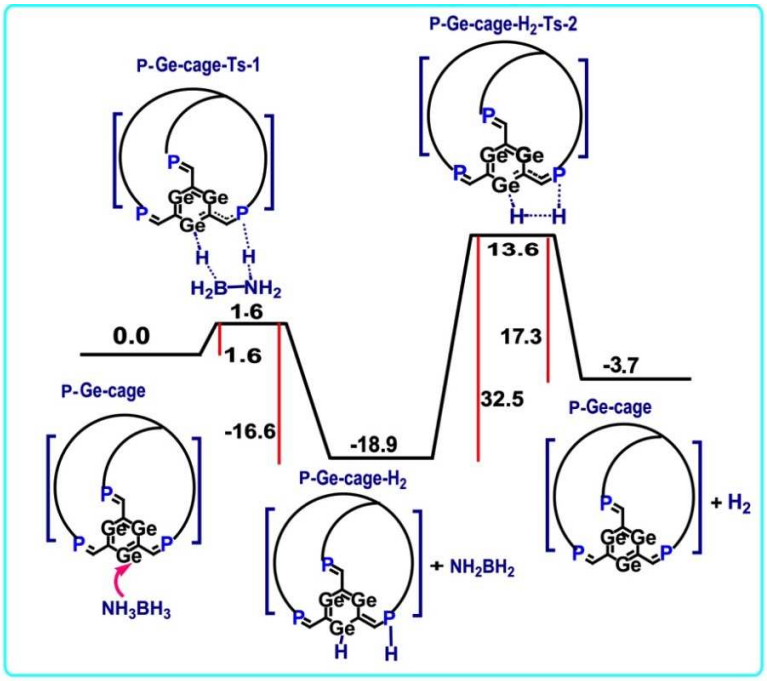

Figure 14. The free energy surface for the dehydrogenation of ammonia borane by the P-Ge cage; all values are in kcal/mol.

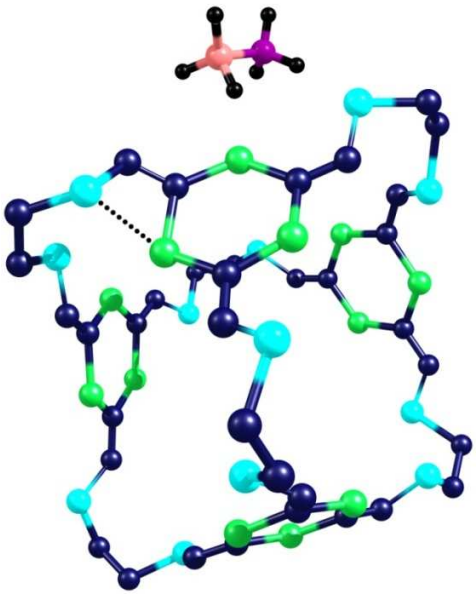

Figure 15. The optimized structure of the reactant adduct species for the case of the P-Ge cage; the colour scheme is the same as in Figure 12; the other hydrogens have been removed for the sake of clarity.

As shown in Figure 16 below, the competing pathway that would lead to the formation of the dormant species has a significantly higher barrier – of 17.2 kcal/mol. Therefore, in all respects, the P-Ge cage case considered here is likely to be the best among all the cases considered for doing AB dehydrogenation catalysis: it has lower barriers for the first and second steps in the dehydrogenation pathway in comparison to all the other cases, and the dehydrogenation pathway is significantly more likely to occur than the competing pathway leading to the dormant species.

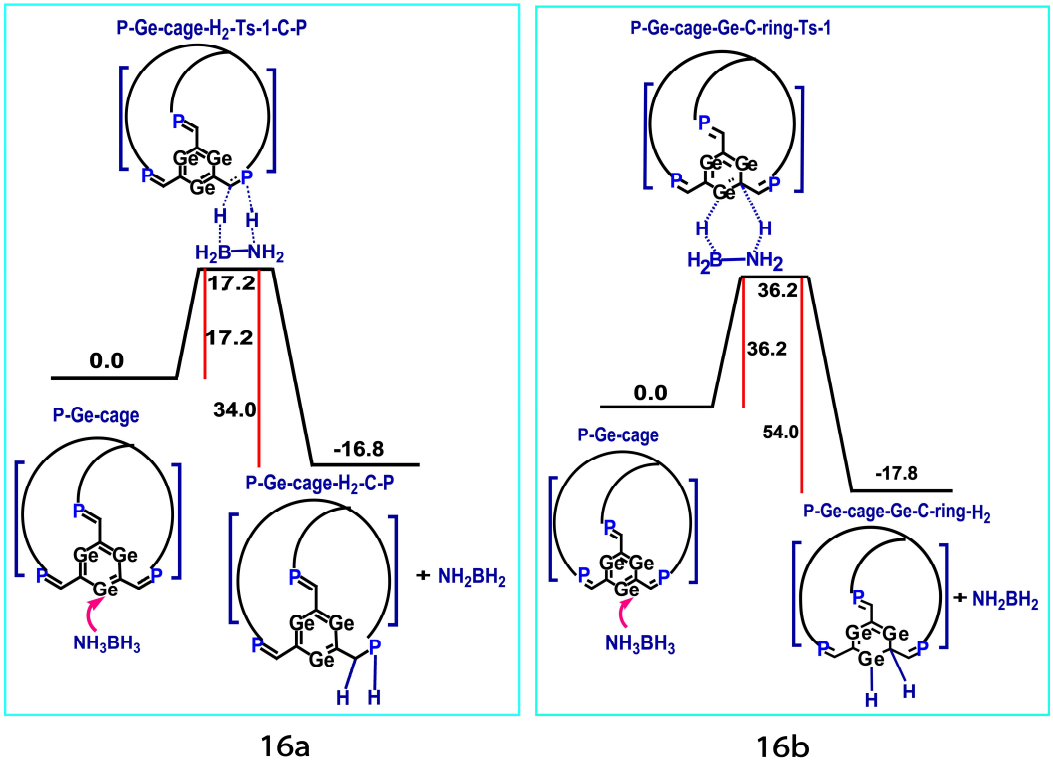

16a 16b

Figure 16a. The free energy surface for the dormant species formation by attack of ammonia borane on the P-Ge cage; Figure 16b. The free energy surface for the dormant species formation by attack of ammonia borane on the P-Ge cage leading to the hydrogenation of the Ge-C bond in the ring; all values in kcal/mol.

Our calculations therefore indicate that there are three cage combinations that are suitable for performing as catalysts for important reactions such as ammonia borane dehydrogenation. They are the N-P, N-Ge and the P-Ge cage cases. As shown and

discussed in the previous sections, the slowest step for AB dehydrogenation catalysis in these cases has a barrier of 32.8 kcal/mol, 34.4 kcal/mol and 32.5 kcal/mol respectively. The corresponding rate constants for each case therefore comes to $0.14*10^{-8}s^{-1}$, $0.12*10^{-9}$ s^{-1} and $0.22*10^{-8}$ s^{-1} for T = 330 K (with the pre-exponential factor estimated as k_bT/h). The rate constants are comparable to, or better than the rate constants that have been obtained for many heterogeneous catalysis processes. For instance, the catalysis of the methane formation over the NiSn[71] catalysts has a rate constant value of $0.53*10^{-9}$ s^{-1} at 330K, and the dissociation of stable diatomic molecules and hydrocarbon cracking reactions have barrier of 1.7eV[72], with the rate constantsthus calculated to be $0.82*10^{-13}$ s^{-1} at 330K. There are several other examples of heterogeneous catalysis processes that have high reaction barriers and low rate constants[73-77]. Therefore, the current work on the solid zero dimensional cage structures as potential catalysts, shows promise. This is especially true when one considers that there are twelve active sites in each cage, which translates to a rate constant per cage of $1.68*10^{-8}s^{-1}$,$1.44*10^{-9}$ s^{-1} and $2.64*10^{-8}$ $s^{-1}$for T = 330 K, for the N-P, N-Ge and the P-Ge cage cases respectively.

4.3.7 Simultaneous Catalysis

As mentioned earlier, a significant advantage that could be gained from using the catalytic 0D structures is the availability, per cage, of many catalytic sites for AB dehydrogenation. This possibility has been explored for the P-C-cage with DFT calculations – the cases where the protic hydrogen of AB is transferred to the phosphorus of the P-C pair being considered. The results are illustrated in Figure 17. The intent is to show how one, two or all three of the phosphorus-carbon (P-C) pairs in each of the four phenyl rings of P-C-cage could simultaneously catalyze AB dehydrogenation from one or two or three AB molecules respectively.

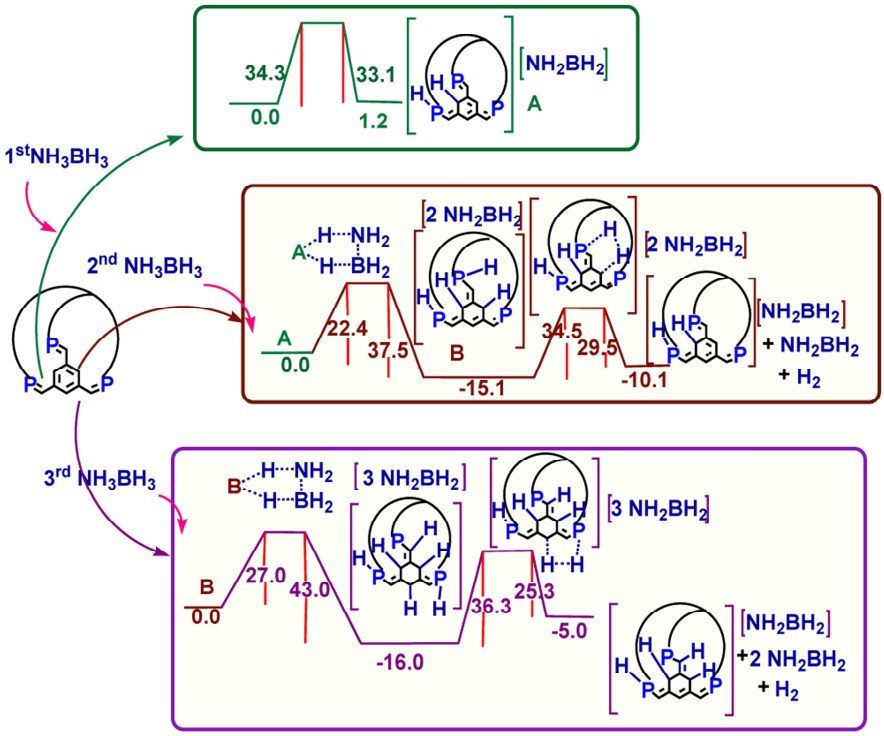

Figure 17. The schematic representation for the second and third simultaneous dehydrogenations of AB molecules by different P-C pairs associated with one phenyl ring of the P-C-cage; considered for the case where the protic hydrogen of AB is being transferred to the phosphorus of the P-C pair; all values are in kcal/mol.

As the middle box in Figure 17 illustrates, after the completion of the first, hydrogen extraction step with one AB molecule (upper box in Figure 17), one of the two adjacent P-C pairs of the same phenyl group can participate in an AB dehydrogenation catalytic cycle (Figure 17). Thus AB dehydrogenation catalysis could proceed simultaneously at both the P-C catalytic centres. Similarly, as the lower box in Figure 17 indicates, the AB dehydrogenation catalysis could also proceed simultaneously with all the three P-C pairs associated with a given phenyl ring of the P-C-cage. A natural extrapolation from these results is that all twelve P-C pairs in every P-C-cage molecule could simultaneously perform as catalytic sites for AB dehydrogenation. The fact that a fourth P-C site, lying adjacent to a phenyl ring with all three P-C centres simultaneously employed in AB dehydrogenation[29], can also catalyze AB dehydrogenation with comparable first and second barrier heights has also been verified – the results are shown in Figure 18 below.

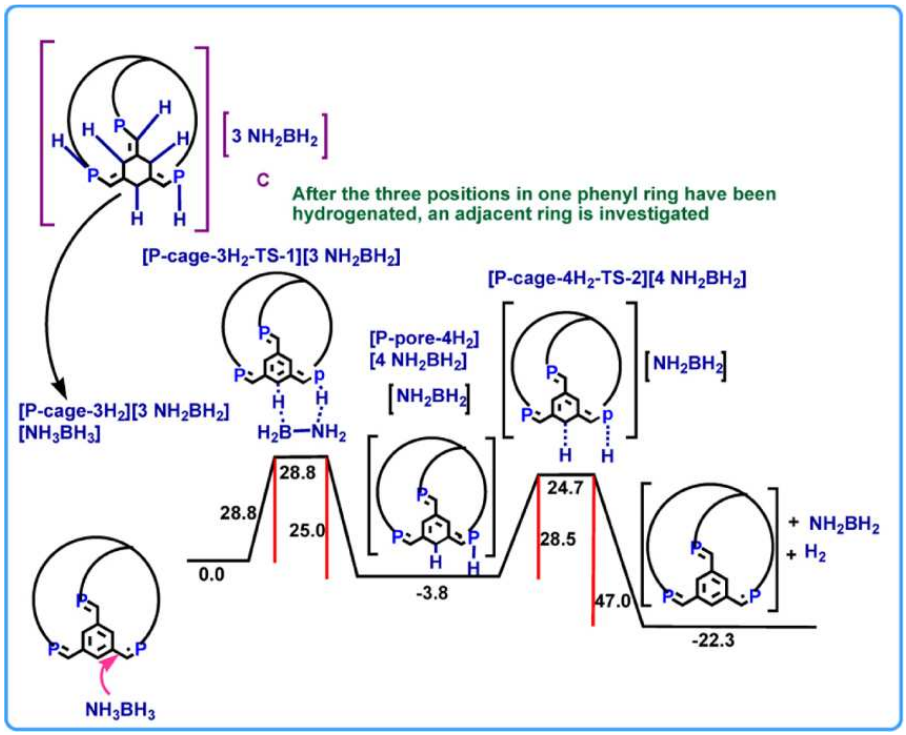

Figure 18. The schematic representation of the catalytic AB dehydrogenation pathway for the P-C cage for the fourth AB dehydrogenation, where a phenyl ring adjacent to a phenyl ring where three dehydrogenation reactions have been completed in part, is taking part in the dehydrogenation process – the protic hydrogen is transferred to the phosphorus of the P-C pair; all values are in kcal/mol.

4.4 Conclusion

The dehydrogenation of ammonia borane (AB) is an important area of research in the field of hydrogen storage, and AB dehydrogenation catalysts containing main-group elements in place of transition metals would be highly desirable. The current work explores computationally the possibility of dehydrogenating AB catalytically by employing cage systems that would be modifications of existing cage structures[28]. Full quantum mechanical (QM) calculations using density functional theory (DFT) show that cages that contain nitrogen-carbon (N-C cage), phosphorus-carbon (P-C cage) and carbon-phosphorus (C-P cage) would not be able to effectively catalyze AB dehydrogenation, due to the feasibility of competing side reactions. However, the

calculations also indicate that cages containing nitrogen-phosphorus (N-P cage), nitrogen-germanium (N-Ge cage) and phosphorus-germanium (P-Ge cage) Lewis pairs would be efficient catalysts for AB dehydrogenation. Of the cases considered, the P-Ge cage case was found to be the most promising, having the lowest barriers for the AB dehydrogenation pathway, and also showing significantly higher preference for the desired dehydrogenation catalytic pathway in comparison to undesired alternative routes that would lead to dormant species.

The calculations therefore show the potential of the 0D cages, if properly modified, for frustrated Lewis pair (FLP) activity. Since there are many exciting possibilities in the field of small molecule activation using FLPs, there is considerable potential in employing 0D cages like the ones discussed in this work, for activating the C-C, C-H and C-O, N-O bonds in small molecules and thereby catalysing important reactions. It is hoped that the current work would provide a fillip to the field of FLPs in this regard.

4.5 References

1. J. Weitkamp, M. Fritz, S. Ernst, *Int. J. Hydrogen Energy*, 1995, 20, 967-970.
2. M. Dinca, J. R. Long, *Angew. Chem. Int. Ed.*, 2008, 47, 6766-6779.
3. J. L. C. Rowsell, O. M. Yaghi, *Angew. Chem. Int. Ed.*, 2005, 44, 4670-4679.
4. B. Sakintuna, F. Lamari-Darkrim, M. Hirscher, *Int. J. Hydrogen Energy*, 2007, 32, 1121-1140.
5. S.-i. Orimo, Y. Nakamori, J. R. Eliseo, A. Zuettel, C. M. Jensen, *Chem. Rev.*, 2007, 107, 4111-4132.
6. M. E. Sloan, A. Staubitz, T. J. Clark, C. A. Russell, G. C. Lloyd-Jones, I. Manners, *J. Am. Chem. Soc.*, 2010, 132, 3831-3841.
7. A. Staubitz, A. P. M. Robertson, I. Manners, *Chem. Rev.*, 2010, 110, 4079-4124.
8. M. C. Denney, V. Pons, T. J. Hebden, D. M. Heinekey, K. I. Goldberg, *J. Am. Chem. Soc.*, 2006, 128, 12048-12049.
9. T. B. Marder, *Angew. Chem. Int. Ed.*, 2007, 46, 8116-8118.
10. J. D. Erickson, J. C. Fettinger, P. P. Power, *Inorg. Chem.*, 2015, ASAP.
11. F. Lips, A. MansikkamÃ¤ki, J. C. Fettinger, H. M. Tuononen, P. P. Power, *Organometallics*, 2014, 33, 6253-6258.
12. A. V. Protchenko, K. H. Birjkumar, D. Dange, A. D. Schwarz, D. Vidovic, C. Jones, N. Kaltsoyannis, P. Mountford, S. Aldridge, *J. Am. Chem. Soc.*, 134, 6500-6503.

13. S. Yao, Y. Xiong, M. Driess, *Organometallics*, 30, 1748-1767.
14. D. Martin, M. Soleilhavoup, G. Bertrand, *Chem. Sci.*, 2, 389-399.
15. U. Siemeling, C. Farber, C. Bruhn, M. Leibold, D. Selent, W. Baumann, M. von Hopffgarten, C. Goedecke, G. Frenking, *Chem. Sci.*, 1, 697-704.
16. G. C. Welch, R. R. S. Juan, J. D. Masuda, D. W. Stephan, *Science*, 2006, 314, 1124-1126.
17. J. S. J. McCahill, G. C. Welch, D. W. Stephan, *Angew. Chem. Int. Ed.*, 2007, 46, 4968-4971.
18. G. Ménard, D. W. Stephan, *J. Am. Chem. Soc.*, 2010, 132, 1796-1797.
19. E. Otten, R. C. Neu, D. W. Stephan, *J. Am. Chem. Soc.*, 2009, 131, 9918-9919.
20. C. M. Mömming, E. Otten, G. Kehr, R. Fröhlich, S. Grimme, D. W. Stephan, G. Erker, *Angew. Chem. Int. Ed.*, 2009, 48, 6643-6646.
21. D. W. Stephan, G. Erker, *Angew. Chem. Int. Ed.*, 2010, 49, 46-76.
22. P. Spies, S. Schwendemann, S. Lange, G. Kehr, R. Fröhlich, G. Erker, *Angew. Chem. Int. Ed.*, 2008, 47, 7543-7546.
23. K. V. Axenov, G. Kehr, R. Fröhlich, G. Erker, *Organometallics*, 2009, 28, 5148-5158.
24. A. J. P. Cardenas, B. J. Culotta, T. H. Warren, S. Grimme, A. Stute, R. Fröhlich, G. Kehr, G. Erker, *Angew. Chem., Int. Ed.*, 2011, 50, 7567-7571.
25. A. M. Chapman, M. F. Haddow, D. F. Wass, *J. Am. Chem. Soc.*, 2011, 133, 18463-18478.
26. A. J. M. Miller, J. E. Bercaw, *Chem. Commun.*, 46, 1709-1711.
27. Y. Guo, X. He, Z. Li, Z. Zou, *Inorg. Chem.*, 2010, 49, 3419-3423.
28. T. Tozawa, J. T. A. Jones, S. I. Swamy, S. Jiang, D. J. Adams, S. Shakespeare, R. Clowes, D. Bradshaw, T. Hasell, S. Y. Chong, C. Tang, S. Thompson, J. Parker, A. Trewin, J. Bacsa, A. M. Z. Slawin, A. Steiner, A. I. Cooper, *Nat. Mater.*, 2009, 8, 973-978.
29. A. Pal, K. Vanka, *Chem. Commun.*, 2011, 47, 11417-11419.
30. R. Ahlrichs, M. Bär, M. Häser, H. Horn, C. Kölmel, *Chem. Phys. Lett.*, 1989, 162, 165-169.
31. A. Schafer, H. Horn, R. Ahlrichs, *J. Chem. Phys.*, 1992, 97, 2571-2577.
32. F. Weigend, *Phys. Chem. Chem. Phys.*, 2002, 4, 4285-4291.
33. F. Weigend, R. Ahlrichs, *Phys. Chem. Chem. Phys.*, 2005, 7, 3297-3305.
34. P. A. M. Dirac, *Proceedings of the Royal Society of London. Series A*, 1929, 123, 714-733.
35. J. C. Slater, *Phys. Rev.*, 1951, 81, 385-390.
36. J. P. Perdew, K. Burke, M. Ernzerhof, *Phys. Rev. Lett.*, 1996, 77, 3865-3868.
37. J. P. Perdew, Y. Wang, *Phys. Rev. B*, 1992, 45, 13244-13249.
38. K. Eichkorn, O. Treutler, H. Öhm, M. Häser, R. Ahlrichs, *Chem. Phys. Lett.*, 1995, 240, 283-290.
39. M. Sierka, A. Hogekamp, R. Ahlrichs, *J. Chem. Phys.*, 2003, 118, 9136-9148.
40. A. D. Becke, *J. Chem. Phys.*, 1993, 98, 5648-5652.
41. C. Lee, W. Yang, R. G. Parr, *Phys. Rev. B*, 1988, 37, 785-789.
42. K. E. Jelfs, F. Schiffmann, J. T. A. Jones, B. Slater, F. Cora, A. I. Cooper, *Phys. Chem. Chem. Phys.*, 13, 20081-20085.

43. E. Kelly, M. Seth, T. Ziegler, *J. Phys. Chem.A*, 2004, 108, 2167-2180.
44. H. Yin, D. Wang, M. Valiev, *J. Phys. Chem.A*, 2011, 115, 12047-12052.
45. V. M. Williams, J. R. Kong, B. J. Ko, Y. Mantri, J. S. Brodbelt, M.-H. Baik, M. J. Krische, *J. Am. Chem. Soc.*, 2009, 131, 16054-16062.
46. W. Janse van Rensburg, C. Grové, J. P. Steynberg, K. B. Stark, J. J. Huyser, P. J. Steynberg, *Organometallics*, 2004, 23, 1207-1222.
47. Y. Qi, Q. Dong, L. Zhong, Z. Liu, P. Qiu, R. Cheng, X. He, J. Vanderbilt, B. Liu, *Organometallics*, 2010, 29, 1588-1602.
48. A. Bagno, W. Kantlehner, R. Kress, G. Saielli, E. Stoyanov, *J. Org. Chem.*, 2006, 71, 9331-9340.
49. J.-N. Li, M. Pu, C.-C. Ma, Y. Tian, J. He, D. G. Evans, *J. Mol. Catal. A: Chem.*, 2012, 359, 14-20.
50. M. Mammen, E. I. Shakhnovich, G. M. Whitesides, *J. Org. Chem.*, 1998, 63, 3168-3175.
51. C. Nickl, D. Joosten, K. Eichele, C. Maichle-Mössmer, K. W. Törnroos, L. Wesemann, *Angew. Chem. Int. Ed.*, 2009, 48, 7920-7923.
52. S. B. Clendenning, P. B. Hitchcock, J. F. Nixon, L. Nyulaszi, *Chem. Commun.*, 2000, 0, 1305-1306.
53. W. J. Shaw, J. C. Linehan, N. K. Szymczak, D. J. Heldebrant, C. Yonker, D. M. Camaioni, R. T. Baker, T. Autrey, *Angew. Chem. Int. Ed.*, 2008, 47, 7493-7496.
54. P. M. Zimmerman, A. Paul, Z. Zhang, C. B. Musgrave, *Inorg. Chem.*, 2009, 48, 1069-1081.
55. M. T. Nguyen, V. S. Nguyen, M. H. Matus, G. Gopakumar, D. A. Dixon, *J. Phys. Chem.A*, 2007, 111, 679-690.
56. A. Berkessel, J. A. Adrio, *J. Am. Chem. Soc.*, 2006, 128, 13412-13420.
57. N. Blaquiere, S. Diallo-Garcia, S. I. Gorelsky, D. A. Black, K. Fagnou, *J. Am. Chem. Soc.*, 2008, 130, 14034-14035.
58. V. Ischenko, U. Englert, M. Jansen, *Chem. Eur. J.*, 2005, 11, 1375-1383.
59. N. Tokitoh, *Acc. Chem. Res.*, 2003, 37, 86-94.
60. Y. Sugiyama, T. Sasamori, Y. Hosoi, Y. Furukawa, N. Takagi, S. Nagase, N. Tokitoh, *J. Am. Chem. Soc.*, 2005, 128, 1023-1031.
61. Y. Mizuhata, T. Sasamori, N. Nagahora, Y. Watanabe, Y. Furukawa, N. Tokitoh, *Dalton Trans.*, 2008, 0, 4409-4418.
62. N. Nakata, N. Takeda, N. Tokitoh, *J. Am. Chem. Soc.*, 2002, 124, 6914-6920.
63. Y. Mizuhata, N. Noda, N. Tokitoh, *Organometallics*, 2010, 29, 4781-4784.
64. D. Ghereg, H. Gornitzka, J. Escudié, S. Ladeira, *Inorg. Chem.*, 2010, 49, 10497-10505.
65. V. Y. Lee, A. Sekiguchi, *Organometallics*, 2004, 23, 2822-2834.
66. J. Berthe, J. M. Garcia, E. Ocando, T. Kato, N. Saffon-Merceron, A. De Cózar, F. P. Cossío, A. Baceiredo, *J. Am. Chem. Soc.*, 2011, 133, 15930-15933.
67. M. Z. Kassaee, M. R. Momeni, F. A. Shakib, M. Ghambarian, *J. Organomet. Chem.*, 2010, 695, 760-765.
68. U. D. Priyakumar, G. N. Sastry, *J. Org. Chem.*, 2001, 67, 271-281.
69. M. Z. Kassaee, N. Jalalimanesh, S. M. Musavi, *J. Mol. Struct.: THEOCHEM*, 2007, 816, 153-160.

70. S. Almstatter, G. Balazs, M. Bodensteiner, M. Scheer, *Chem. Commun.*, 2011, 47, 9998-10000.
71. J.W. Shabaker, R.R. Davda, G.W. Huber, R.D. Cortright,, J.A. Dumesic, *J. Catal.*, 2003, 215, 344-352.
72. A. Michaelides, Z. P. Liu, C. J. Zhang, A. Alavi, D. A. King,, P. Hu, *J. Am. Chem. Soc.*, 2003, 125, 3704-3705.
73. F. Kapteijn, J. R. Mirasol , J. A. Moulijn, *Appl. Catal. B: Environmental*, 1996, 9, 25-64.
74. G. I. Panov, V. I. Sobolev, A. S. Kharitonov, *J. Mol. Catal*., 1990, 61, 85-97.
75. S. Dahl, A. Logadottir, R. C. Egeberg, J. H. Larsen, I. Chorkendorff, E. Törnqvist, J. K. Nørskov, *Phys. Rev. Lett*., 1999, 83, 1814-1817.
76. T. Bligaard, J.K. Nørskov, S. Dahl, J. Matthiesen, C.H. Christensen, J. Sehested, *J. Catal.*, 2004, 224, 206-217.
77. V.I. Sobolev, G.I. Panov, A.S. Kharitonov, V.N. Romannikov, A.M. Volodin, K.G. Ione, *J. Catal*., 1993, 139, 435-443.

Chapter 5

Silylenes Can Rival Transition Metal Systems in Bond-Strengthening π-Back Donation

Abstract

Full quantum chemical calculations with density functional theory (DFT) show that bond-strengthening back-donation to a π-diborene, recently discovered for transition metal systems (Braunschweig and co-workers, *Nat. Chem*., 2013, 5, 115-121), would be just as favored for Main Group silylene complexes. This result not only shows the range and applicability of the bond-strengthening back-bonding interaction, but also showcases the potential of silylene complexes to do new chemistry, such as the cooperative activation of carbon monoxide and carbon dioxide.

5.1 Introduction

The most distinctive feature of transition metal catalysis, indeed, the very basis of it, is the interaction between the metal and the ligand through the donation of electron density from a filled metal orbital to an empty, anti-bonding ligand orbital. This serves to weaken one of the bonds in the ligand, thus giving rise to most of the transition metal chemistry known today [1,2]. However, a radical new development by Braunschweig and co-workers shows that bond-weakening back-donation is not the sole possibility in metal-ligand interactions. They have found[3] that donation of electron density can take place from a filled metal orbital (of a palladium and a platinum based complex) to a singly occupied orbital (the SOMO) of the ligand (a π-diborene: PhB=BPh), an interaction that leads to the stabilization of the bond in the π-diborene ligand. This unprecedented finding is not only interesting conceptually, but is also likely to lead to important developments in transition metal catalysis. However, an important question that needs to be asked is: would such a bond-strengthening back-donating interaction also be possible for non-transition metal systems? It is known that Main Group systems such as carbenes [4-7] and silylenes [8-11] can activate small molecules [12-14] by weakening ligand bonds, just like transition metal complexes. What we decided to investigate was whether Main Group complexes such as silylenes might also be able to demonstrate the unusual bond-strengthening back-donation interaction. Such an interaction, if also possible for silylene systems, would not only expand the scope of applicability of this newly discovered form of bonding, but would also showcase the potential of the Main Group complexes to do new chemistry. It is to be noted here that while several recent papers[15-26] have discussed the implications of the work of Braunschweig and coworkers, our study is the first one that considers the possibility of bond strenghtening back-donation by a Main Group system.

5.2 Computational Details

The current computational study explores this possibility for three different silylene complexes (I, II and III in Figure 2), representing both cyclic and acyclic silylenes. The full quantum chemical calculations in this study have been done with density functional

theory (DFT). The DFT calculations have been done with the Turbomole suite of programs, using Turbomole 6.0[27]. The TZVP basis set (triple-z basis set augmented by a polarization function) and the PBE functional have been employed in all the calculations[28-34]. The dispersion correction[35] was used to incorporate dispersion effects. The resolution of identity (RI), along with the multipole accelerated resolution of identity (marij) approximations were employed for an accurate and efficient treatment of the electronic Coulomb term in the DFT calculations. Furthermore, solvent effects have been included for the solvent benzene (ε = 2.3) through single point calculations with the Conductor Like Screening Model – COSMO[36]. For the case of silylene **I-bb** the geometry optimization has also been done with the hybrid functional such as b3-lyp. Frequency calculations have been done at the DFT level in order to obtain the zero point energy, the internal energy and entropic contributions (calculated at 298.15 K). All the numbers reported are ΔG values. The molecular orbital (MO) diagrams have been generated for all the proposed complexes by the Gaussian 09[37] program with PBEPBE functional and 6-31g* basis set. Only the transition metal atom in the geometries has been treated with the 3-21g* basis set. It is to be noted that full geometry calculations done with a higher basis set (DGDZVP) for the palladium atom in the Pd-Me-bb complex leads to no change in the results, indicating the reliability of the calculations. All the bond lengths and the nature of the HOMO and HOMO-1 orbitals for Pd-Me-bb (Pd with DGDZVP) are shown in the figure 4 below. The Wiberg bond indices[38] and NBO analysis were also calculated with Gaussian 09.

5.3 Results and Discussion

The reason we have focused attention on silylenes is because they are likely to have HOMOs that would be closer in energy to the SOMOs of complexes such as π-diborene. For example, our calculations indicate that the gap between the HOMO of the silylene (Si{Si($SiMe_3$)$_3$}{N($SiMe_3$)Dipp}) (I in Figure 2 below) and the SOMO of the π-diborene complex is only 2.4 kcal/mol. This would indicate that bond-strengthening back-donation interactions can happen between the silylene and the π-diborene complex, as illustrated in Figure 1 below.

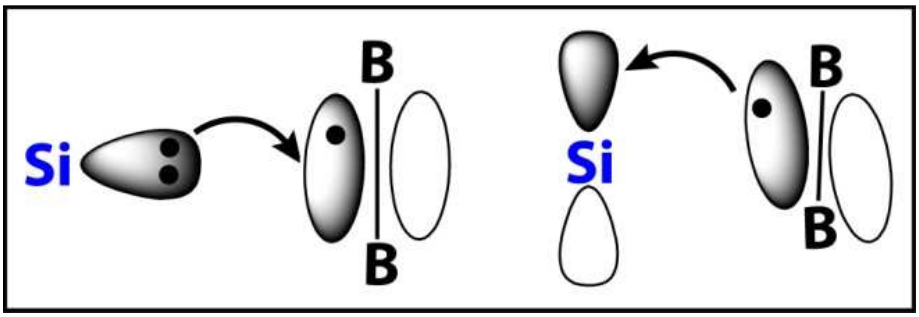

Figure 1. The schematic representation of bond-strengthening back-donation interactions between a silylene complex and a π-diborene.

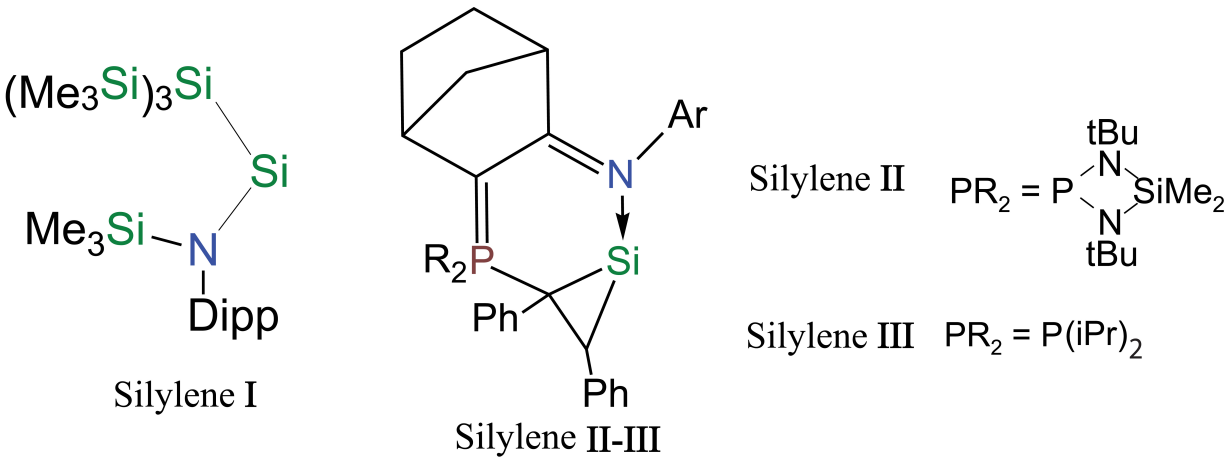

Figure 2. The three silylene complexes considered in the current chapter.

As shown in Table 1 below, the HOMO-SOMO gap between the silylene and the π-diborene is small for all the three cases considered. Encouraged by this result, we proceeded to optimize the geometries of the π-diborene complexed to the cyclic and acyclic silylenes, and compared them to the metal-π-diborene complexes, which were also optimized.

Orbital name	Diborene	Silylene I	Silylene II	Silylene III
SOMO	-0.1532, -0.1696			
HOMO		-0.1571	-0.1630	-0.1632

Table 1. The SOMO and HOMO energy values for model free diborene, transition metal and silylene systems; the energy values are in hartree.

In the free diphenyl diborene, the B-B bond distance is 1.526 Å (since diphenyl diborene does not exist in isolation, this can be considered a reference calculation). As discussed by Braunschweig *et al.*[3], the experimentally observed interaction of this molecule with the zero valence platinum complex exhibits considerable lowering of the B-B bond distance (to 1.510 Å) from its free form. Our calculation optimizing the reported model Pd based diborene complex, Pd-Me-bb (see Figure 3), confirms the strengthening of the B-B bond. The C-B bond distances in Pd-Me-bb are seen to have increased from 1.510 Å to 1.528 Å and 1.530 Å, which indicates that the strengthening of the B-B bond comes at a cost to the C-B bonds. Pd-Me-bb is seen to show almost equal Pd-B bond distances of 2.102 Å and 2.107 Å, which signifies the bonding contribution involving both the boron atoms. The C-B-B bond angles are 169.2° and 174° respectively, which indicate an almost planar structure, which is also in accordance with the proposed model by Braunschweig and co-workers. The other two metal complexes, (Pd-et-bb) and (Pt-et-bb) exhibit similar structural characteristics. The corresponding values are shown in Table 2. Furthermore, as also discussed by Braunschweig and co-workers[3], the HOMO and HOMO-I of Pd-Me-bb, shown in Figure 4 below, indicate the bonding and back-bonding interactions between the metal center and the π-diborene ligand.

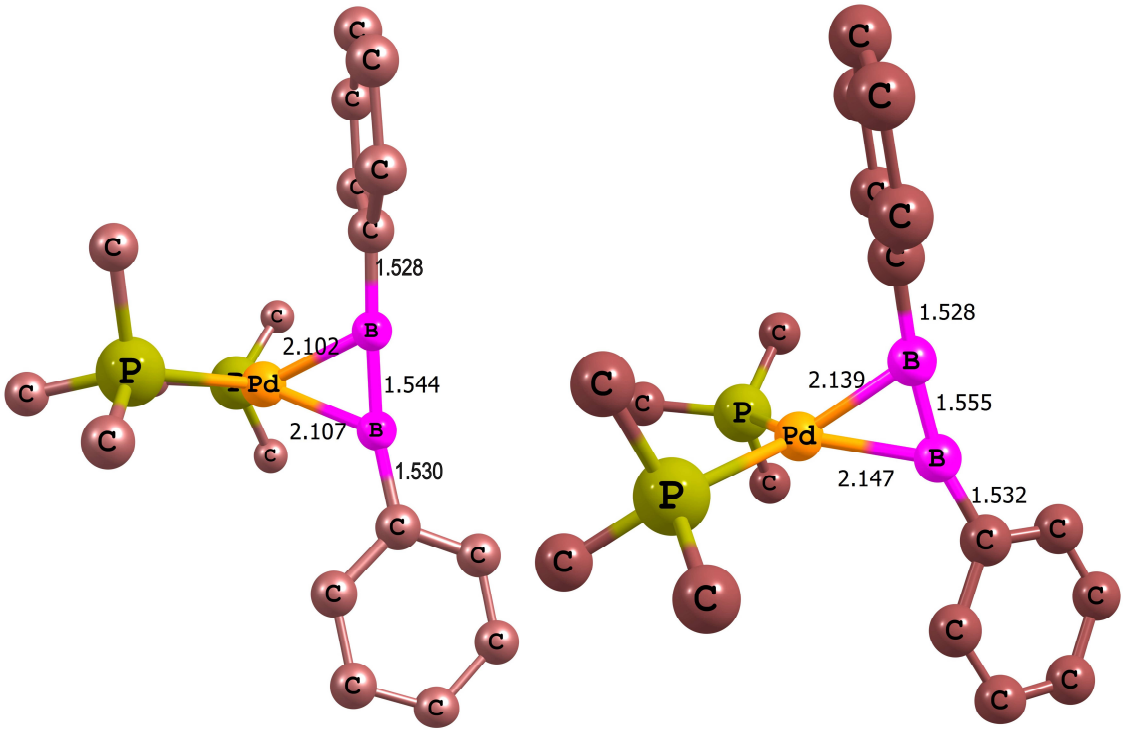

Figure 3. The optimized structures for $Pd(PMe_3)_2$, Pd complexed to the π-diborene employing the 3-21g* basis set and a higher basis set DGDZVP for the transition metal atom; hydrogen atoms have not been shown for the purpose of clarity.

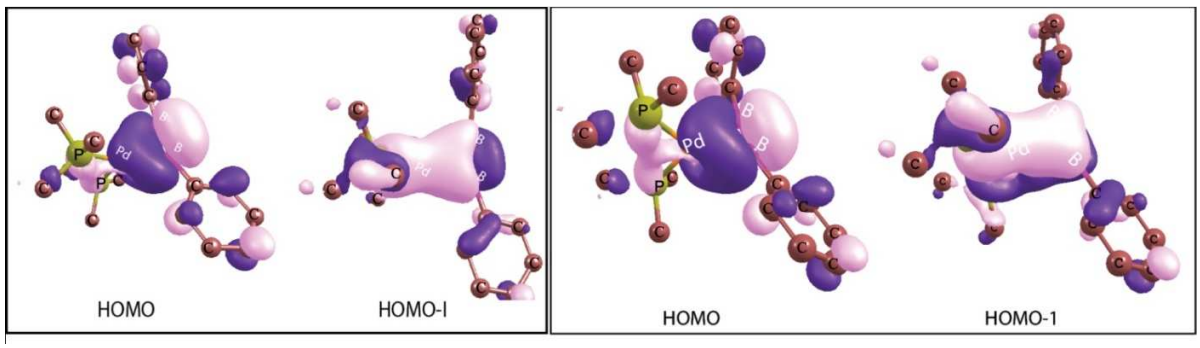

Figure 4. The HOMO and the HOMO-I for the $Pd(PMe_3)_2$ complexed with diborene employing the 3-21g* basis set and a higher basis set DGDZVP for the transition metal atoms.

Now, moving on to the silylenes I-III, the optimized structure of π-diborene coordinated to I (I-bb) is shown in Figure 5 below. It is seen that I-bb not only has the same bonding features as Pd-Me-bb, but also shows evidence of greater interaction between the silicon and the π-diborene. The B-B bond distance is 1.544 Å in Pd-Me-bb, but it is only 1.516 Å in I-bb. Moreover, the Si-B bond lengths (2.047 Å and 2.116 Å) are also comparable to the Pd-B bond lengths. The C-B-B bond angles are 156.3° and 166.2°, which again indicate the slight distortion from planarity, as in the case of Pd-Me-bb. Also, like in Pd-Me-bb, there is an increase in the C-B bond distances (1.546 Å and 1.531 Å respectively), which suggests that the B-B strengthening in the presence of the silylene leads to a concomitant reduction in the bond strength of the C-B bonds. Furthermore, as shown in Figure 6 below, the HOMO and the HOMO-I of I-bb also reveal the same bonding and back-bonding interactions as observed in Pd-Me-bb, though, interestingly, the HOMO of I-bb resembles the HOMO-I of Pd-Me-bb, and the HOMO-I of I-bb resembles the HOMO of Pd-Me-bb. The reason for this is that the shapes of the HOMO and the LUMO are switched for the bare $Pd(PMe_3)_2$ and silylene I complexes. (The HOMO and LUMO for both the cases are shown below in Figure 7 and Figure 8.) Finally, the ΔG of the formation of the π-diborene with I (ΔG = -39.8 kcal/mol) is in the same range as the corresponding Pd-Me-bb formation (ΔG = -39.2 kcal/mol) (see Table 2). All of these structural, electronic and energetic features therefore strongly indicate that silylene I would be either as effective, or more effective at bond-strengthening back-donation with π-diborene than the palladium complex.

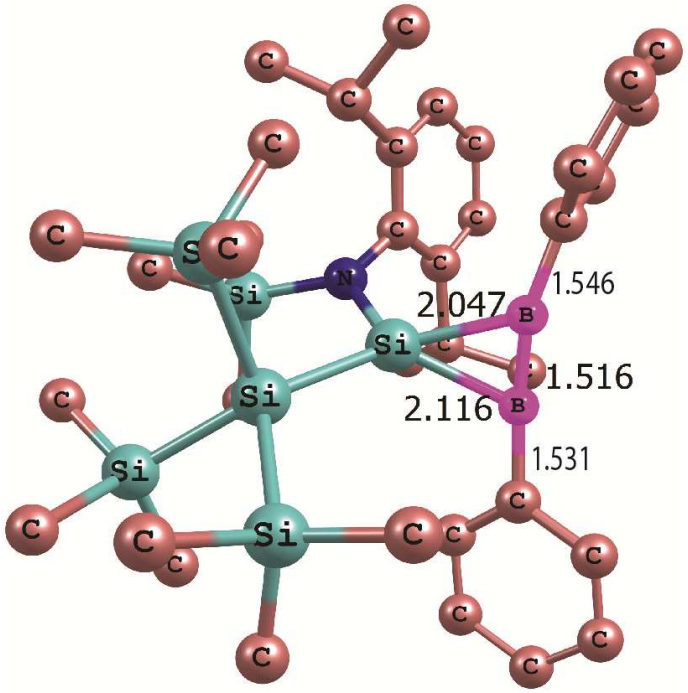

Figure 5. The optimized structure for silylene I complexed to the π-diborene; hydrogen atoms have not been shown for the purpose of clarity.

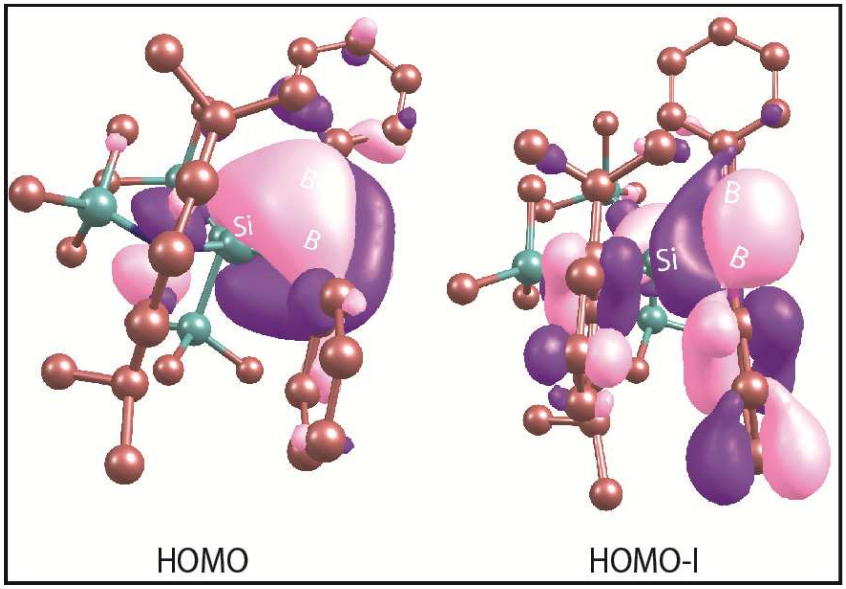

Figure 6. The HOMO (-0.15 Ha) and the HOMO-I (-0.17 Ha) for the complex shown in Figure 5 above.

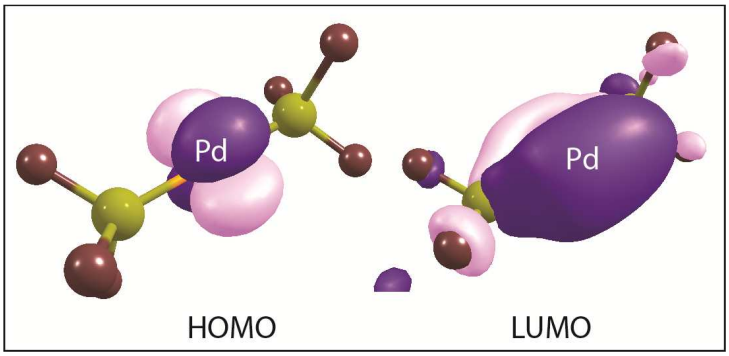

Figure 7. The HOMO (-0.124 Ha) and the LUMO (-0.016Ha) for the bare $Pd(Me_3)_2$ complex.

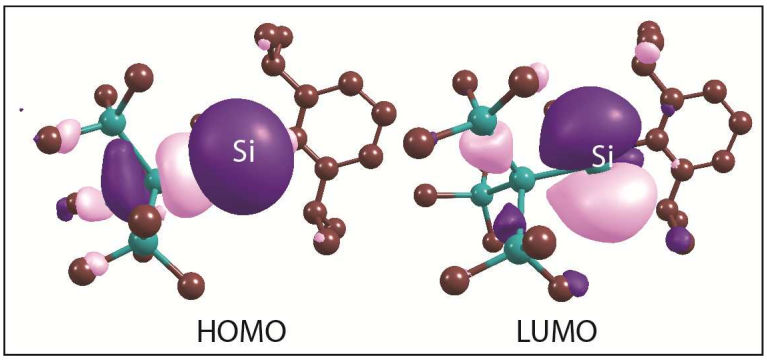

Figure 8. The HOMO (-0.157 Ha) and LUMO (-0.085 Ha) for silylene I.

No	Name of the complexes	Binding energy (Gas phase in kcal/mol)	Binding energy (benzene solvent in kcal/mol)
1.	**Pd-me-bb**	-39.5	-39.2
2.	**Pd-et-bb**	-34.0	-34.6
3.	**Pt-et-bb**	-39.8	-40.3
4.	**I-bb**	-41.1	-39.8
5.	**II-bb**	-40.4	-39.3
6.	**III-bb**	-38.9	-37.7

Table 2. The binding energy values for both the transition metal and silylenediborene complexes.

The same structural, energetic and electronic features are also observed in the cases of the silylenes II and III. The optimized structures of II-bb and III-bb are shown in the Figure 9

and Figure 10 below. Also, the relevant bond lengths and bond angles for II-bb and III-bb have been compiled in Table 3.

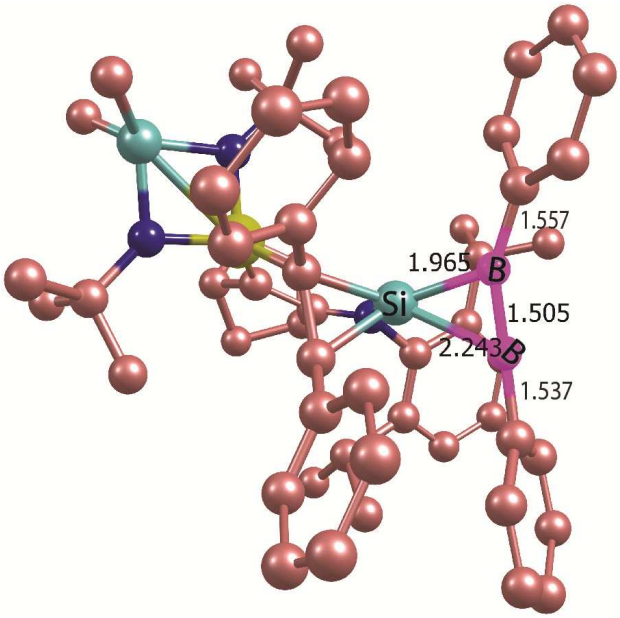

Figure 9. The optimized structure for silylene II complexed to the π-diborene; hydrogen atoms have not been shown for the purpose of clarity.

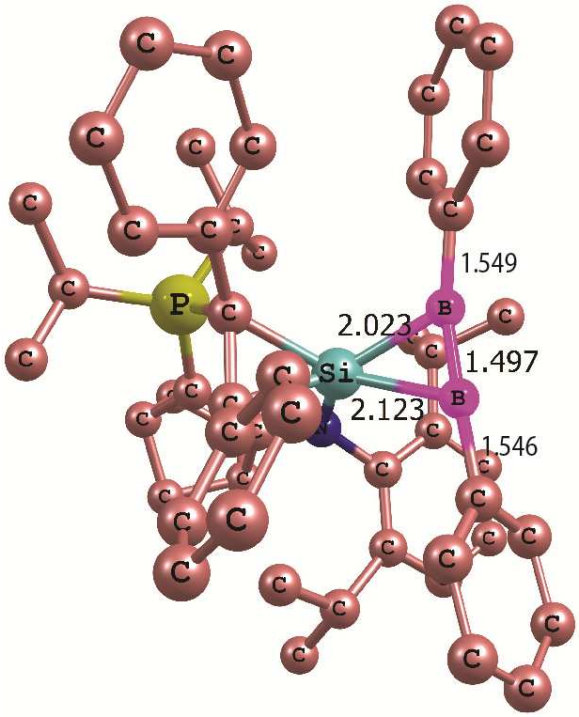

Figure 10. The optimized structure of silylene III complexed to the π-diborene; hydrogen atoms have not been shown for the purpose of clarity.

No	Name of the complexes	d(B-B)	d(C-B)	d(M/Si-B)	angle(C-B-B)
1.	**Free π-diborene**	1.526	1.510 1.510		
2.	**Pd-me-bb**	1.544	1.528 1.530	2.102 2.107	169.2 174.0
3.	**Pd-et-bb**	1.545	1.528 1.529	2.101 2.097	171.4 177.3
4.	**Pt-et-bb**	1.549	1.540 1.537	2.092 2.091	164.4 172.4
5.	**I-bb**	1.516	1.546 1.531	2.047 2.116	156.3 166.2
6.	**II-bb**	1.505	1.557 1.537	1.965 2.243	152.2 171.7
7.	**III-bb**	1.496	1.549 1.546	2.023 2.123	169.2 162.0

Table 3. All the relative bond length and bond angle values for both the transition metal and silylene structures.

The HOMO and HOMO-II of II-bb and III-bb are shown in Figure 11 and Figure 12 below. Since I is an acyclic silylene and II is a cyclic silylene (both have been synthesized [39,40]), the results suggest that the bond-strengthening back-donation interaction with π-diborene would be present in a range of silylenes. Silylene III is a proposed cyclic silylene structure, where isopropyl groups have been suggested for the cyclic backbone (see Figure 2 above). The calculations indicate that this proposed silylene complex would show the best bond-strengthening back-bonding interaction, reducing the B-B bond distance to 1.496 Å. This result suggests that new silylenes can be designed, with greater electron donation to the silylene center, which would lead to the further stabilization of the π-diborene. Indeed, the pronounced B-B bond shortening observed in all the optimized silylene-bb cases suggests that the strengthening will be measurable and observable as shortened bonds, should the compounds be synthesized. This is in contrast to the calculations done by Braunschweig *et al.*[3], where the calculated

B-B bond length in the palladium-bb complex was found to be longer than the experimental value. It is to be noted here that, the B-B bond-shortening has also been observed in the case of III-bb with hybride functional such as b3lyp. The B-B bond is seen to strengthen (value: 1.502 Å) in the silylene complexed case (III-bb) in comparison to the free diborene (value: 1.512 Å).

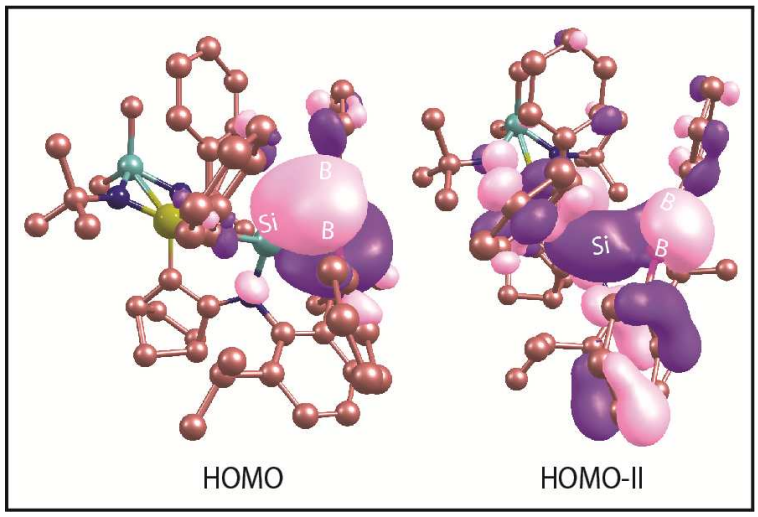

Figure 11. The HOMO (-0.12 Ha) and the HOMO-II (-0.165 Ha) for the complex shown in Figure 9 above.

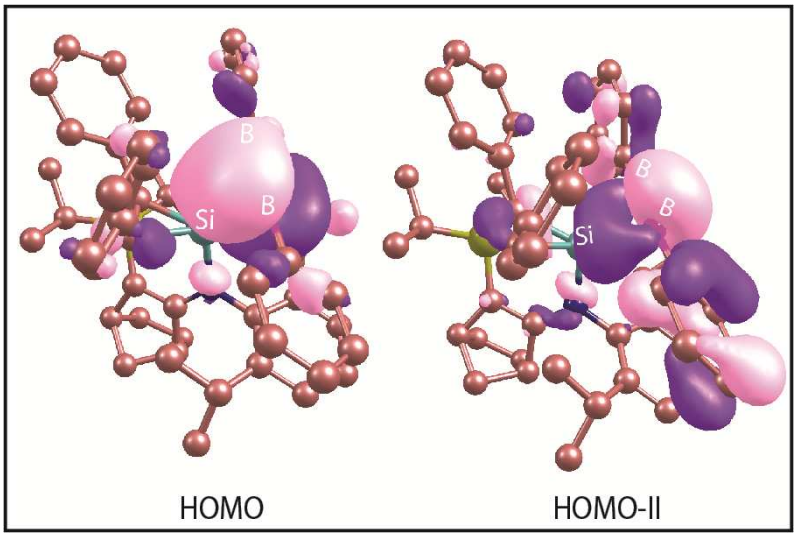

Figure 12. The HOMO (-0.125 Ha) and the HOMO-II (-0.161 Ha)for the complex shown in Figure 10 above.

A final point in this regard is about the calculation of the Wiberg Bond Indices (WBI), which was also done for the three silylene-diborene complexes. The values obtained further indicate the strengthening of the B-B bond. As shown in Table 4 below, the WBI for the B-B bond is found to be 1.43 and 1.50 for the Pd-me-bb and Pd-et-bb case, while it is 1.63 for I-bb, 1.70 for II-bb, and 1.78 for III-bb. The value of the WBI in the free diborene was found to be 1.44, thereby indicating the significant bond strengthening in all the silylene cases considered.

No	**Name of the complexes**	**WBI of first Metal/Si-B bond**	**WBI of second Metal/Si-B bond**	**WBI of B-B bond in the complexes**
1.	**Pd-me-bb**	0.60	0.62	1.43
2.	**Pd-et-bb**	0.60	0.60	1.50
3.	**I-bb**	0.82	0.68	1.63
4.	**II-bb**	0.93	0.44	1.70
5.	**III-bb**	0.78	0.58	1.78

Table 4. The Wiberg Bond Indices (WBI) for the palladium and all the silylenediborene complexes.

NBO analysis done for the Pd-Me-bb complex shows that the occupancies for the bonds between the two borons are 1.91 and 1.52. The data also indicates that both the borons contribute almost equally to the bonds. The analysis for the I-bb complex indicates that the bonds between the borons have characteristics identical to the Pd-Me-bb case: the occupancies for the B-B bonds are 1.9 and 1.6, and the other parameters are almost the same as for the Pd-Me-bb complex. Hence this again indicates the similarity in bonding between the silylene-bb and palladium-bb complexes.

The current calculations show the potential of silylenes to rival transition metal complexes in doing the newly discovered bond-strengthening back-bonding interaction. This indicates that the scope of the Main Group silylenes can be considerably expanded outside the range of dihydrogen activation[41]. For instance, silylenes can activate the π-diborene, leading to the bonding and activation of molecules such as CO and CO_2. As seen from Figure 13 below, showing CO coordination to I-bb, the carbon oxygen bond length in the coordinated CO is 1.16 Å, which is much higher than the bond length (1.138 Å) in the free form of CO. As a result, the boron-boron bond length is also seen to increase to 1.6 Å. Further indication of the favorable binding of CO to the silyene complexed π-diborene is seen from the fact that CO coordination to I-bb is exergonic by 29.7 kcal/mol. The calculations also indicate that this would a barrierless process: a linear transit approach where the distance between the carbon of CO and the boron was decreased from 2.0 Å to 1.4 Å showed a steady decrease in energy till the product was formed.

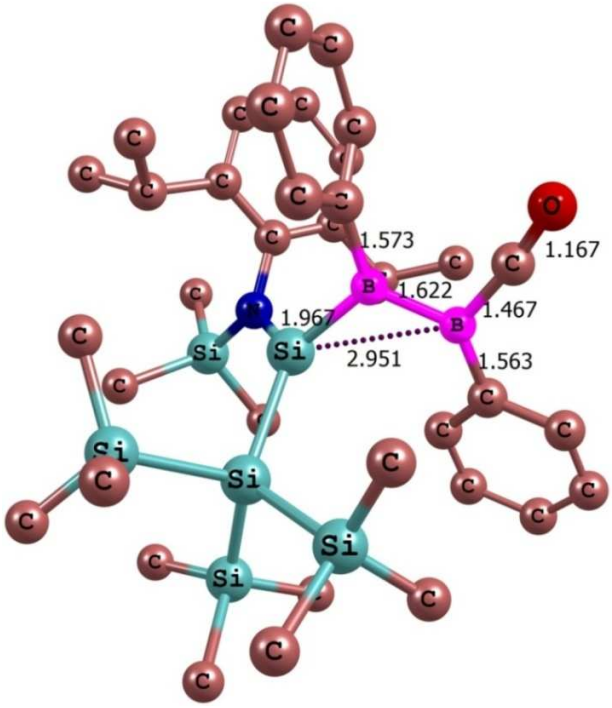

Figure 13. The optimized structure for I-bb complexed to carbon monoxide; hydrogen atoms have not been shown for the purpose of clarity.

The analogous calculation of CO_2 binding to I-bb also indicates high favorability, being exergonic by 25.9 kcal/mol. The transition state for this binding reaction was obtained, and the barrier was calculated to be 13.8 kcal/mol, which indicates that the process would be very feasible at ambient temperatures. It is to be noted that the binding of the free silylene I to CO_2 is only exergonic by 6.0 kcal/mol, and that I does not bind CO at all. Also, the free π-diborene does not exist, and can only be formed when stabilized, as experimentally done[3] with the platinum complex, and computationally shown to be possible here. In other words, the chemistry that can be done with the silylene-π-diborene complex would not be possible by either isolated component. This indicates the importance of the bond-strengthening back-bonding interaction for the Main Group silylene complexes.

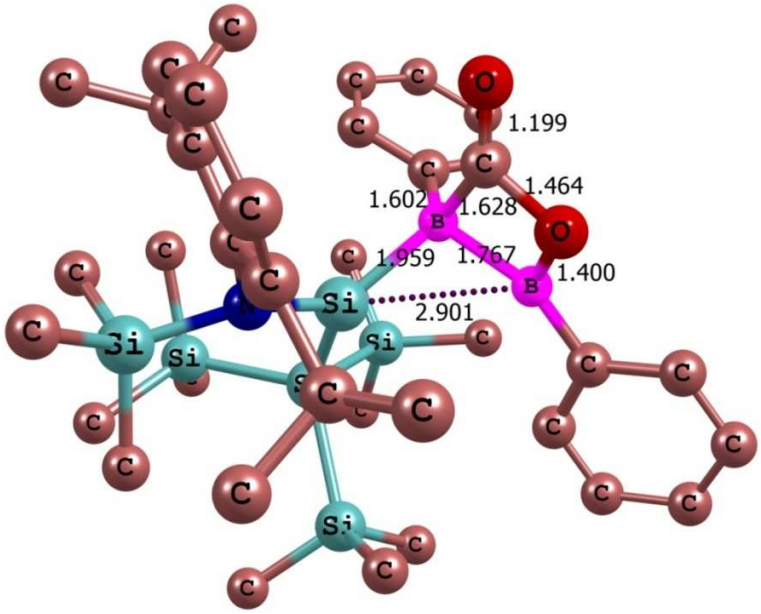

Figure 13. The optimized structure of I-bb complexed to carbon dioxide; hydrogen atoms have not been shown for the purpose of clarity.

5.4 Conclusions

To summarize, the current computational investigations reveal that bond-strengthening π-back donation, which has been recently discovered for transition metal systems[3], can be

done just as effectively by Main Group silylene complexes. This finding has significant implications with regard to the scope and range of the reactivity of silylenes. Moreover, since it is known that Main Group complexes are cheaper and greener than their transition metal counterparts, the current work has both conceptual and practical significance.

5.5 References

1. G. Frenking, N. Fro¨hlich, *Chem. Rev.*, 2000, 100, 717-774.

2. G. J. Kubas, *J. Organomet. Chem*., 2001, 635, 37-68.

3. H. Braunschweig, A. Damme, R. D. Dewhurst, A. Vargas, *Nat. Chem.*, 2013, 5, 115-121.

4. E. Despagnet-Ayoub, K. Miqueu, J.-M. Sotiropoulos, L. M. Henling, M. W. Day, J. A. Labinger, J. E. Bercaw, *Chem. Sci.*, 2013, 4, 2117-2121.

5. C. D. Martin, M. Soleilhavoup, G. Bertrand, *Chem. Sci.*, 2013, 4, 3020-3030.

6. G. D. Frey, V. Lavallo, B. Donnadieu, W. W. Schoeller, G. Bertrand, *Science*, 2007, 316, 439-441.

7. A. J. Arduengo, R. L. Harlow, M. Kline, *J. Am. Chem. Soc*., 1991, 113, 361-363.

8. B. Gehrhus, M. F. Lappert, J. Heinicke, R. Boese, D. Blaser, *J. Chem. Soc., Chem. Commun.*, 1995, 1931-1932.

9. M. Denk, R. Lennon, R. Hayashi, R. West, A. V. Belyakov, H. P. Verne, A. Haaland, M. Wagner, N. Metzler, *J. Am. Chem. Soc*., 1994, 116, 2691-2692.

10. M. Haaf, T. A. Schmedake, R. West, *Acc. Chem. Res*., 2000, 33, 704-714.

11. G. Bender, T. Wiegand, H. Eckert, R. Fröhlich, C. G. Daniliuc, C. Mück-Lichtenfeld, S. Ndambuki, T. Ziegler, G. Kehr, G. Erker, *Angew. Chem. Int. Ed*., 2012, 51, 8846-8849.

12. G. C. Welch, R. R. S. Juan, J. D. Masuda, D. W. Stephan, *Science*, 2006, 314, 1124-1126.

13. P. R. Schreiner, *Chem. Soc. Rev.*, 2003, 32, 289-296.

14. P. P. Power, *Nature*, 2010, 463.

15. H. Braunschweig, A. Damme, R. D. Dewhurst, T. Kramer, I. Krummenacher, A. K. Phukan, *Organometallics*, 2014, 33, 604-606.

16. Z. Li, H. T. Chifotides, K. R. Dunbar, *Chem. Sci*., 2013, 4, 4470-4485.

17. H. Braunschweig, K. Radacki, R. Shang, *Chem. Commun*., 2013, 49, 9905-9907.

18. T. Miyada, M. Yamashita, *Organometallics*, 2013, 32, 5281-5284.

19. J. Brand, H. Braunschweig, S. S. Sen, *Acc. Chem. Res*., 2014, 47, 180-191.

20. K. Hari Krishna Reddy, E. D. Jemmis, *Dalton. Trans*., 2013, 42, 10633-10639.

21. H. Braunschweig, A. Damme, *Chem. Commun*., 2013, 49, 5216-5218.

22. H. Braunschweig, A. Damme, T. Kupfer, *Inorg. Chem*., 2013, 52, 7822-7824.

23. H. Braunschweig, R. Bertermann, A. Damme, T. Kupfer, *Chem. Commun*., 2013, 49, 2439-2441.

24. H.-J. Himmel, *Nat. Chem*., 2013, 5, 88-89.

25. Y. Shoji, N. Tanaka, K. Mikami, M. Uchiyama, T. Fukushima, *Nat. Chem*., 2014, 6, 498-503.

26. R. S. Anju, D. K. Roy, B. Mondal, K. Yuvaraj, C. Arivazhagan, K. Saha, B. Varghese, S. Ghosh, *Angew. Chem. Int. Ed.*, 2014, 53, 2873-2877.

27.TURBOMOLE V6.0 2009, a development of University of Karlsruhe and Forschungszentrum Karlsruhe GmbH, 1989-2007, TURBOMOLE GmbH, since 2007; available from http://www.turbomole.com.

28. F. Weigend, *Phys. Chem. Chem. Phys.*, 2002, 4, 4285-4291.

29. F. Weigend, R. Ahlrichs, *Phys. Chem. Chem. Phys.*, 2005, 7, 3297-3305.

30. A. Schafer, H. Horn, R. Ahlrichs, *J. Chem. Phys*., 1992, 97, 2571-2577.

31. P. A. M. Dirac, Proceedings of the Royal Society of London. Series A 1929, 123, 714-733. (31)

32. J. C. Slater, *Phys. Rev*., 1951, 81, 385-390.

33. J. P. Perdew, K. Burke, M. Ernzerhof, *Phys. Rev.Lett*., 1996, 77, 3865-3868.

34. J. P. Perdew, Y. Wang, *Phys. Rev. B*, 1992, 45, 13244-13249.

35. S. Grimme, *J. Comp. Chem*., 2004, 25, 1463.

36. A. Klamt, G. Schuurmann, *J. Chem. Soc., Perkin Transactions 2*, 1993, 799-805.

37. M. J. Frisch, G. W. Trucks, H. B. Schlegel, G. E. Scuseria, M. A. Robb, J. R. Cheeseman, G. Scalmani, V. Barone, B. Mennucci, G. A. Petersson, H. Nakatsuji, M. Caricato, X. Li, H. P. Hratchian, A. F. Izmaylov, J. Bloino, G. Zheng, J. L.

Sonnenberg, M. Hada, M. Ehara, K. Toyota, R. Fukuda, J. Hasegawa, M. Ishida, T. Nakajima, Y. Honda, O. Kitao, H. Nakai, T. Vreven, J. A. Montgomery, J. E. Peralta, F. Ogliaro, M. Bearpark, J. J. Heyd, E. Brothers, K. N. Kudin, V. N. Staroverov, R. Kobayashi, J. Normand, K. Raghavachari, A. Rendell, J. C. Burant, S. S. Iyengar, J. Tomasi, M. Cossi, N. Rega, J. M. Millam, M. Klene, J. E. Knox, J. B. Cross, V. Bakken, C. Adamo, J. Jaramillo, R. Gomperts, R. E. Stratmann, O. Yazyev, A. J. Austin, R. Cammi, C. Pomelli, J. W. Ochterski, R. L. Martin, K. Morokuma, V. G. Zakrzewski, G. A. Voth, P. Salvador, J. J. Dannenberg, S.Dapprich, A. D. Daniels, J. B. Farkas Foresman, J. V. Ortiz, J. Cioslowski, D. J. Fox, Wallingford CT, 2009.

38. J. P. Foster, F. Weinhold, *J. Am. Chem. Soc*., 1980, 102, 7211-7218.

39. R. Rodriguez, T. Troadec, T. Kato, N. Saffon-Merceron, J.-M. Sotiropoulos, A. Baceiredo, *Angew. Chem*., 2012, 124, 7270-7273.

40. A. V. Protchenko, A. D. Schwarz, M. P. Blake, C. Jones, N. Kaltsoyannis, P. Mountford, S. Aldridge, *Angew. Chem. Int. Ed.*, 2013, 52, 568-571.

41. A. V. Protchenko, K. H. Birjkumar, D. Dange, A. D. Schwarz, D. Vidovic, C. Jones, N. Kaltsoyannis, P. Mountford, S. Aldridge, *J. Am. Chem. Soc.*, 2012, 134, 6500-6503.

Chapter 6

Small Molecule Activation by Constrained Phosphorus Compounds

Abstract

An exciting new development in main group chemistry has been the use of a constrained, “flat”, phosphorus based complex to mediate in reactions such as the dehydrogenation of ammonia borane (AB), and the activation of the N-H bond in primary amines. Its importance is based on the fact that it shows that main group compounds, when properly designed, can be as effective as transition metal complexes for doing significant chemical transformations. What the current computational study, employing density functional theory (DFT), reveals is that a common, general mechanism exists that accounts for the behavior of the flat phosphorus compound in the different reactions that have been experimentally reported to date. This mechanism, which involves the mediation by a base as a proton transfer agent, is simpler and energetically more favorable than the previous mechanisms that have been proposed for the same reactions in the literature. It is likely that the knowledge gained from the current work about the chemical behavior of this phosphorus compound can be utilized to design new constrained phosphorus based compounds.

6.1 Introduction

Since its discovery in 1669[1], phosphorus and its chemistry has acquired great significance. The remarkable property of spontaneous flammability of phosphorus found wide usage in war[1, 2]. Its oxidation product, phosphate (PO_4^{3-}), was discovered to be an essential nutrient in all living organisms[2]. Furthermore, a variety of phosphorus based phosphine ligands that can cooperate with various transition metal systems in many metal-catalyzed transformations[3, 4] have been designed in more recent years. The rhodium catalyzed hydroformylation reaction[5-7], the ruthenium catalyzed[8-10] olefin metathesis and the palladium catalyzed C-C bond formation[11] reactions are prominent examples where the organophosphine ligands play a significant role. Thus, phosphorus based ligands have emerged as one of the most important chemical components of modern industrial processes.

However, while phosphorus compounds have proved to be very effective as ligands in transition metal chemistry, their use in main group chemistry as independent compounds has not met with similar success, unlike compounds based on carbon[12-19], silicon[20-24] and germanium[25-27]. Indeed, chemistry with compounds based on purely Group 15 elements, such as nitrogen or phosphorus, has usually led to stoichiometric behavior for the oxidative addition or reductive elimination steps[28], which are so significant in transition metal chemistry[29, 30]. This includes the chemistry of main group compounds known as frustrated Lewis pairs (FLPs)[31] that can activate dihydrogen[32-34] and ammonia-borane[35, 36], as well as hydrogenate the C=C[37], C=N[38-40] and C=O[41, 42] bonds. Very few studies have been reported in the literature for systems based on Group 15 elements where the chemical behavior has been shown to be catalytic in nature[43]. As a result, although phosphorus based ligands are exceptionally functional in the metal systems, the design of phosphorus based main group catalysts has been proved to be very challenging.

In this context of main group catalysis, an important development is that of Radosevich and co-workers, who have recently demonstrated that a phosphorus based system can catalytically mimic the redox reactivity of transition metal catalysts[43]. The flat, T-shaped, tri-coordinated phosphorus compound, which had been originally described by the group

of Arduengo[44-46] and Driess[47], is significant for its ability to dehydrogenate ammonia borane (AB) and do subsequent transfer hydrogenation[43]. This pincer coordinated phosphorus complex is shown in Figure 1 below. It is interesting to also note that other phosphorus compounds having the conventional pyramidal structure are ineffectual for the same AB dehydrogenation-transfer hydrogenation process[43, 48]. This shows the importance of constraining the geometry of the phosphorus compound to the T shape[48]. The mechanism proposed by Radosevich and coworkers for this process invokes single-site behavior, involving a P(III)/P(V) switching at the phosphorus center, analogous to transition metal complexes[29, 49-52].

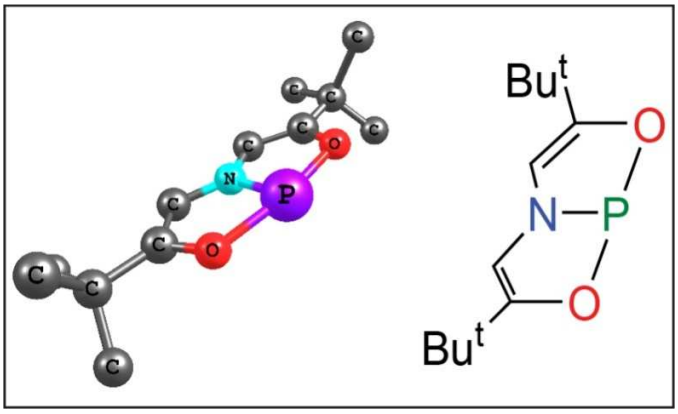

Figure 1. The structure of the flat, T-shaped, tri-coordinate phosphorus based pincer compound.

The AB dehydrogenation pathway by this T-shaped phosphorus pincer complex has been computationally investigated by Sakaki and coworkers[53]. Interestingly, they have found that phosphorus is not, as stated by Radosevich *et al*, a single-site activator in the reaction. In their mechanism, shown in Figure 2a below (and denoted as the "Sakaki Mechanism" in this chapter) one of the coordinating oxygens cooperates with the central phosphorus atom in the presence of AB, resulting in the cleavage of the phosphorous oxygen bond (P-O), and the simultaneous transfer of both the hydridic and protic hydrogens of AB to the phosphorus and the oxygen atoms respectively. This type of ligand cooperativity is well known in certain transition metal systems[54-56]. The Sakaki Mechanism[53] also involves further assistance of the amino-borane (NH_2BH_2, generated

from AB in the first step of the catalytic cycle) with the backbone nitrogen of the pincer complex for the completion of the overall dehydrogenation process (see Figure 2 below).

In more recent work, Radosevich *et al*. have observed N-H bond cleavage in the reaction of the phosphorus pincer complex with ammonia, as well as with a series of primary amines[57]. This is a significant result, since the splitting of the N-H bond in ammonia is a highly challenging reaction[58-61], with only a few examples known in the literature[57, 62, 63]. However, what is also interesting to note is that, for this set of reactions, the N-H bond cleavage would have to proceed *without the involvement of the N-P backbone in the pincer complex*. In other words, a mechanism significantly different from the Sakaki Mechanism[53] for AB dehydrogenation would have to be operating in this case. This suggests that

(i) either the Sakaki Mechanism[53] is only limited to the AB dehydrogenation process and a different reaction mechanism is operating for the N-H bond cleavage reaction (indeed, Radosevich *et al.* have proposed an intermolecular N-H bond cleavage mechanism – denoted as the "Radosevich Mechanism" - for this set of reactions[57], which is also shown in Figure 2b), or

(ii) there is a general, common mechanism that is operative for the two different reactions, AB dehydrogenation and N-H activation; a mechanism that is different from both the Sakaki[53] and Radosevich[57] mechanisms and more efficient than both.

The purpose of the current work is to demonstrate that there indeed does exist a common, general mechanism for both the AB dehydrogenation and N-H activation processes. This mechanism is also shown in the Figures 2c and 2d, along with the Sakaki and Radosevich Mechanisms. The mechanism involves, in its first step, the cleavage of the P-O bond, a feature common with the Sakaki Mechanism, but subsequently proceeds through the mediation of a primary amine molecule in the N-H activation reaction, and of an ammonia molecule in the AB dehydrogenation reaction, leading to the observed products (see Figure 2). Such mediation by proton shuttling molecules, such as water, is known in biological systems[64-67]. As will be discussed in the Results and Discussion section, this

proposed mechanism is competitive with the Radosevich Mechanism, and is both simpler and energetically more favorable than the Sakaki Mechanism. This strongly indicates that it is likely to be the operative mechanism in both the reactions with the T-shaped phosphorus complex that have been reported to date. The significance of this result is that it provides insights that allow the development of new phosphorus based complexes that can participate and mediate in important reactions such as AB dehydrogenation and the N-H activation of primary amines.

a) Sakaki Mechanism: (Ammonia-borane dehydrogenation)

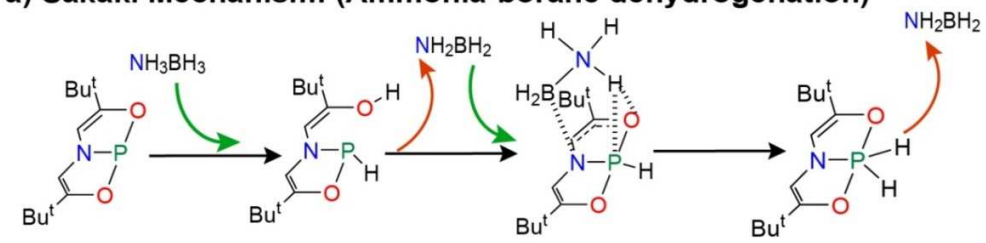

b) Radosevich Mechanism: (N-H oxidative addition of methylamine)

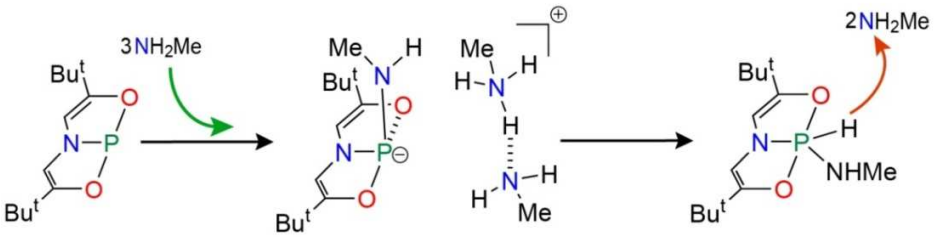

c) Our Mechanism: (N-H oxidative addition of methylamine)

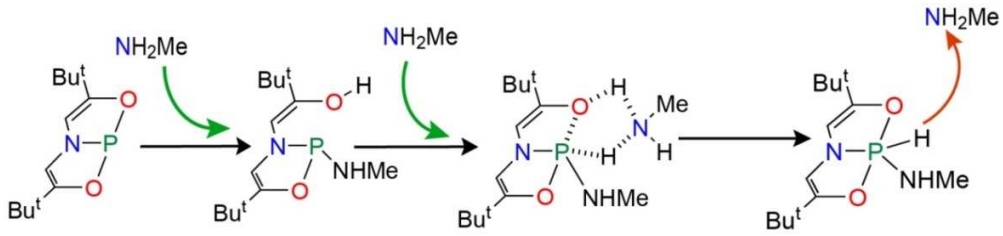

d) Our Mechanism: (Ammonia-borane dehydrogenation)

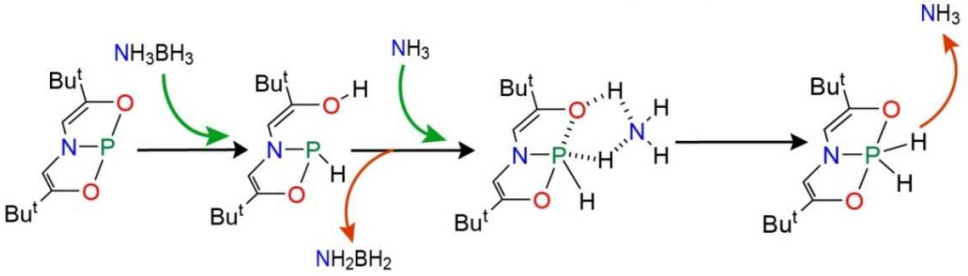

Figure 2. (a) The mechanism proposed by Sakaki and coworkers for the dehydrogenation of ammonia borane (AB) by the T-shaped phosphorus pincer complex. (b) The mechanism proposed by Radosevich and coworkers for the N-H activation by the T-shaped phosphorus pincer complex. (c) and (d) The general mechanism that we have proposed for the N-H activation and the AB dehydrogenation reactions.

6.2 Computational Details

The DFT calculations have been done with the Gaussian 09 program[68] with M06-2X[69] functional and 6-311++G (2d, 2p)[70-72] basis set. It is to be noted that specific to only the 2,4,6-trimethylaniline substrate case, pertaining to the N-H activation of the primary amine, the proposed mechanism has been calculated with the M06-2X functional with the 6-31g*[73] basis set in order to reduce the computational expenses. Solvent effects[74] have been included throughout the optimization of reactants, intermediates, products, and transition states for all the mechanisms discussed in the chapter for AB dehydrogenation and amine activation reactions. For AB dehydrogenation, acetonitrile (ε = 35.688) has been employed as the solvent and benzene (ε = 2.270) has been applied for the N-H oxidative addition reactions of amines. Two different solvents have used in order to be consistent with the respective experiments. Frequency calculations[75, 76] have been done in order to obtain and include the zero point energy, the internal energy and entropy contributions (calculated at 298.15 K). Therefore, all the numbers reported in the chapter are the free energy (ΔG) values.

6.3 Results and Discussion

6.3.1 The Radosevich Mechanism for N-H Activation.

The “Radosevich Mechanism” involves the creation of a P-N bond by the interaction of the phosphorus center with three molecules of the amine, followed by a P-H bond formation by hydrogen transfer from the ammonium cation to the amidophosphoranide anion (see Figure 2b). Radosevich *et al.* have determined the energy profile for this mechanism for the case of methylamine (NH_2Me). We have obtained the free energy

profile for the same mechanism and with the same primary amine, so that this mechanism can be compared to our proposed mechanism (which will be discussed later) at the same level of theory as employed by Radosevich and coworkers[57] {MO6-2X/6-311++g (2d, 2p)}. As shown in Figure 3 below, there are four reactant species: 1 and the three NH_2Me molecules. The three NH_2Me molecules can form an adduct complex: $(NH_2Me)_3$ which then reacts with 1. However, this adduct complex formation bears an entropic cost, and therefore 1 and $(NH_2Me)_3$ lie 11.3 kcal/mol above the four separate reactant species on the free energy surface. Subsequent to this, the mechanism proceeds with the interaction of $(NH_2Me)_3$ with the phosphorus pincer complex to form an adduct INT1: the hydrogen-bonding cluster of three methylamine molecules with 1. This has been found to be 22.1 kcal/mol endergonic in comparison to the starting reactants. INT1 is then converted to a zwitterionic species INT2 by the formation of a phosphorus nitrogen bond through the first transition state (TS1). Subsequent to this, the mechanism suggests that the deprotonation of the ammonium cation would occur, followed by a proton transfer step (overcoming the transition state TS2) to the amidophosphoranide anion, leading to the final product. TS1 is seen to be endergonic by 28.3 kcal/mol in comparison to the separated reactants, while the barrier corresponding the crossing of TS2 has been calculated to be 30.9 kcal/mol from the separated reactants, and is therefore the barrier that has to be overcome for the reaction to be completed. The final product, 6, is endergonic by 4.0 kcal/mol.

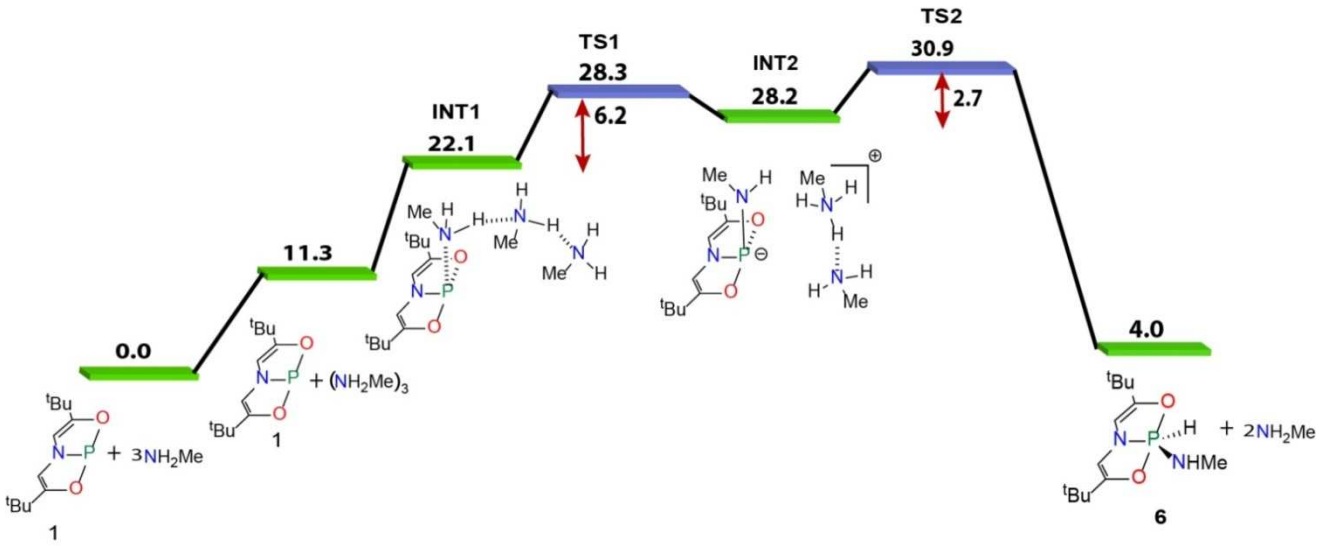

Figure 3. The free energy profile of the Radosevich Mechanism for the N-H oxidative addition reaction of methylamine to the pincer ligated phosphorus compound; all values are in kcal/mol.

6.3.2 Our Mechanism for N-H Activation.

In our mechanism, the first step is the interaction between the phosphorus of the pincer complex and the oxygen of the ONO ligand with the nitrogen and hydrogen respectively of the N-H bond in methylamine. This step, involving phosphorus-oxygen cooperativity in 1, is analogous to what Sakaki *et al.* have proposed for the case of AB dehydrogenation by 1[53]. This leads to the intermediate 2_NMe, in which the nitrogen of the amine is bonded with the phosphorus of the pincer complex and the proton is attached to one of the oxygens of the ONO ligand. This is seen to be endergonic by 9.7 kcal/mol (see Figure 4). After 2_NMe is formed, several reactions are possible: (i) the proton can take part in tautomerism with the vicinal carbon-carbon double bond, or (ii) the proton attached to the oxygen can directly transfer to the phosphorus centre, or (iii) the proton can shift from oxygen to phosphorus with the help of another amine molecule, which can act as a proton transfer agent (see Figure 2c), or (iv) the tautomerism may occur through the help of the second amine molecule.

All four possibilities have been investigated. The free energy profile obtained for the possibilities (i) and (ii) is shown in Figure 5I below. The results make it clear that Possibility is highly unlikely, since the barrier for this process is seen to be 61.0 kcal/mol. Possibility (ii) is also unlikely, because the barrier for this process was calculated to be 30.8 kcal/mol. Since the intermediate 2_NMe is itself 9.7 kcal/mol higher in energy in comparison to the separated reactants, this means that the transition state for this process would be 40.5 kcal/mol higher in energy in comparison to the original separated reactants. This suggests an unfavorable reaction pathway for getting from the reactants to the observed final product.

However, as shown in Figure 5II, Possibility (iii) is seen to have a barrier of only 20.0 kcal/mol, thus being about 10.8 kcal/mol lower in energy than the barrier for Possibility (ii). Such a lowering of the energy barrier (about 10.0 kcal/mol) in the presence of an extra substrate is also known for other main group systems. For example, Sicilia and co-workers have demonstrated the mechanism of introducing a second molecule of ammonia for the 1,1 and 1,4 addition of ammonia by silylene and germylene systems[77]. The participation of the extra NH_2Me also suggests an entropically unfavorable reaction, having an ordered transition state with high molecularity. This, indeed, matches the observed experimental findings for the reaction of the amines with 1. Our calculations indicate that the ΔS for the reaction would be 79.0 cal/mol/K (the value obtained for the ΔS by comparing the entropy of the transition state TS2/5_NMe and the original reactant species). This compares very favorably with the ΔS value obtained experimentally from the Eyring plot by Radosevich and coworkers for the N-H bond splitting reaction involving 1 and the *n*-propylamine (72.0 +/- 2.0 cal/mol/K)[57], further suggesting the feasibility of our proposed mechanism.

The reason the barrier is decreased by the intervention of an additional amine is because of the conversion of a sterically encumbered three membered transition state (O-H-P) to a more sterically relaxed five membered transition state (O-H-N-H-P). A similar mediation of an additional amine can also be envisaged for the tautomerism case as well (Possibility (iv)). As Figure 6 shows, the presence of an additional amine indeed reduces the barrier

significantly for this case – from 61.0 kcal/mol to 21.3 kcal/mol. Since this barrier is only 1.3 kcal/mol higher than the barrier obtained for Possibility (iii) (see Figure 5II), the results indicate that the possibility of a *keto* species being formed cannot be ruled out: it may be formed as an undesired side product during the reaction. Furthermore, in comparison to the Radosevich Mechanism, discussed in the earlier section, the barrier for our proposed mechanism {Possibility (iii)} is lower, but the difference between the barriers for the slowest steps of the two mechanisms is only 1.2 kcal/mol (see Figure 6). This indicates that both the mechanisms could be operative during the amine oxidative addition process. This may explain the experimental observation of the order of the reaction being 3 for this process, as noted by Radosevich and co-workers[57]. Also, it should be noted that for the specific case of the N-H activation of the ammonia substrate, the Radosevich Mechanism could be the preferred mechanism, since the experiments were done employing liquid ammonia as the solvent[57], and hence the entropic cost of bringing three ammonia molecules to the vicinity of the phosphorus catalyst would be reduced in this specific case. Nevertheless, the present calculations do indicate that our proposed reaction mechanism has a slightly lower barrier in general in comparison to the Radosevich Mechanism for primary amine cases, and would thus be very competitive during the reaction process for the N-H activation of the primary amines by the constrained phosphorus based system. It can also be envisaged that two amine molecules can mediate to form a seven membered transition state (O-H-N-H-N-H-P), and this may also be a competitive pathway during the reaction. Although such a pathway has not been studied in the current work, due to the computational constraints, it is clear that such possibilities, based on our proposed mechanism, would also provide a reaction cycle having order 3 with respect to the primary amine.

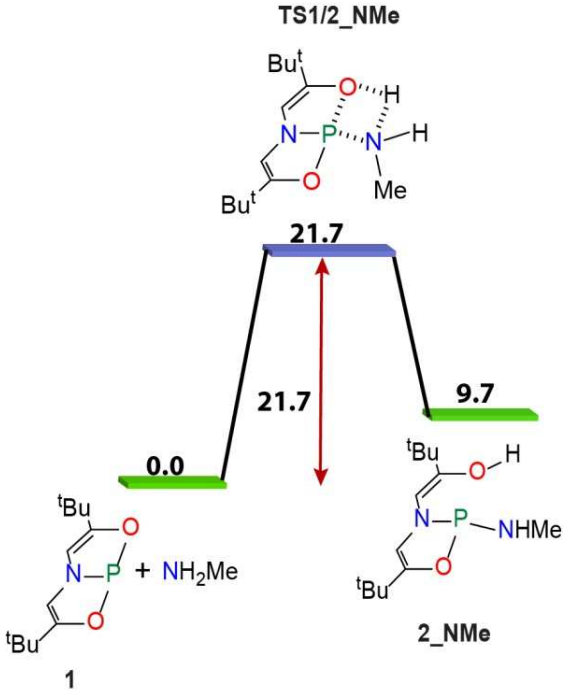

Figure 4. The free energy profile of the phosphorus oxygen bond cleavage by the primary amine molecule; all values are in kcal/mol.

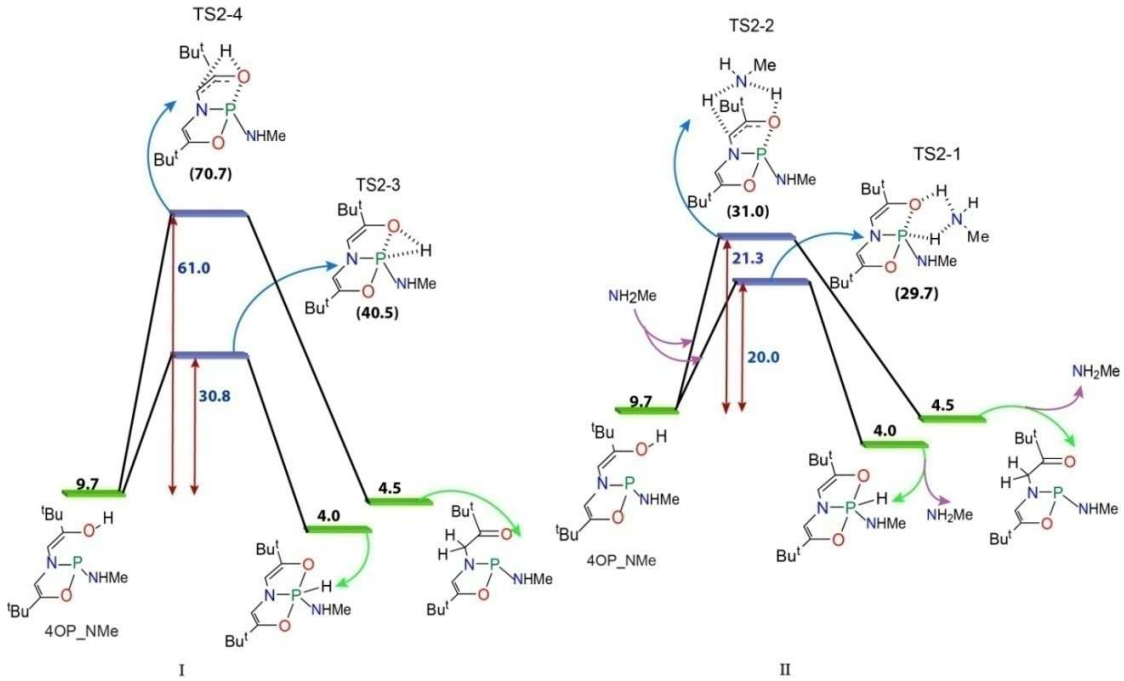

Figure 5. (I) The free energy profile of the possibilities (i) and (ii) for proton transport from oxygen to phosphorus for amine activation reaction. (II) The free energy profile of

the possibilities (iii) and (iv) for proton transport from oxygen to phosphorus with the help of second amine molecule for amine activation reaction all values are in kcal/mol.

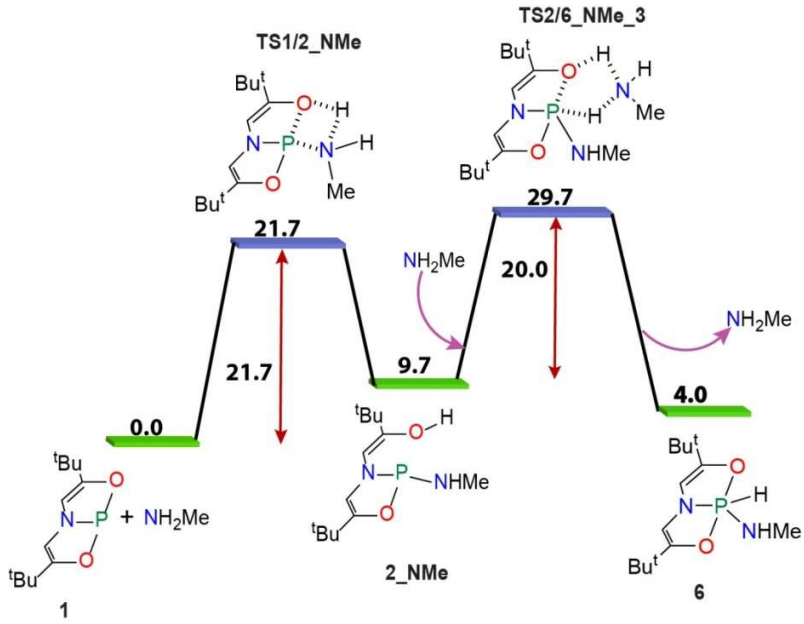

Figure 6. The free energy profile of our proposed mechanism for the N-H oxidative addition reaction of methylamine; all values are in kcal/mol.

6.3.3 The Sakaki Mechanism for Ammonia Borane (AB) Dehydrogenation.

In this section, we discuss the calculations pertaining to the "Sakaki Mechanism" for AB dehydrogenation by 1 (discussed in the Introduction, and shown in Figure 2(a)) with the intention of comparing the free energy surface with that of our proposed mechanism for the same reaction (which will be discussed in the next section).

As shown in Figure 13 below, the first step of the Sakaki Mechanism is the phosphorous ONO ligand cooperation that leads to P-O bond cleavage and forms the intermediate 2 *via* the transition state TS1/2, a process that is seen to have a barrier of 26.6 kcal/mol. This first step is common to the Sakaki mechanism as well our newly proposed mechanism (which is discussed in the next section). The reason this step is feasible for the constrained geometry phosphorus complex, and not for pyramidal geometry phosphorus complexes (since they have not been found to be effective at AB

dehydrogenation[43]) can be understood from a perusal of the HOMO and the LUMO for 1, and comparing them to the HOMO and the LUMO of the pyramidal phosphorus complex $P(OMe)_3$. As shown in the Figure 7, the HOMO for the planar phosphorus complex 1 is found to be located over the phosphorus and the two oxygen atoms, while the LUMO is found to be located on the central phosphorus atom. This suggests that the initial phosphorus oxygen bond cleavage by the simultaneous transfer of both the hydridic and protic hydrogens of AB to the phosphorus and the oxygen atoms for the case of AB dehydrogenation is likely for the phosphorus complex, because the LUMO on phosphorus can interact with the hydride of AB, while one of the coordinated oxygens can donate electron density to the protic hydrogen of AB, since the HOMO extends over the coordinated oxygens. However, for the case of pyramidal phosphorus complexes, represented by $P(OMe)_3$ in our calculations, the HOMO is solely present over the phosphorus atom, while the LUMO is present over the methyl groups (see Figure 8). The antibonding orbital, i.e., the lowest unoccupied molecular orbital (LUMO), which is based on the phosphorus atom, is much higher in energy and thus unable to participate in accepting electron density from the incoming substrate. This means that the donation of electron density from the hydridic hydrogen of AB to the phosphorus or oxygen atoms would not be possible in the pyramidal $P(OMe)_3$ case. This shows the importance of employing a constrained phosphorus complex in order to ensure that the first step of the AB dehydrogenation process can proceed in a facile manner. It is to be noted, however, that there are some other examples where distorted, constrained tricoordinated phosphorus systems are capable of similar bond activation reactions. For instance, Radosevich and coworkers have reported a distorted, tricoordinated, pyramidal phosphorus complex recently that can activate the O-H bond[78]. The structure of this complex is shown in Figure 9 below. In this chapter, we have analyzed the frontier molecular orbitals of this complex, and compared them with both the T-shaped phosphorus complex and the pyramidal phosphorus $P(OMe)_3$ type complexes. The frontier orbitals of this complex are shown in Figure 10. The highest bonding orbital (i.e. the HOMO) of this complex is located on the phosphorus and the adjacent nitrogen atoms and the LUMO for this complex is located away from the phosphorus atom. However, the

LUMO+1 orbital for this complex is located significantly on the phosphorus, and its energy is significantly lower than the LUMO of the inert pyramidal phosphorus based systems. For the T-shaped, planar phosphorus system[43], the LUMO is centered on the phosphorus atom and is even lower in energy than the LUMO+1 in the distorted pyramidal system. Thus, the calculations indicate that the reason the planar and the distorted pyramidal structures are more effective at bond activation than the pyramidal $P(OMe)_3$ type phosphorus based structures is because of the high energy of the antibonding orbital that is present on the phosphorus atom in the pyramidal systems.

Recently, Kinjo *et al.* have reported another phosphorus based pyramidal structure and found that it is able to activate the N-H bond in ammonia[62]. We have also performed calculations for this complex, the structure of which is shown in Figure 11. It is to be noted that the frontier orbitals (shown in Figure 12) for the single point geometry (calculation done by taking the coordinates from the .cif file) and the final optimized geometry for the distorted pyramidal complex reported by Radosevich and coworkers[78] and discussed in the previous paragraph, are similar. Hence, for the phosphorus based pyramidal structure reported by Kinjo *et al.*, the frontier orbitals have been obtained from only a single point calculation of the structure obtained from the reported .cif file[62]. For this complex, the LUMO+5 orbital is located on the phosphorus atom. The LUMO, LUMO+1, LUMO+2, LUMO+3 and the LUMO+4 are all located on atoms at a distance from the proton accepting nitrogen atom (on which the HOMO is located). However, it is important to note that the structure has another phosphorus atom in the backbone, where the LUMO+5 orbital is also located. Thus, some alternative mechanism of N-H activation by this complex involving both the phosphorus atoms along with the nitrogen is also likely. This indicates that the activation mechanism for such type of complexes may be substantially different than the mechanism discussed for the planar phosphorus structure, as well as the distorted pyramidal structure discussed in the previous paragraph.

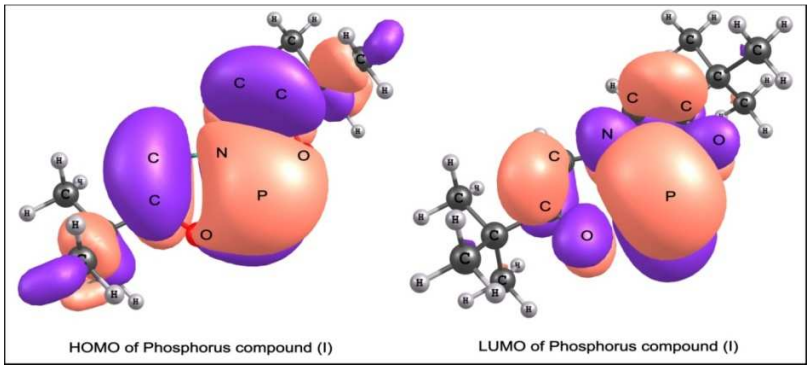

Figure 7. The HOMO and the LUMO for the planar phosphorus complex (1).

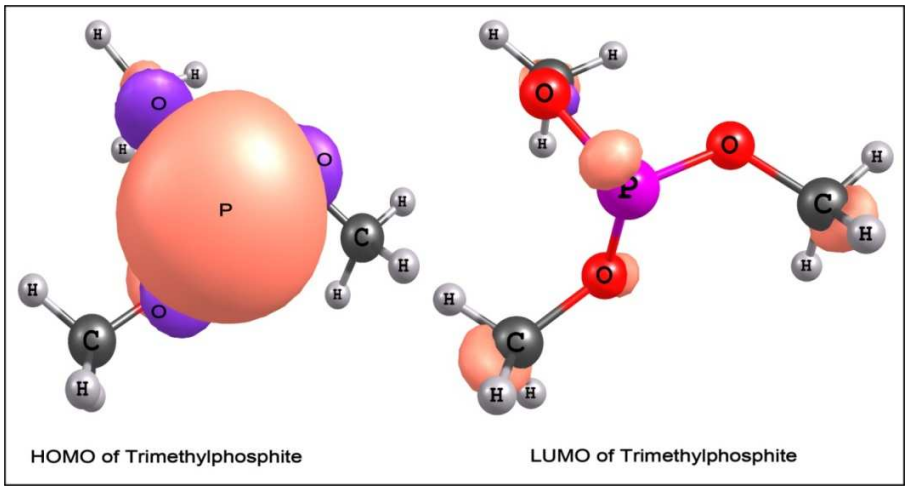

Figure 8. The HOMO and the LUMO for the pyramidal phosphorus complex P(OMe)3.

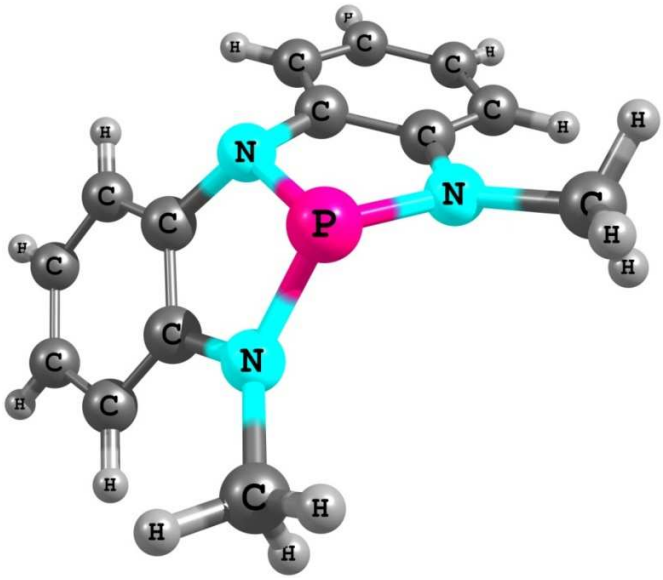

Figure 9. The structure of the distorted tricoordinated phosphorus complex.

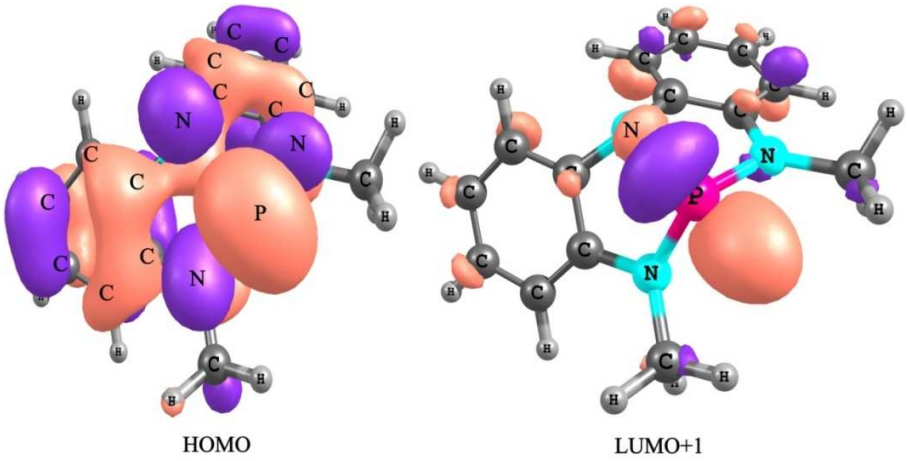

Figure 10. The HOMO and LUMO+1 orbitals of the distorted tricoordinated phosphorus complex shown in Figure 9.

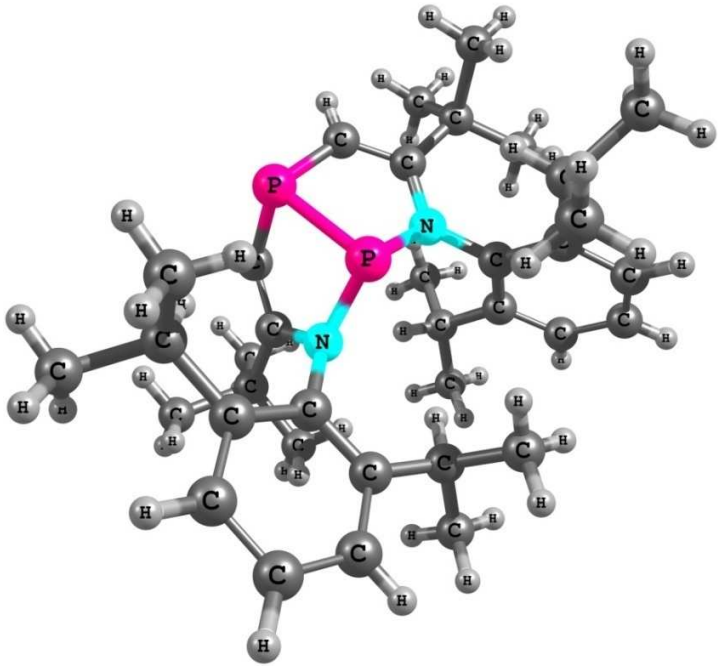

Figure 11. The structure of the pyramidal phosphorus complex.

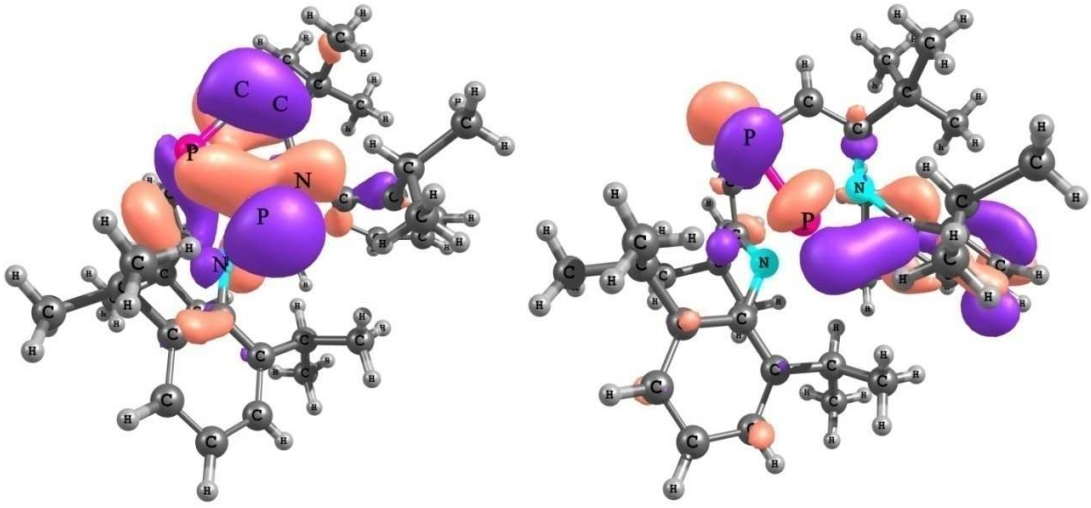

Figure 12. The HOMO and LUMO+5 orbitals of the pyramidal phosphorus complex shown in Figure 11.

Now coming back to the mechanism proposed by Sakaki and co-workers, the subsequent steps in the Sakaki mechanism involve the amino borane assisted transformation of 2 into 5. The BH_2 moiety of amino borane interacts with the nitrogen atom of 2, while simultaneously, the nitrogen atom of amino borane shifts the proton from the oxygen to the phosphorus atom. This process involves two intermediates and three transition states, with the final transition state TS4/5, lying 30.5 kcal/mol higher in energy than the initial separated reactants (see Figure 13).

The first step of the Sakaki Mechanism, as mentioned, is the same as our proposed mechanism. However, the subsequent steps are significantly different. An alternative mechanism that is simpler, with fewer steps, and having barriers that are lower than the barriers of the Sakaki Mechanism would certainly be preferred during AB dehydrogenation by 1. The next section describes our proposed mechanism, which will be seen to satisfy these criteria.

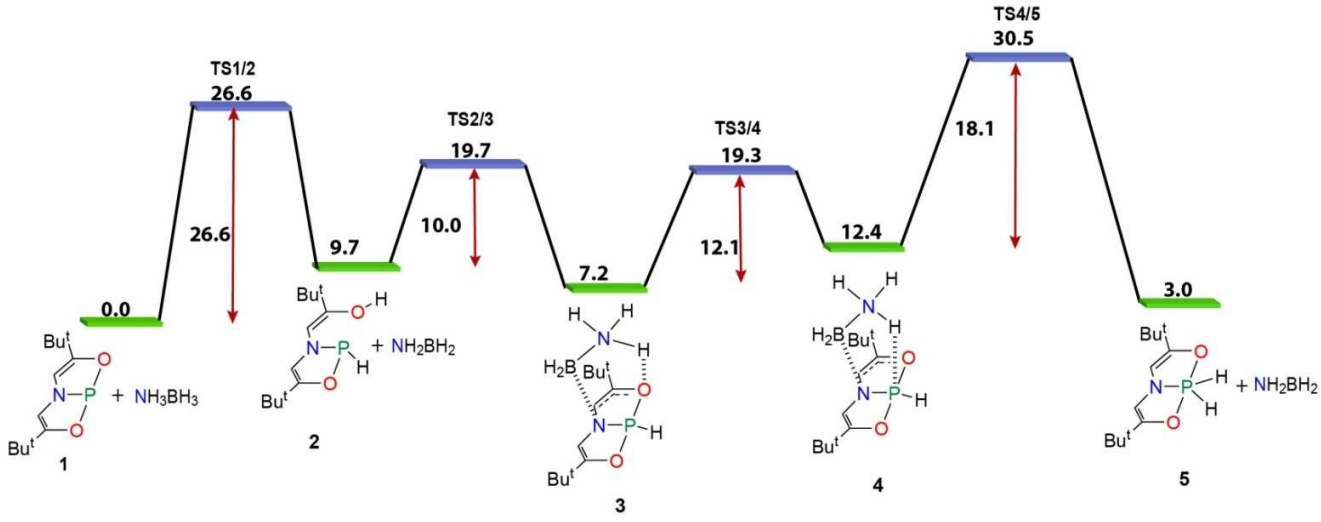

Figure 13. The free energy profile of the Sakaki Mechanism for the ammonia borane dehydrogenation reaction; all values are in kcal/mol.

6.3.4 The Proposed Mechanism for Ammonia Borane (AB) Dehydrogenation by 1.

Before the discussion of the results of our proposed mechanism for AB dehydrogenation by 1, one pertinent question that can be asked is whether the Radosevich Mechanism might be operational for this reaction. The Radosevich Mechanism, applied to AB

dehydrogenation, would involve at least two AB molecules, with the hydridic hydrogen of the first AB molecule being transferred from boron to phosphorus, forming a zwitterionic species that would be the intermediate for this reaction. However, such an intermediate was not obtained, with the system structure reverting back to the reactants in every optimization attempt. An alternative concerted Radosevich-type mechanism was also considered. In this mechanism, shown in Figure 14 below, the hydridic hydrogen attached to boron would shift to the phosphorus center, while, simultaneously, the protic hydrogen of the first AB molecule would be shifted to the second AB molecule. The second AB molecule, while accepting the proton, would, at the same time, transfer a proton to the phosphorus center, leading to the observed experimental product. As seen from Figure 14, this concerted reaction would be highly unfavorable, having a barrier of 60.4 kcal/mol. Such a process is, therefore, not possible. By extension, a similar reaction involving three AB molecules would also be likely to be highly unfavorable. Hence, one can safely state that the equivalent of the Radosevich Mechanism would not be feasible for AB dehydrogenation by 1. Furthermore, the possibility of tautomerization between the O-H and the adjoining C=C groups, after the formation of the first intermediate, 2, in the Sakaki Mechanism has not been investigated because of experimental observations of Radosevich and coworkers indicating no tautomerization in this system for the case of AB dehydrogenation[79].

Our proposed mechanism, when applied to AB dehydrogenation by 1, would require the presence of a base that would act as the proton transfer agent, after two hydrogens have been provided to 1 from an AB molecule (the first step that is shared with the Sakaki Mechanism). Now, in the case of the primary amines, discussed in the previous section, the amine itself could act as the proton transferring base. However, in the case of AB dehydrogenation, it is unlikely that an extra AB molecule can serve this function. This is because the nitrogen in NH_3BH_3 (AB) is four-coordinated, and would be unlikely to be stable as a five coordinated species during the proton transferring transition state. There remains the possibility, however, that other bases may be present in the system that can act as proton transfer agents. The most likely candidate for this is ammonia, NH_3, which can be formed by the dissociation of AB in solution. Indeed, the formation of free

ammonia in reactions involving AB has been observed in experimental studies[80]. Moreover, theoretical studies in the past have shown that the cleavage of the N-B bond in AB to yield NH_3 and BH_3 is preferred over the formation of NH_2BH_2 and H_2 in free AB[81-84], and so free NH_3 would be present in the system, especially when excess of AB is employed. In this regard, it is notable that in the experiments done by Radosevich and coworkers, a significant excess of AB was employed during the dehydrogenation of AB by 1; the ratio of AB to 1 was 4:1[43]. Hence, a significant amount of ammonia was likely to have been present when 1 was converted to the hydrogenated species, 2, denoted in Figure 15 below.

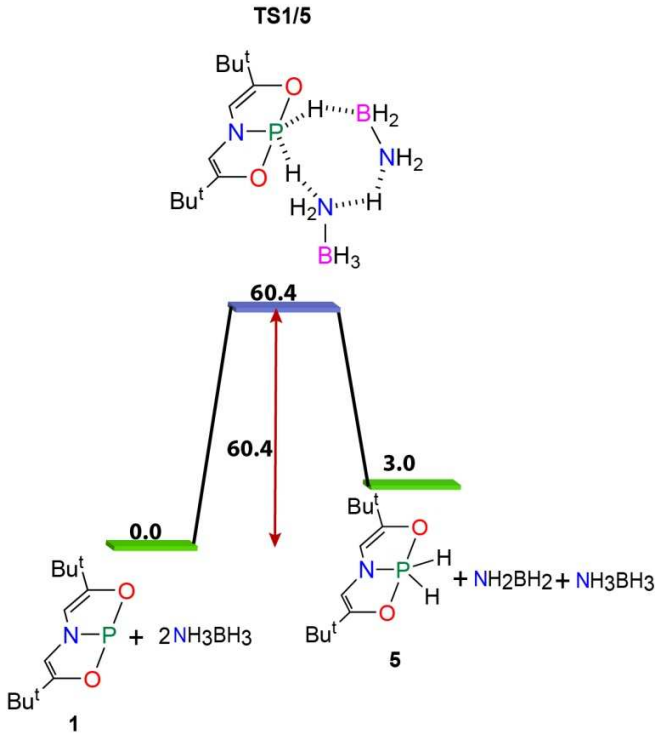

Figure 14. The free energy profile of the concerted mechanism for ammonia borane dehydrogenation; all values are in kcal/mol.

It may be argued that a Radosevich type of mechanism might be possible with one ammonia and one AB molecule, in place of the two AB molecules case that was discussed earlier in this section. However, all attempts made to obtain an intermediate structure having an anionic phosphorus complex, with the corresponding cationic

$[NH_3BH_2NH_3]^+$ – which would be the intermediate in the Radosevich Mechanism – failed, indicating that this, too, is an unlikely possibility. Hence, the only means by which ammonia can influence the reaction would be by our newly proposed base mediated mechanism.

We also note here that we have also looked into an alternative mechanism proposed by Uhl and co-workers for a similar system, where the proton of AB was proposed to have been transferred to the phosphorus atom of a phosphorus-aluminium based FLP[35], which thereby formed a zwitterionic intermediate. Such a mechanism is unlikely for the AB dehydrogenation by the flat phosphorus complex, discussed here, as our calculations indicated that a similar type of zwitterionic intermediate was not stable, and reverted back to the original reactants.

The first step in our proposed mechanism is common with the Sakaki Mechanism: two hydrogens are transferred from AB, one to the phosphorus atom and one to the oxygen, leading to the formation of the species denoted as 2 in Figure 15, and amino borane, NH_2BH_2. The subsequent step in the mechanism involves the mediation by an ammonia molecule, which would lead to a five membered (O-H-N-H-P) transition state, TS2/5, and then to the final product 5. The barrier for this reaction was found to be 15.3 kcal/mol from the intermediate and 25.0 kcal/mol from the original reactant species. This means that the slowest step of the reaction is the first step, with a barrier of 26.6 kcal/mol. In contrast to the Sakaki Mechanism, where the barrier for the slowest step was 30.5 kcal/mol (see Figure 13), the current proposed mechanism therefore is seen to (i) have fewer steps: only two steps in comparison to the four steps of the Sakaki Mechanism, and (ii) have a slowest step barrier that is 3.9 kcal/mol lower in energy than the barrier for the slowest step in the Sakaki Mechanism. These results, therefore, strongly indicate that the newly proposed mechanism would be the prevalent one during AB dehydrogenation by 1.

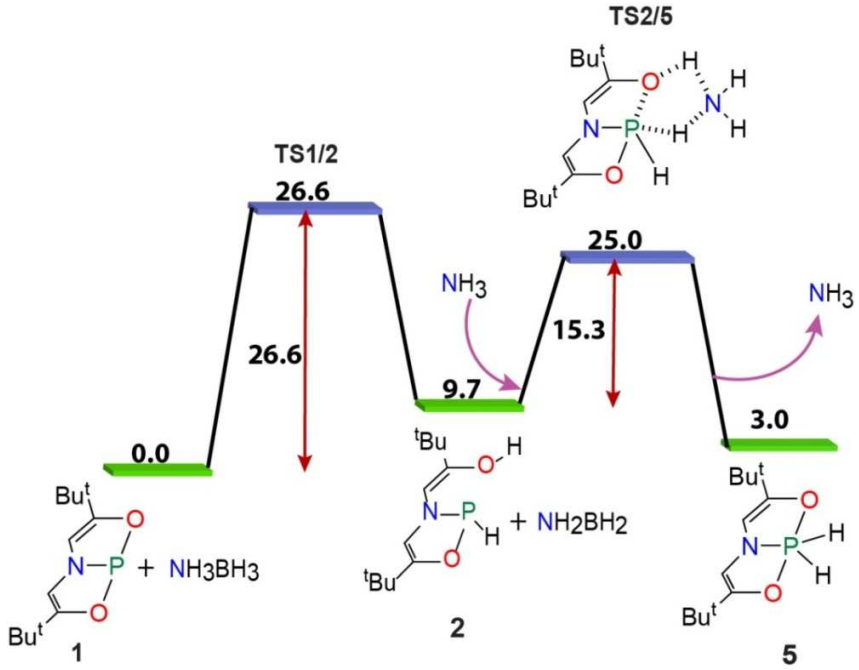

Figure 15. The free energy profile of the newly proposed mechanism for ammonia borane (AB) dehydrogenation by 1; all values are in kcal/mol.

A perusal of the Figures 6 and 15, which show the free energy surfaces for our proposed mechanism for the N-H activation reactions and AB dehydrogenation respectively, indicates that the base mediated step is the slowest step in the N-H activation case, while it is the more facile step in the AB dehydrogenation case. An explanation for this can be found from a charge analysis (using NBO[85-87]) of the intermediates along the reactions pathways for the two cases. The charge analysis on the central phosphorus atom indicates that in the intermediate 2, for the case of AB dehydrogenation reaction, the central phosphorus atom is less electrophilic than in complex 1, but, in the intermediate 2_NMe for the corresponding N-H activation case, the central phosphorus atom is more electrophilic (see Table 1). This suggests that it will be more difficult to transfer the proton from the oxygen to the more electrophilic phosphorus centre for the amine activation case. This provides an explanation for why the barrier for proton transfer from oxygen to phosphorus for the case of AB dehydrogenation *via* the base has been found to be 4.7 kcal/mol lower than the corresponding barrier for the N-H activation case.

Compound Name	1	2	2_NMe	$P(OMe)_3$
Charge on Phosphorus	1.13	1.11	1.47	1.6

Table 1.The charges on the central phosphorus atom in various optimized phosphorus complexes.

6.4 Conclusions

Finding main group systems to do chemistry that has traditionally been done with transition metal complexes is an important area of research. In this regard, newly designed[43] constrained phosphorus based systems hold much promise. Such a "flat" phosphorus based complex, having a tridentate pincer ligand, "1" (see Figure 1), has been reported to participate in interesting and important chemistry, such as the dehydrogenation of ammonia borane (AB)[43], and the activation of the N-H bond in primary amines[57]. The current computational work, employing full quantum chemical calculations with density functional theory (DFT), shows that a general mechanism exists that is common to the different reactions involving 1. This general, base mediated mechanism has been shown to be both simpler and energetically more favorable in comparison to mechanisms that have been proposed earlier in the literature[53, 57]. The significance of these findings is that it reveals that the ligand backbone in the phosphorus complex is not involved in interacting with the substrates during the reactions. This finding is important because it indicates that the phosphorus complex can be altered, with new structures being designed having a different ligand backbone, without potentially affecting the ability of the new complexes to do interesting chemistry, such as AB dehydrogenation. Therefore, the current work has expanded the understanding of these important new systems, and revealed new possibilities that can be explored to improve upon the existing phosphorus based systems.

6.5 References

1. J. Emsley, The Shocking History of Phosphorus, *Pan Macmillan*, 2000.
2. J. R. Nitschke, *Nat. Chem.*, 2011, 3, 90-90.
3. C. A. Tolman, *Chem. Rev.*, 1977, 77, 313-348.
4. D. W. Stephan, *Angew. Chem. Int. Ed.*, 2000, 39, 314-329.

5. N. Sakai, S. Mano, K. Nozaki, H. Takaya, *J. Am. Chem. Soc.*, 1993, 115, 7033-7034.
6. S. H. Chikkali, J. I. van der Vlugt, J. N. H. Reek, *Coord. Chem. Rev.*, 2014, 262, 1-15.
7. C. P. Casey, G. T. Whiteker, M. G. Melville, L. M. Petrovich, J. A. Gavney, D. R. Powell, *J. Am. Chem. Soc.*, 1992, 114, 5535-5543.
8. J. A. Tallarico, P. J. Bonitatebus, M. L. Snapper, *J. Am. Chem. Soc.*, 1997, 119, 7157-7158.
9. M. S. Sanford, M. Ulman, R. H. Grubbs, *J. Am. Chem. Soc.*, 2001, 123, 749-750.
10. L. Cavallo, *J. Am. Chem. Soc.*, 2002, 124, 8965-8973.
11. J. Ye, S. Ma, *Acc. Chem. Res.*, 2014, 47, 989-1000.
12. D. Enders, U. Kallfass, *Angew. Chem. Int. Ed.*, 2002, 41, 1743-1745.
13. M. N. Hopkinson, C. Richter, M. Schedler, F. Glorius, *Nature*, 2014, 510, 485-496.
14. J. W. Bode, S. S. Sohn, *J. Am. Chem. Soc.*, 2007, 129, 13798-13799.
15. R. S. Menon, A. T. Biju, V. Nair, *Chem. Soc. Rev.*, 2015, 44, 5040-5052.
16. F. Li, Z. Wu, J. Wang, *Angew. Chem. Int. Ed.*, 2014, 54, 656-659.
17. J. W. Bode, *Nat. Chem.*, 2013, 5, 813-815.
18. J. Mahatthananchai, J. W. Bode, *Acc. Chem. Res.*, 2014, 47, 696-707.
19. M. Albrecht, *Angew. Chem. Int. Ed.*, 2015, 54, 5822-5822.
20. F. Lips, A. Mansikkamäki, J. C. Fettinger, H. M. Tuononen, P. P. Power, *Organometallics*, 2014, 33, 6253-6258.
21. F. Lips, J. C. Fettinger, A. Mansikkamäki, H. M. Tuononen, P. P. Power, *J. Am. Chem. Soc.*, 2014, 136, 634-637.
22. Y.-L. Shan, W.-L. Yim, C.-W. So, *Angew. Chem.*, 2014, 126, 13371-13374.
23. M. Majumdar, I. Omlor, C. B. Yildiz, A. Azizoglu, V. Huch, D. Scheschkewitz, *Angew. Chem.*, 2015, 127, 8870-8874.
24. Y. Li, B. Ma, C. Cui, *Dalton Trans.*, 2015, DOI: 10.1039/C5DT01290B.
25. S. Krupski, C. Schulte to Brinke, H. Koppetz, A. Hepp, F. E. Hahn, *Organometallics*, 2015, 34, 2624-2631.
26. M. Driess, S. Yao, M. Brym, C. van Wüllen, *Angew. Chem. Int. Ed.*, 2006, 45, 4349-4352.
27. J. D. Erickson, J. C. Fettinger, P. P. Power, *Inorg. Chem.*, 2015, 54, 1940-1948.
28. S. Oae, Y. Uchida, *Acc. Chem. Res.*, 1991, 24, 202-208.
29. J. Halpern, *Acc. Chem. Res.*, 1970, 3, 386-392.
30. L. Vaska, *Acc. Chem. Res.*, 1968, 1, 335-344.
31. G. C. Welch, R. R. S. Juan, J. D. Masuda, D. W. Stephan, *Science*, 2006, 314, 1124-1126.
32. T. A. Rokob, A. Hamza, A. Stirling, T. Soós, I. Pápai, *Angew. Chem. Int. Ed.*, 2008, 47, 2435-2438.
33. V. Sumerin, F. Schulz, M. Nieger, M. Leskelä, T. Repo, B. Rieger, *Angew. Chem. Int. Ed.*, 2008, 47, 6001-6003.
34. V. Sumerin, F. Schulz, M. Atsumi, C. Wang, M. Nieger, M. Leskelä, T. Repo, P. Pyykkö, B. Rieger, *J. Am. Chem. Soc.*, 2008, 130, 14117-14119.

35. C. Appelt, J. C. Slootweg, K. Lammertsma, W. Uhl, *Angew. Chem. Int. Ed.*, 2013, 52, 4256-4259.
36. Y. Guo, X. He, Z. Li, Z. Zou, *Inorg. Chem.*, 2010, 49, 3419-3423.
37. L. Greb, P. Oña-Burgos, B. Schirmer, S. Grimme, D. W. Stephan, J. Paradies, *Angew. Chem. Int. Ed.*, 2012, 51, 10164-10168.
38. L. Zhao, H. Li, G. Lu, Z.-X. Wang, *Dalton Trans.*, 2010, 39, 4038-4047.
39. P. A. Chase, G. C. Welch, T. Jurca, D. W. Stephan, *Angew. Chem. Int. Ed.*, 2007, 46, 8050-8053.
40. P. A. Chase, T. Jurca, D. W. Stephan, *Chem. Commun.*, 2008, 1701-1703.
41. H. Li, L. Zhao, G. Lu, F. Huang, Z.-X. Wang, *Dalton Trans.*, 2010, 39, 5519-5526.
42. T. Privalov,Chem. Eur. J., 2009, 15, 1825-1829.
43. N. L. Dunn, M. Ha, A. T. Radosevich, *J. Am. Chem. Soc.*, 2012, 134, 11330-11333.
44. A. J. Arduengo, C. A. Stewart, *Chem. Rev.*, 1994, 94, 1215-1237.
45. A. J. Arduengo, C. A. Stewart, F. Davidson, D. A. Dixon, J. Y. Becker, S. A. Culley, M. B. Mizen, *J. Am. Chem. Soc.*, 1987, 109, 627-647.
46. S. A. Culley, A. J. Arduengo, *J. Am. Chem. Soc.*, 1984, 106, 1164-1165.
47. M. Driess, N. Muresan, K. Merz, M. Päch, *Angew. Chem. Int. Ed.*, 2005, 44, 6734-6737.
48. E. E. Coyle, C. J. O'Brien, *Nat Chem*, 2012, 4, 779-780.
49. M. Albrecht, G. van Koten, *Angew. Chem. Int. Ed.*, 2001, 40, 3750-3781.
50. N. Selander, K. l. n. J. Szabó, *Chem. Rev.*, 2010, 111, 2048-2076.
51. J. P. Collman, *Acc. Chem. Res.*, 1968, 1, 136-143.
52. S. Niu, M. B. Hall, *Chem. Rev.*, 2000, 100, 353-406.
53. G. Zeng, S. Maeda, T. Taketsugu, S. Sakaki, *Angew. Chem. Int. Ed., 2014,* 53, 4633-4637.
54. M. Vogt, A. Nerush, Y. Diskin-Posner, Y. Ben-David, D. Milstein, *Chem. Sci.*, 2014, 5, 2043-2051.
55. B. Askevold, J. T. Nieto, S. Tussupbayev, M. Diefenbach, E. Herdtweck, M. C. Holthausen, S. Schneider, *Nat. Chem.*, 2011, 3, 532-537.
56. G. A. Filonenko, M. P. Conley, C. Copéret, M. Lutz, E. J. M. Hensen, E. A. Pidko, *ACS Catal.*, 2013, 3, 2522-2526.
57. S. M. McCarthy, Y.-C. Lin, D. Devarajan, J. W. Chang, H. P. Yennawar, R. M. Rioux, D. H. Ess, A. T. Radosevich, *J. Am. Chem. Soc.*, 2014, 136, 4640-4650.
58. E. Morgan, D. F. MacLean, R. McDonald, L. Turculet, *J. Am. Chem. Soc.*, 2009, 131, 14234-14236.
59. M. A. Salomon, A.-K. Jungton, T. Braun, *Dalton Trans.*, 2009, 7669-7677.
60. T. E. Hanna, E. Lobkovsky, P. J. Chirik, *Eur. J. Inorg. Chem.*, 2007, 2007, 2677-2685.
61. A. C. Sykes, P. White, M. Brookhart, *Organometallics*, 2006, 25, 1664-1675.
62. J. Cui, Y. Li, R. Ganguly, A. Inthirarajah, H. Hirao, R. Kinjo, *J. Am. Chem. Soc.*, 2014, 136, 16764-16767.
63. G. D. Frey, V. Lavallo, B. Donnadieu, W. W. Schoeller, G. Bertrand, *Science*, 2007, 316, 439-441.

64. M. A. Lill, V. Helms, *Proceedings of the National Academy of Sciences*, 2002, 99, 2778-2781.
65. F.-Q. Shi, X. Li, Y. Xia, L. Zhang, Z.-X. Yu, *J. Am. Chem. Soc.*, 2007, 129, 15503-15512.
66. K. M. Jude, S. K. Wright, C. Tu, D. N. Silverman, R. E. Viola, D. W. Christianson, *Biochem.*, 2002, 41, 2485-2491.
67. M. r. Wikström, M. I. Verkhovsky, G. Hummer, *Biochimica et Biophysica Acta (BBA) - Bioenergetics*, 2003, 1604, 61-65.
68. M. J. T. Frisch, G. W.; Schlegel, H. B.; Scuseria, G. E.; Robb, M. A.; Cheeseman, J. R.; Scalmani, G.; Barone, V.; Mennucci, B.; Petersson, G. A.; Nakatsuji, H.; Caricato, M.; Li, X.; Hratchian, H. P.; Izmaylov, A. F.; Bloino, J.; Zheng, G.; Sonnenberg, J. L.; Hada, M.; Ehara, M.; Toyota, K.; Fukuda, R.; Hasegawa, J.; Ishida, M.; Nakajima, T.; Honda, Y.; Kitao, O.; Nakai, H.; Vreven, T.; Montgomery, J. A., Jr.; Peralta, J. E.; Ogliaro, F.; Bearpark, M.; Heyd, J. J.; Brothers, E.; Kudin, K. N.; Staroverov, V. N.; Kobayashi, R.; Normand, J.; Raghavachari, K.; Rendell, A.; Burant, J. C.; Iyengar, S. S.; Tomasi, J.; Cossi, M.; Rega, N.; Millam, M. J.; Klene, M.; Knox, J. E.; Cross, J. B.; Bakken, V.; Adamo, C.; Jaramillo, J.; Gomperts, R.; Stratmann, R. E.; Yazyev, O.; Austin, A. J.; Cammi, R.; Pomelli, C.; Ochterski, J. W.; Martin, R. L.; Morokuma, K.; Zakrzewski, V. G.; Voth, G. A.; Salvador, P.; Dannenberg, J. J.; Dapprich, S.; Daniels, A. D.; Farkas, Ö.; Foresman, J. B.; Ortiz, J. V.; Cioslowski, J.; Fox, D. J. , *Gaussian, Inc. Wallingford CT*, 2009, Gaussian 09.
69. Y. Zhao, D. Truhlar, *Theor. Chem. Acc.*, 2008, 120, 215-241.
70. K. Raghavachari, G. W. Trucks, *J. Chem. Phys.*, 1989, 91, 1062-1065.
71. R. Krishnan, J. S. Binkley, R. Seeger, J. A. Pople, *J. Chem. Phys.*, 1980, 72, 650-654.
72. A. D. McLean, G. S. Chandler, *J. Chem. Phys.*, 1980, 72, 5639-5648.
73. G. A. Petersson, A. Bennett, T. G. Tensfeldt, M. A. Al-Laham, W. A. Shirley, J. Mantzaris, *J. Chem. Phys.*, 1988, 89, 2193-2218.
74. J. Tomasi, B. Mennucci, R. Cammi, *Chem. Rev.*, 2005, 105, 2999-3094.
75. W. H. Miller, N. C. Handy, J. E. Adams, *J. Chem. Phys.*, 1980, 72, 99-112.
76. M. Page, J. W. McIver, *J. Chem. Phys.*, 1988, 88, 922-935.
77. M. E. Alberto, N. Russo, E. Sicilia, Chem. Eur. J., 2013, 19, 7835-7846.
78. W. Zhao, S. M. McCarthy, T. Y. Lai, H. P. Yennawar, A. T. Radosevich, *J. Am. Chem. Soc.*, 2014, 136, 17634-17644.
79. A. T. Radosevich, 2014, Information acquired from personal communication with Dr. Alexander Radosevich.
80. Z. Li, G. Zhu, G. Lu, S. Qiu, X. Yao, *J. Am. Chem. Soc.*, 2010, 132, 1490-1491.
81. P. M. Zimmerman, Z. Zhang, C. B. Musgrave, *J. Phys. Chem. Lett.*, 2011, 2, 276-281.
82. M. T. Nguyen, V. S. Nguyen, M. H. Matus, G. Gopakumar, D. A. Dixon, *J. Phys. Chem. A*, 2007, 111, 679-690.
83. D. J. Grant, D. A. Dixon, *J. Phys. Chem. A*, 2006, 110, 12955-12962.
84. D. A. Dixon, M. Gutowski, *J. Phys. Chem. A*, 2005, 109, 5129-5135.
85. J. P. Foster, F. Weinhold, *J. Am. Chem. Soc.*, 1980, 102, 7211-7218.

86. A. E. Reed, F. Weinhold, *J. Chem. Phys.*, 1983, 78, 4066-4073.
87. A. E. Reed, L. A. Curtiss, F. Weinhold, *Chem. Rev.*, 1988, 88, 899-926.

CHAPTER 7

Summary of All the Chapters

Throughout this thesis, the potential of catalysts has been scrutinized based on their efficacy for small molecule activation such as the ammonia borane dehydrogenation reaction. For this purpose, several metallic and non-metallic catalysts have been investigated by density functional theory (DFT).

Chapter 1 discusses the state of the art in terms of reaction pathways and the application of the same in small molecule activation and ammonia borane dehydrogenation.

Chapter 2 describes the theoretical underpinnings of the computational tools that have been employed to perform the work presented in this dissertation.

In chapter 3, the design of late transition metal frustrated Lewis pairs (FLPs) has been discussed, based on a α diimine ligand with a labile phosphorus bond with the metal centre. DFT/MP2 methods have been employed to explore such late transition metal containing FLPs for their catalytic role in the dehydrogenation of ammonia borane (AB) and the hydrogenation of ethylene. The possibility of side reactions has also been investigated and it has been shown that the resulting products can serve as excellent FLPs for the catalysis of the dehydrogenation process. Thus, the study has opened up new possibilities of metal-ligand cooperativity in small molecule activation reactions. (*Dalton Trans.*, 2013, 42, 13866-13873.)

In chapter 4, the possibility of the catalytic dehydrogenation of AB has been evaluated computationally by employing various cage systems. Full quantum mechanical (QM) calculations using density functional theory (DFT) show that the cages that contain nitrogen-carbon (N-C cage), phosphorus-carbon (P-C cage) and carbon-phosphorus (C-P cage) would have competing side reactions in catalyzing AB dehydrogenation. Further calculations show that the cages having nitrogen-phosphorus (N-P cage), nitrogen-

germanium (N-Ge cage) and phosphorus-germanium (P-Ge cage) Lewis pairs would be efficient AB dehydrogenation catalysts. Among the cages, the P-Ge cage was observed to be the most promising, with the lowest energy barriers for the AB dehydrogenation pathway. In addition, it also exhibits a noticeably higher preference towards the desired dehydrogenation pathway compared to the undesired alternative directions that would lead to the formation of dormant species. Such calculations pinpoint the potential of the zero dimensional cages for frustrated Lewis pair (FLP) behavior. (*Chem. Commun.,* 2011, 47, 11417-11419 and *Phys. Chem. Chem. Phys.*, 2013, 15, 20857-20867.)

In chapter 5, we have concluded that the bond-strengthening π-back donation that has been recently discovered for transition metal systems can also be applied effectively for main group silylene complexes. This observation has significant impact on the broader scope of the reactivity for a range of silylenes that had been considered unstable previously. In addition, such complexes are cheaper and greener than conventional transition metal counterparts, which highlight the practical significance of this finding. (*Chem. Commun.*, 2014, 50, 8522-8525.)

In chapter 6, newly designed constrained “flat” phosphorus based complex systems with the tridentate pincer ligand have been demonstrated to participate in important reactions such as the dehydrogenation of ammonia borane and the activation of the N-H bond in primary amines. Full quantum chemical calculations utilizing density functional theory (DFT) show that a general mechanism exists i.e., a base mediated mechanism that has been proposed to be both simpler and energetically more favorable than the literature accounts till date. These findings provide important predictions of the chemical behavior of such main group compounds. The scope of having different ligand backbones without affecting their ability to do similar chemistry will open up new design strategies for phosphorus based complexes. (*Inorg. Chem.*, 2016, 55, 558–565)